University of Alberta

Nonlinear Observer-based Fault Detection and Diagnosis

by

Amr Moustapha Pertew

A thesis submitted to the Faculty of Graduate Studies and Research in partial fulfillment of the requirements for the degree of Doctor of Philosophy

Department of Electrical and Computer Engineering

Edmonton, Alberta
Spring 2007

Canada

To Walaa, Abderrahman and Mostafa

Abstract

With the advent of efficient computational algorithms, real-time solutions to the non-linear Fault Detection and Diagnosis problem are nearing a reality. In this thesis, we propose a new dynamical observer structure to solve this problem for a class of nonlinear systems referred to as Lipschitz systems. Lipschitz systems constitute a very important class, since any nonlinear system with continuously differentiable nonlinearities can be locally expressed in this form. Examples include trigonometric nonlinearities occurring in robotics, as well as nonlinearities which are square or cubic in nature. The new observer structure adds extra degrees of freedom over the classical observer structure, and lays the ground to the addition of the Fault Diagnosis objective in the design problem. It is shown that the Lipschitz observer design problem can be carried out using a systematic design procedure which is less restrictive than the existing design approaches and that can be solved using commercially available software. Within this new framework, the sensor Fault Diagnosis problem is formulated as a standard convex optimization problem solvable using Linear Matrix Inequalities (LMIs). It is shown that the classical observer structure could not solve the problem in this case. The case of additive uncertainties is considered by extending the Unknown Input Observer (UIO) technique to the class of Lipschitz systems.

The new Lipschitz observer and sensor Fault Diagnosis designs are applied to a practical example, namely the *Rotary Inverted Pendulum* (ROTPEN) which falls in the category of planar robot manipulators. The experimental results illustrate the applicability of the proposed techniques in the robotics field, showing: (i) How to model a robot manipulator as a standard Lipschitz system, (ii) The importance of the dynamic Lipschitz observer in large operating regions and for large Lipschitz constants, (iii) The accurate velocity estimation

obtained using the dynamic observer, alleviating the need to introduce velocity sensors in real-time, (iv) The efficiency of the dynamic observer in diagnosing and tolerating sensor faults of different frequencies.

Acknowledgements

The work in this thesis would not have been possible without the help of many individuals. I would like to express my gratitude to Prof. Horacio Marquez for his valuable advices and constant support in all aspects of this research. His enthusiasm in control theory, skillful ideas for investigation in new areas to correlate the two fields of nonlinear control and fault detection, and meticulous attention to the details are predominantly responsible for the completion of this work. It has been my privilege to work with him and I am deeply indebted for his interest.

I would also like to thank Dr. Qing Zhao for the guidance she has given me throughout the course of my work. Her ideas and points of view have been a constant source of inspiration, and our endless discussions have taught me to be more inquisitive. Thanks for widening my views and helping me achieving my goals, and for teaching me how to systematically approach research projects, and organize my work coherently.

Thanks to all the great friends I met here at University of Alberta. I am indebted to my colleagues at the Advanced Control Systems Laboratory for the endless and valuable discussions that we had throughout the years. I owe gratitude to Thomas Grochmal for providing the switching swingup control scheme used in Experiment C.

I would like to thank my family, to whom I have dedicated this thesis, for their support throughout the years. My wife, Walaa, has always been loving throughout this difficult experience while working full-time and raising our family. She has always been my greatest source of energy to finish this thesis. For this, I am forever grateful. To her and her smile I owe everything I attained.

Table of Contents

List of Tables

List of Figures

List of Nomenclature

ARE : Algebraic Riccati Equation

FDD : Fault Detection and Diagnosis

FDI : Fault Detection and Isolation

LFDI : Lipschitz Fault Detection and Isolation

LFT : Linear Fractional Transformation

LMI : Linear Matrix Inequality

LQR : Linear Quadratic Regulator

LTI : Linear Time Invariant

MIMO : Multiple Input Multiple Output

SDO : Sampled Data Observer

UIO : Unknown Input Observer

Chapter 1

Introduction

Motivated by a growing demand for higher reliability in modern control systems, the *Fault Diagnosis Problem* is gaining increasing consideration world-wide in both theory and application. This problem is defined as the synthesis of a monitoring system to detect faults and specify their location and significance in a control system [13]. Broadly speaking, the term *Fault* means failures, errors, malfunctions or disturbances in the functional units that can lead to undesirable or intolerable behavior of the system [10]. Fault Diagnosis is becoming of crucial importance in a wide variety of applications, including:

i) Safety-critical systems such as nuclear reactors, chemical plants, aircraft control systems, fire alarms and medical devices, where the need for fast and accurate detection of anomalous situations is of utmost importance.

ii) Systems operating in remote and hazardous environments, where a high degree of autonomy and safety is required (such as free-flying space robots and advanced unmanned combat aircraft).

iii) Applications in which a safe and reliable man-machine interaction is of primary concern. Today's automobile industry is a good example where the auto manufacturers have introduced many electronic functions such as anti-lock brake, chassis control, climate control, traction control, etc [10].

In addition to safety concerns, Fault Diagnosis is very important from an economical perspective. This is due to the fact that fast fault detection could prevent unexpected and total failure that can lead to plant shutdown and loss of revenues. Besides, the environmental

1

concern is now becoming an important factor in the incorporation of Fault Diagnosis techniques in many industries. A good example is the California Air Resource Board (CARB) and Environmental Protection Agency (EPA) legislations concerning all light duty vehicles sold in North American fleet as of 1998. The law requires on board fault detection capability for all vehicle components whose failure can result in emission levels beyond a certain value [10].

The Fault Diagnosis problem (referred to as Fault Detection, Isolation and Identification in the literature, abbreviated as FDI henceforth) is also very important in fault-tolerant control. A fault-tolerant control system is designed to retain some portion of its control integrity in the event of a set of possible component faults. This is achieved by incorporating an element of automatic reconfiguration, once a malfunction has been detected. FDI plays an important role in this case, as before any control law reconfiguration is possible, the fault must be reliably detected, isolated and the information should be passed to a supervision mechanism to make proper decisions [13]. Fault-tolerance is considered as one of the characteristics of intelligent systems [3, 104].

1.1 History of FDI

A large amount of knowledge on model-based fault diagnosis has been accumulated through the literature since the beginning of the 1970s [13]. The term *model-based* is used to characterize the application of the powerful techniques of mathematical modelling, state estimation and system identification for FDI. Model-based FDI is also referred to as *analytical redundancy* in contrast with *hardware redundancy*, the other widely applied approach for FDI such as the well-known triple module redundancy (TMR) schemes used in industries. Figure 1.1, [13], demonstrates the concepts of the two approaches when applied for sensor fault diagnosis.

In hardware redundancy, e.g. sensor redundancy, multiple lanes of sensors are used to measure a particular variable, and a voting scheme is applied to decide if and when a fault has occurred and to specify its likely location. On the other hand, in the model-based approach, redundant analytical relationships between various measured variables of the monitored process are used to solve the problem. The major advantages of analytical redundancy over hardware redundancy is that the former is cost-effective, can be implemented in software on the same computer used for process control and offers high reliability. Figure 1 also shows that only additional storage capacity and possibly greater computer power is needed for the
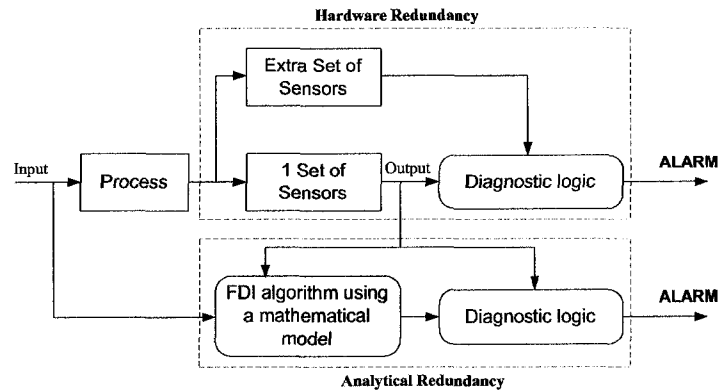
Figure 1.1: Analytical versus Hardware Redundancy.

implementation of a model-based FDI algorithm.

The most extensive period of development of model-based FDI took place between late 1970s and early 1990s. During this period, many fundamental definitions were established and a general model-based FDI system structure was proposed [13, 44]. The objectives of a model-based FDI algorithm have become widely accepted as the monitoring of the plant during its normal working conditions so as to detect the occurrence of faults (Fault Detection), recognize their location (Fault Isolation) and, if possible, their time evolution (Fault Identification). Within this context, many techniques have been proposed and much work has considered the practical side of the problem. From the early important works in this direction are the works by Clark et. al in 1975 [19] who first applied classical observers to develop sensor fault isolation schemes. Mironovski [81] originally proposed the parity relation approach, in 1979, based upon consistency checking on system input and output data over a time window. The parameter estimation approach, which is based directly on system identification techniques, was first illustrated by Bakiotis et. al in 1979 [4].

All of these methods share the same framework in which the diagnosis objective is achieved by comparing the actual system's behavior with the corresponding expected behavior derived via its mathematical model. The result of this comparison is a set of variables (referred to as *residuals*) which are sensitive to the occurrence of a fault. In other words, when a fault occurs, a fault signature affects the residuals, and this information is then processed to identify the size and the location of the fault by using numerical and statistical techniques.

1.2 Robust and Nonlinear FDI

Since the existence of a good mathematical model is the basic building block of all model-based approaches used in FDI, mathematical modelling and system identification techniques are of crucial importance for all these techniques. An important problem occurs when a perfectly accurate and complete mathematical model for the system under hand is not available or is hard to obtain. This is due to the fact that discrepancies between the actual process and its model cause fundamental methodology difficulties in FDI applications. They constitute a source of false and missed alarms which can corrupt the FDI system performance to such an extent that it may become totally ineffective. This problem has encouraged much work towards the so-called "Robust FDI" problem where the effects of modelling uncertainties as well as noise and disturbances are considered.

The main objective of "Robust FDI" is to design residuals that can differentiate between faults and uncertainties. Although the best case scenario is to design residuals which are insensitive or even invariant to uncertainties, this is a challenging problem and a more meaningful formulation of the Robust FDI problem is to reduce the effect of uncertainties, without losing (or even with an increase of) fault sensitivity. A number of methods have been proposed to tackle this problem, for example the *unknown input observer* by Frank et. al [31, 32, 38], *the eigenstructure assignment approach* by Patton et. al [85, 86, 88, 90], *the optimal robust parity relation method* by Gertler et. al [45, 48, 49], *the optimal fault detection filter design* by Frank, Ding et. al [27]. However, the research is still under the way to develop more practically applicable methods.

Another important problem that results from mathematical modelling is when a model exists but is highly nonlinear. This yields the "Nonlinear FDI" problem which is the main focus of this thesis. Nonlinear FDI has traditionally been approached in three different directions: (i) Linearization methods, (ii) Observer-based approaches and (iii) Learning methodologies. In linearization, the model is first linearized at an operating point, and robust FDI techniques are then applied for residual generation. This method only works well when the linearization does not cause a large mismatch between linear and nonlinear models and the system operates near the operating point. On the other hand, the observer-based methods deal with systems with high nonlinearity and wide operating range by tackling the FDI problem directly using *Nonlinear observer* techniques. This approach will be discussed in more detail in Chapter 2.

Learning methodologies (or sometimes referred to as "knowledge-based" methods) are conceptually different techniques that attempt to overcome the difficulty of analytical treatment of the nonlinearity by using non-analytical (qualitative and knowledge-based) methodologies such as neural networks or fuzzy system techniques. The main idea is to find an approximate model which can be used to represent the nonlinear system, as well as a mechanism which can automatically identify this model. The Neural Network has therefore been used as a powerful tool of handling such problems, and there have been a large number of publications on neural networks-based FDI, e.g [37, 57, 82, 103, 114]. Some typical problems in these methods include the network selection, the training algorithms and the representation of system dynamics. Therefore, research focusing on the practical side of the problem is still under the way.

As a conclusion, the Fault Diagnosis (FDI) problem is an important problem from both the theoretical and practical perspectives. Different approaches have been adopted to solve this problem. However, challenges still exist and many questions need to be answered for this field to become maturely established. Besides, the gap between theory and practice is yet to be explored.

1.3 Overview and Statement of Contributions

In this thesis, we restrict attention to model-based FDI, focusing on a class of nonlinear systems known as "Lipschitz systems". Although sufficient conditions for observer convergence have been known for many years, observer design for Lipschitz systems has remained an open problem. Using the concept of "Dynamical Observers" we provide a general solution to the Lipschitz observer synthesis problem. Furthermore, we use this concept for diagnosing different faults affecting the system as well as for cancelling the effect of disturbances that may cause false alarms. We show the effectiveness of the introduced strategies in the Robotics field, by conducting experiments on a two-degrees of freedom manipulator (the Rotating Inverted Pendulum).

The rest of the thesis is organized as follows:

- Chapter 2: In this chapter, we survey the techniques currently used for model-based fault diagnosis focusing on the nonlinear observer-based approach. Within this context, different Nonlinear FDI techniques are discussed and the motivation of our research is

highlighted.

- Chapter 3: In this chapter, we consider the problem of observer design for Lipschitz nonlinear systems. A new dynamic framework which is a generalization of previously used Lipschitz observers is introduced and the generalized sufficient condition that ensures asymptotic convergence of the state estimates is presented. The equivalence between this condition and an H_∞ optimal control problem which satisfies the standard regularity assumptions in H_∞ optimization theory is shown and a parameterization of all possible observers is also presented. A design procedure which is less restrictive than the existing design approaches is proposed, and a simulation example is given to illustrate the observer design.

- Chapter 4: In this chapter, we apply the dynamic observer structure introduced in chapter 3 to the FDI problem. The extra degrees of freedom are used for treating the sensor fault diagnosis problem with the objective to make the residual converge to the faults vector achieving detection and identification at the same time. The use of appropriate weightings to solve this problem in a standard convex optimization framework is also demonstrated. A Linear Matrix Inequality (LMI) design procedure solvable using commercially available software is presented with a simulation example to illustrate the proposed design.

- Chapter 5: In this chapter, we consider the robust FDI problem by studying the case of additive uncertainties. Firstly, the standard *Unknown Input Observer* (UIO) approach (used to deal with additive uncertainties in linear systems) is generalized to nonlinear Lipschitz systems. The new observer is then applied in the robust fault diagnosis problem, by modelling the problem as a two-objectives optimization problem that is solved using numerical techniques. In this problem, the first objective is to achieve observer stability, while the second is to decouple the effect of uncertainties from faults in the estimation error.

- Chapter 6: In this chapter, we consider the application of the proposed techniques in the Robotics field. Techniques of modelling robot manipulators as standard Lipschitz systems are first introduced. Experimental results on a two-degrees of freedom manipulator (the Rotating Inverted Pendulum) are also presented.

- Chapter 7: In this chapter, we explore the idea of additional dynamics in the sampled-data state reconstruction problem. We consider the linear time invariant case proposing

a new full order observer structure that can generate intersample state estimation. The observer synthesis is carried out using the H_∞ framework and is shown to have some important advantages over the classical lifting technique that has been used to study similar problems. The introduced techniques are applied through simulations in the fast rate fault detection problem.

- Chapter 8: In this chapter, concluding remarks are presented, and future research topics are proposed.

Chapter 2

Background and Mathematical

Framework

In this chapter we survey the techniques that are currently used for model-based fault diagnosis, followed by background material that motivates our research. The mathematical framework and notation used throughout the thesis are introduced[1].

2.1 The Model-based FDI Approach

As seen in Figure 1.1, analytical redundancy (model-based) techniques have many advantages over the hardware redundancy schemes used in fault diagnosis. Therefore, the trend is to use the model-based FDI approach represented by the structure in Figure 2.1. This two-stage structure was first suggested by Chow and Willsky in 1980 [16], and is now widely accepted by the fault diagnosis community [13]. It consists of the following:

a) Residual generation: Its purpose is to generate a fault indicating signal (residual), using available input and output information from the monitored system. This auxiliary signal is designed to reflect the onset of a possible fault in the analyzed system. The residual should be normally zero or close to zero only when no fault is present.

b) Decision making: The residuals are examined and a decision rule is then applied to determine if a fault has occurred. The decision process usually consists of a simple

---

[1]This chapter is a pure survey of previous work in areas related to the thesis. No new results can be found in this chapter.

8

threshold test on instantaneous values or moving average of the residuals. It may also consist of methods of statistical decision theory, such as Generalized Likelihood Ratio (GLR) testing or Sequential Probability Ratio Testing (SPRT) [5, 6, 20, 112, 116].
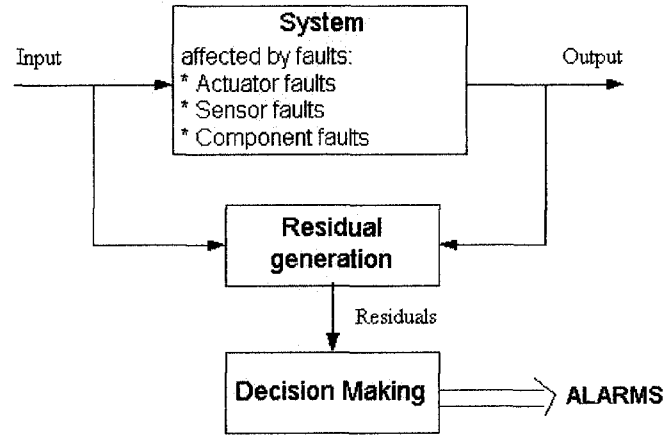
Figure 2.1: Structure of the Model-based FDI System.

Most of the work done in this field is focused on the residual generation problem because the decision making based on well designed residuals is relatively easy [13, 116]. Several approaches appeared in the literature for the residual generation problem of linear systems. These are briefly described below [13], focusing on the applicability to the nonlinear case:

1. The observer-based approach: an observer is designed and the residual is constructed as a weighted difference between the measured and estimated output. This approach is very well developed for the linear case and standard techniques exist in the literature providing solutions to both the theoretical and practical aspects of the problem (see [31, 33, 35, 36, 116] for good surveys). Extension of the above results to nonlinear systems requires the design of a nonlinear observer. However, the nonlinear observer design is not yet mature due to the complexity of this problem [41].

2. Parity space techniques: these techniques are mainly applied to discrete time systems. Unlike the observer-based approach, the residual generator has no dynamics but uses instead a collection of measurements through a time window of appropriate size [13, 17, 31, 36, 49]. Again, almost all results employing this technique assume a linear model.

3. Factorization methods: this is a frequency domain approach. It has been shown that

all these factorization methods can be made equivalent to the observer-based methods except that the design is done in frequency domain [13, 27, 36]. These methods can not be applied to the nonlinear case.

4. Parameter estimation: this method uses system identification techniques assuming that faults are reflected in the system parameters. It is the input-output mathematical model of the system that is usually employed. It is possible to handle nonlinearities using identification techniques for nonlinear systems [13, 36, 64].

Many variations of these techniques also appeared in the literature; including extensions to stochastic systems, and robustness issues, etc. However, the basic building block of the residual generation invariably accommodates to one of the four techniques described above.

2.2 The Observer-based Approach

Motivated by the future extension to nonlinear systems, we will focus in this section on the observer-based approach trying to cover different aspects of the problem. Two steps are needed to get a valid residual using this approach: *modelling* and *design*. The former consists of choosing a model for the monitored system including the effect of faults to be considered. For example, a widely accepted model for the Linear Time-Invariant (LTI) case (considering the three types of faults shown in Figure 2.1) is the following state-space model [13, 36]:

$$\dot{x}(t) = Ax(t) + Bu(t) + Bf_a(t) + f_c(t), \qquad x \in \mathbb{R}^n, u \in \mathbb{R}^m \qquad (2.1)$$

$$y(t) = Cx(t) + Du(t) + Df_a(t) + f_s(t), \qquad y \in \mathbb{R}^p \qquad (2.2)$$

where $f_a(t) \in \mathbb{R}^m$, $f_c(t) \in \mathbb{R}^n$ and $f_s(t) \in \mathbb{R}^p$ are vectors representing actuators, components and sensors faults respectively. It is important to consider how a possible fault fits in a model and the importance of (2.1)-(2.2) is that this model can accommodate several types of faults for the LTI case.

Once a model has been determined, the next step consists of the synthesis of an output estimator as a part of the residual generation. For the LTI case, the simplest residual form is $r(t) = Q(y(t) - \hat{y}(t))$ where $\hat{y}$ is an output estimation using a *Luenberger* type observer and Q is an appropriate weighting. The observer structure is as follows:

$$\dot{\hat{x}}(t) = (A - LC)\hat{x}(t) + Bu(t) + Ly(t) - LDu(t) \qquad (2.3)$$

$$\hat{y}(t) = C\hat{x}(t) + Du(t) \qquad (2.4)$$

where L, the observer gain, is the design parameter responsible for achieving asymptotic convergence of the state estimates "$\hat{x}$" to the actual system states "x". As a result of the observer stability, the residual is guaranteed to converge to zero only if no fault affects the system. Other than the Luenberger observer, many other observer techniques are also available in literature such as: the Unknown Input Observer (UIO), Beard Fault Detection Filter (BFDF), the combined UIO and BFDF observer, and the eigenstructure assignment approach, etc [13, 36]. These methods will be briefly discussed later.

Regardless of the particular observer structure used in the residual generation, the FDI algorithm requires certain conditions to be met. These conditions are either related to the FDI application, such as *fault detectability, detection delay, fault isolability, fault identifiability*, etc; or they are related to the modelling assumptions such as the *Robustness issue*, the *Stochastic and Nonlinear problems*, etc. Some of these important concepts are briefly discussed below [13] (the Nonlinear case is left to section 2.3 where it is discussed in more details):

- Fault detection: The technique must guarantee that the occurrence of every fault (in the considered fault vector) has a remarkable effect on the response of the residual. Missed alarms should be avoided. Besides, the detection delay (the time interval between the occurrence of a fault and its successful detection by the FDI algorithm) should be as small as possible.

- Fault isolation: To distinguish a particular fault, its effect on the residual should be not only remarkable, but also different in a certain way from the effect of other faults. Two approaches have been traditionally used to solve this problem:

  (i) Using *fixed directional residuals* (or residuals that lie in a fixed and fault-specified direction in the residual space). The Beard Fault Detection Filter (BFDF) [7] is one of the famous techniques that use this approach for the LTI case.

  (ii) Using *structured residual sets*, or a bank of residual generators where each residual is designed to be sensitive to a subset of faults, whilst remaining insensitive to the remaining faults [45].

- Fault identification: This is defined as the objective of estimating the size as well as the type and nature of the fault. Whilst undoubtedly helpful, it may not be as essential as detection and isolation if no reconfiguration action is involved.

- The stochastic case: In the case of random noise, the residual generator has to be designed to suppress the effect of noise on residuals. A common approach is the use of

Kalman-filter based residual generators which, although having a similar structure to the observer, are based on a stochastic model of the dynamic system (instead of a deterministic one). In normal operation, the Kalman filter residual vector is a zero-mean white noise process with known covariance matrix, and the use of different statistical tests to detect faults in the system was first proposed in [78]. Since then, many variants of the idea of hypothesis testing for FDI have been published [5, 116, 124]. As each fault has its own signature, a set of hypotheses can be used and checked for the likelihood that a particular fault has occurred, and the idea common to all these approaches is to test, amongst all possible hypotheses, that the system has a fault or is fault-free.

- Robustness: The observer used for FDI should be robust to system uncertainties (disturbances, modelling errors, discretization errors, etc) to avoid missed and false alarms. This is more important for the detection of incipient faults than for hard and abrupt faults, since incipient faults have a small effect on the residuals and can be hidden as a consequence of uncertainty. However, unlike the use of observers in output feedback applications, it is only the output estimation error that has to be robust to these uncertainties in FDI. Techniques available in the literature range from total cancellation of the uncertainty effect (Unknown Input Observers (UIO) [14] and Nonlinear UIO (NUIO) [117] are examples of disturbance decoupling techniques for linear and nonlinear cases respectively) to the minimization of its effect using optimization techniques (multiobjective, frequency domain and H_∞ optimization techniques are some examples) [13]. However, a tradeoff between cancelling (or minimizing) the uncertainty effect and maintaining fault detectability is a main concern. Robustness is very important for the nonlinear case especially when using the discretized model (which is always an approximation of the actual discrete model unlike the LTI case). It is also very important when using linearization, considering the linearization error as an uncertainty affecting an LTI model. When residuals can not be made robust against system uncertainty, another approach has been used to achieve robustness at the decision making stage by using Adaptive Thresholds. This was studied extensively by Ding et. al [24, 25, 26] and some application examples were reported in [11, 58].

2.3   The Nonlinear Observer-based Approach

The most important part of the nonlinear observer-based FDI is the design of a nonlinear observer. In this section, we first focus on this part of the problem (which is the design of an observer that estimates the full state of a nonlinear system), then we discuss the application of this observer in FDI.

2.3.1   Nonlinear Observer Synthesis

Unlike the LTI case, nonlinear observer design is still an open area of research. Contributions to this field are scattered and range from continuous-time to discrete-time systems, from ordinary to partial differential equations and from special applications (mechanical, electrical, chemical, etc.) to general nonlinear system models [83]. A general class of nonlinear continuous systems can be represented as follows

$$\dot{x} = g(x, u), \qquad\qquad x \in \mathbb{R}^n, u \in \mathbb{R}^m \qquad (2.5)$$

$$y = h(x, u), \qquad\qquad y \in \mathbb{R}^p \qquad (2.6)$$

Before designing an observer, the observability of (2.5)-(2.6) needs to be considered and this problem has been widely investigated. The definition of observability is the same for both linear and nonlinear systems:

Definition 2.1 *[83] (Observability): Observability is the property that for any pair of different initial conditions (x_0^1, x_0^2), there exists an input u such that this pair is distinguishable from the output.*

Despite the similar definition, the conditions for observability are totally different in linear and nonlinear systems. For the linear case, the well known *observability rank condition* $\left(\mathrm{rank} \left[C^T \quad (CA)^T \quad ... \quad (CA^{n-1})^T \right] = n \right)$ is necessary and sufficient for global observability and does not depend on the input u. On the other hand, the nonlinear case *lacks a similar condition, may be only locally observable* and *may have singular inputs*. The concept of singular inputs is a special characteristic of nonlinear systems and can be clarified by the following example [83]

$$\dot{x}_1 = ux_2 \qquad (2.7)$$

$$\dot{x}_2 = -x_2 \qquad (2.8)$$

$$y = x_1 \qquad (2.9)$$

which is observable according to the previous definition and yet $u \equiv 0$ is called a singular input since it makes the pairs (x_0^1, x_0^2) having the same x_1 indistinguishable from the output. Therefore, a stronger definition of observability (referred to as uniform observability) is widely accepted for nonlinear systems.

Definition 2.2 *[83] (Uniform observability): A system is uniformly observable if it has no singular inputs.*

It is important to note that both observability and uniform observability are equivalent in the linear case.

In view of the above definitions, testing the observability of nonlinear systems is much more involved than that in a linear case. The *observability rank condition* is the most widely known **sufficient** condition for a local version of observability [74, 75]. For single output systems it states that the observation space $q(x) = \begin{bmatrix} h; & L_g h; & \ldots; & L_g^{n-1} h \end{bmatrix}$ has a full rank codistribution at the origin, i.e,

$$\text{rank}\left(\begin{bmatrix} \nabla h(0); & \nabla L_g h(0); & \ldots; & \nabla L_g^{n-1} h(0) \end{bmatrix}\right) = n$$

where ∇ and L_g are the gradient and Lie derivative operators respectively. A weaker sufficient condition, yet more difficult to test, is that $q(x)$ constitutes an injective (one to one) map in a local region [119]. Many variations of these results also exist in the literature.

Another problem with a nonlinear observer is that even with observability satisfied, there is no universal technique available to design the observer. Linearization could be helpful, however, it only guarantees local convergence and is not the best choice if the dynamic system has multiple operating points. Therefore, a nonlinear observer is required in order to achieve a better performance. Several methods have been employed and we can briefly classify them into the following groups:

- Geometric techniques [9, 43, 59, 63, 66, 67, 73, 74, 107]: They all share the idea of providing conditions under which a nonlinear system may be transformed into an observer canonical form by means of coordinate transformations. They are the only techniques that make explicit use of the sufficient conditions on observability discussed earlier. The observability condition is always one of the necessary conditions for the existence of the transformation described above. This approach is very elegant since it guarantees exact linearization of the observer error dynamics, however, the existence conditions are very restrictive and various modifications have been employed.

- Linearization techniques [23, 83, 96]: In addition to the well known technique of operating point linearization, another widely used approach is the linearization around state estimate trajectories and the design of an observer for the resulting Linear Time-Varying (LTV) system. For both techniques, neglecting higher order terms is the main concern and among solutions to this problem is the use of the nonlinear identity approach [55], the extended Kalman filter, etc. An important drawback of these approaches is the local convergence.

- Lyapunov-like techniques: The earliest and most famous among them is the one developed for the special class of Lipschitz nonlinear systems of the form $(\dot{x} = Ax + \Phi(x,u);\ y = Cx)$, under a Lipschitz restriction for the function Φ. The techniques in [92, 93, 106, 121] make use of quadratic Lyapunov function for the observer error system and try to develop sufficient conditions and methods for design. The main drawback is the lack of necessary conditions for stability and of simplified methods for design.

- Algebraic techniques: These techniques make use of linear algebra to deal with special forms of nonlinearities as disturbances affecting a linear part whose effects have to be cancelled. The design of bilinear observers is a famous example where various techniques have been developed to deal with the class of nonlinear systems having the form $(\dot{x} = Ax + \sum_{i=1}^{m} u_i A_i x\ ;\ y = Cx)$ (see for example [62]). However, conditions are very restrictive and better design techniques are still required.

- Adaptive techniques [41, 83, 111]: Adaptive observers have been considered for robustness against unknown parameters. They combine the state estimation and the parameter estimation approaches. Special forms are usually considered and the main hindrance is to find a suitable parameter update law.

- Numerical techniques [50, 84]: These can be classified as techniques that either use numerical differentiation when input and output derivatives are needed, or that formulate the estimation problem as a nonlinear algebraic system of equations which must be solved periodically (using for example Newton's method or formulating it as an optimization problem over some finite horizon). Local results are always expected.

As a conclusion, the nonlinear observer design is a challenging problem and an active area of research. The available techniques usually deal with special cases of the general form

in (2.5)-(2.6), or give restrictive conditions that guarantee its transformation into a simpler form, or develop assumptions that only guarantee local convergence. The need of better design techniques still attracts researchers worldwide to work in this field.

2.3.2 Application of Nonlinear Observers in Fault Diagnosis

Before discussing the application of a nonlinear observer in FDI particularly, it is important to mention the different applications of a nonlinear observer in general. This helps to compare their implications on the observer design problem discussed in section 2.3.1. We will categorize four different applications of observers, either linear or nonlinear; namely: **output feedback control, system monitoring, process identification, and FDI.** For the first two, a complete knowledge of the model is implicitly assumed and the observer is needed to estimate the states that can not be measured. A reduced order observer that only estimates the unmeasured states may be acceptable. On the other hand, the last two applications are considered as model validation ones where the model is not trusted either due to uncertain parameters to be identified or due to faults affecting the system. The observer, in this case, is needed to estimate the output in order to compare it with the actual measurements.

It is now clear that the application of a nonlinear observer is an important factor that affects the design requirements and hence the design problem. Moreover, nonlinearity is an important factor that needs to be considered in practice since it may cause the loss of some desired properties that hold for the linear case. For example, in output feedback control applications, the well known separation principle is not satisfied for nonlinear systems. Nonlinearity is also expected to affect many aspects of the FDI problem. In the following discussion, we focus on these aspects such as fault detection, fault isolation and robustness.

Compared to the LTI system model with faults in (2.1)-(2.2), the general nonlinear faulty system model is shown below

$$\dot{x} = g(x,\ u,\ f,\ d), \qquad\qquad x \in \mathbb{R}^n, u \in \mathbb{R}^m \qquad (2.10)$$

$$y = h(x,\ u,\ f,\ d), \qquad\qquad y \in \mathbb{R}^p \qquad (2.11)$$

where $f(t) \in \mathbb{R}^s$, $d(t) \in \mathbb{R}^q$ are vectors representing faults (actuators, components and sensors) and uncertainties respectively. During the research of the last two decades on nonlinear observers in FDI, important results have been achieved for special cases of interest of the general form (2.10)-(2.11). In the following, we will briefly discuss some of these results focusing on the open problems that motivate our research:

- The Nonlinear Identity approach: This was the first reported work in nonlinear observer-based FDI and was carried by Hengy and Frank in 1986 [55]. They suggested the use of the nonlinear identity observer (understood as one that uses linearization around estimated state trajectories) for fault detection of the general class in (2.10)-(2.11). It was reconsidered in [2] for sensor fault isolation using structured residual sets. However, only local convergence was achieved.

- Geometric techniques: For the class of systems (2.12)-(2.13):

$$\dot{x} = g_o(x) + \sum_{i=1}^{m} g_i(x)u_i + e_1(x)f_1 + e_2(x)f_2 \tag{2.12}$$

$$y = h(x) \tag{2.13}$$

geometric techniques combined with high gain observers have been used for fault detection and isolation when only two faults (modelled by f_1 and f_2 respectively) are considered [54]. The same techniques have also been used [53] for the class of *state affine to output injection*, i.e systems modeled as:

$$\dot{x} = A(u)\ x + \psi(y, u) + e_1(x)f_1 + e_2(x)f_2 \tag{2.14}$$

$$y = C\ x \tag{2.15}$$

The robustness issue have been considered in [101] for the more general class (2.16)-(2.17):

$$\dot{x} = g(x,\ u) + E(x)\ d + K(x,\ u)\ f \tag{2.16}$$

$$y = h(x) \tag{2.17}$$

where, under some restrictive assumptions, a transformation $z = T(x)$ can be found to cancel the effect of the uncertainty term "$E(x)\ d$" and hence robust fault detection is guaranteed. Fault isolation has also been considered when the fault term in (2.16) is not a function of the input and has the form "$K(x)\ f$".

- The adaptive approach: Adaptive observers are more efficient than other robust observers in detecting incipient faults. A non adaptive technique which is robust to model uncertainties would normally have low sensitivity to incipient faults [109]. To overcome this difficulty, adaptive observers are used to estimate the states and the unknown parameters simultaneously. A good example is the work in [25] where the class of systems

(2.18)-(2.19) was considered:

$$\dot{x} = A\ x + g_1(y, u) + g_2(y, u)\theta + g_3(x, u)f \tag{2.18}$$

$$y = C\ x \tag{2.19}$$

An adaptive observer was designed to estimate both the states "x" and the unknown parameter vector "θ". This observer was further used for fault detection. Adaptive observers were also used as a way for fault identification in [68] for the class of nonlinear systems in (2.20)-(2.21):

$$\dot{x} = g_o(x) + \sum_{i=1}^{m} g_i(x)\ u_i + \sum_{i=1}^{s} e_i(x)\ f_i \tag{2.20}$$

$$y = h(x) \tag{2.21}$$

where geometrical conditions guaranteeing input observability were combined with adaptive update laws to estimate the fault inputs f_i (considered here as unknown parameters).

• Bilinear systems: The study of bilinear systems is important since many physical systems (nuclear reactors, suspension systems, fermentation processes, hydraulic drives, heat exchange systems, etc.) can be modelled by bilinear equations. Therefore, much work has been done on FDI for this class of systems focusing on practical applications. For example, the fault isolation was considered in [52] for (2.22)-(2.23) where only two faults were considered:

$$\dot{x} = A_0\ x + B\ u + \sum_{i=1}^{m} u_i\ A_i\ x + \sum_{i=1}^{2}(E_i\ x + F_i)\ f_i \tag{2.22}$$

$$y = C\ x \tag{2.23}$$

while *robust* fault (actuator and sensor) detection was considered in [120] for (2.24)-(2.25):

$$\dot{x} = A_0\ x + B\ u + \sum_{i=1}^{m} u_i\ A_i\ x + E\ d + G\ f_a \tag{2.24}$$

$$y = C\ x + Q\ f_s \tag{2.25}$$

Constructive necessary and sufficient conditions for observer design of (2.24)-(2.25) were given in [62]. However, they are very restrictive and have not been used for fault isolation.

- Lipschitz systems: We conclude this section by Lipschitz systems, since this class of nonlinear systems will be the main focus of this thesis. Tremendous work has been done for the observer design of Lipschitz systems, or nonlinear systems of the form $(\dot{x} = Ax + \Phi(x, u))$ with a linear read-out equation for the output $(y = Cx)$ and with a Lipschitz condition on the function Φ (A full discussion of the importance of Lipschitz systems and of the observer synthesis problem is left to Chapter 3, where some new results are proposed). However, not much work has been reported concerning their applications in FDI. The most important work reported to date is the one related to the faulty case in (2.26)-(2.27):

$$\dot{x} = A\ x + B\ u + \Phi(x, u) + \sum_{i=1}^{s} F_i\ \Phi_i(x, u)\ f_i \tag{2.26}$$

$$y = C\ x \tag{2.27}$$

where Φ is a Lipschitz function and f_i represents the ith fault with mode F_i and all failure modes are assumed independent in the output space. The design has been considered in [41, 42] where under an assumption of some algebraic conditions as well as the solvability of the Riccati equation needed for the observer design, an observer that guarantees the fault detection and isolation (through directionality of residuals) can be found. An important drawback of this method is that the robustness issue was not considered. Open problems also include the sensor fault diagnosis, the relaxation of the existing design conditions, and the study of the discretization issue resulting from the practical sampled-data implementation.

As a conclusion, the observer-based FDI problem for many nonlinear systems is still open for research. The approaches reviewed solve the problem partially and many questions still remain unanswered. In this thesis, we will focus on the class of Lipschitz systems. A new observer design will be introduced in Chapter 3, while its application in the sensor FDI problem will be the focus of Chapter 4. New results for robustness against additive uncertainties will be introduced in Chapter 5, while Chapter 6 will focus on the application of these results in the robotics field. Some reflections on the sampled-data problem will be presented in Chapter 7.

2.4 Notation

Throughout the thesis, we will use lower-case letters for scalars, vectors and functions, and capital letters for matrices, systems and operators. We will also make use of the following definitions and notation:

Definition 2.3 *($\mathcal{L}_2$ space): The space $\mathcal{L}_2$ consists of all Lebesgue measurable functions u :* $\mathbb{R}^+ \to \mathbb{R}^q$, *having a finite $\mathcal{L}_2$ norm $\|u\|_{\mathcal{L}_2}$, where $\|u\|_{\mathcal{L}_2} \triangleq \sqrt{\int_0^\infty \| u(t) \|^2 \, dt}$, with $\|u(t)\|$ as the Euclidean norm of the vector $u(t)$.*

Definition 2.4 *(Eigenvalues and Singular values): Let A, a square $n \times n$ matrix, then the eigenvalues of A are the n roots of its characteristic polynomial $p(\lambda) = det(\lambda I - A)$. This set of roots is called the spectrum of A and is denoted by $\lambda(A)$. The set of singular values of a $n \times m$ matrix R, $\sigma(R)$, is equal to $\sqrt{\lambda(R^T R)}$.*

For a system $H : \mathcal{L}_2 \to \mathcal{L}_2$, we will represent by $\gamma(H)$ the $\mathcal{L}_2$ gain of H defined by $\gamma(H) = \sup_u \frac{\|Hu\|_{\mathcal{L}_2}}{\|u\|_{\mathcal{L}_2}}$. It is well known that, for a linear system $H : \mathcal{L}_2 \to \mathcal{L}_2$ (with a transfer matrix $\hat{H}(s)$), $\gamma(H)$ is equivalent to the H-infinity norm of $\hat{H}(s)$ defined as follows:

$$\gamma(H) \equiv \| \hat{H}(s) \|_\infty \triangleq \sup_{\omega \in \mathbb{R}} \sigma_{\max}(\hat{H}(j\omega))$$

where $\sigma_{\max}$ represents the maximum singular value of $\hat{H}(j\omega)$. The matrices I_n, 0_n and 0_{nm} represent the identity matrix of order n, the zero square matrix of order n and the zero n by m matrix respectively. $Diag_r(a)$ represents the diagonal square matrix of order r with $\begin{bmatrix} a & a & \cdots & a \end{bmatrix}_{1 \times r}$ as its diagonal vector, while $Diag(a_1, a_2, \cdots, a_r)$ represents the diagonal square matrix of order r with $\begin{bmatrix} a_1 & a_2 & \cdots & a_r \end{bmatrix}$ as its diagonal vector. The symbol $\hat{T}_{yu}$ represents the transfer matrix from input u to output y. The symbol RH_∞ denotes the space of all proper and real rational stable transfer matrices. The partitioned matrix $H = \begin{bmatrix} A & B \\ \hline C & D \end{bmatrix}$ (when used as an operator from u to y, i.e, $y = Hu$) represents the state space representation ($\dot{\xi} = A\xi + Bu$, $y = C\xi + Du$), and in that case the transfer matrix of the system is $\hat{H}(s) = C(sI - A)^{-1}B + D$. We will also make use of the following property on the rank of $\hat{H}(s)$ [122]:

$$\text{rank} \begin{bmatrix} A - sI & B \\ C & D \end{bmatrix} = n + \text{rank} \left(\hat{H}(s) \right) \tag{2.28}$$
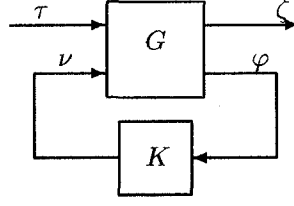
Figure 2.2: Standard Setup.

if s is not an eigenvalue of A and where n is the dimension of the matrix A. The standard setup in Figure 2.2 will also be used throughout the thesis along with the state space representation for the plant G of the form:

$$\hat{G}(s) = \left[\begin{array}{c|cc} A & B_1 & B_2 \\ \hline C_1 & D_{11} & D_{12} \\ C_2 & D_{21} & D_{22} \end{array}\right] \tag{2.29}$$

The following result on the H_∞ norm of $\hat{T}_{\zeta\tau}$ is useful in this case:

Theorem 2.1 [40] *For the generalized plant in (2.29), assume stabilizability and detectability of (A, B_2, C_2) and that $D_{22} = 0$, and let $\mathcal{N}_{12}$ and $\mathcal{N}_{21}$ denote orthonormal bases of the null spaces of (B_2^T, D_{12}^T) and (C_2, D_{21}) respectively. There exists a controller K such that $\|\hat{T}_{\zeta\tau}\|_\infty < \gamma$ if and only if there exist two symmetric matrices $R, S \in \mathbb{R}^{n \times n}$ satisfying the following system of Linear Matrix Inequalities (LMIs):*

$$\left[\begin{array}{c|c} \mathcal{N}_{12} & 0 \\ \hline 0 & I \end{array}\right]^T \left[\begin{array}{cc|c} AR + RA^T & RC_1^T & B_1 \\ C_1 R & -\gamma I & D_{11} \\ \hline B_1^T & D_{11}^T & -\gamma I \end{array}\right] \left[\begin{array}{c|c} \mathcal{N}_{12} & 0 \\ \hline 0 & I \end{array}\right] < 0 \tag{2.30}$$

$$\left[\begin{array}{c|c} \mathcal{N}_{21} & 0 \\ \hline 0 & I \end{array}\right]^T \left[\begin{array}{cc|c} A^T S + SA & SB_1 & C_1^T \\ B_1^T S & -\gamma I & D_{11}^T \\ \hline C_1 & D_{11} & -\gamma I \end{array}\right] \left[\begin{array}{c|c} \mathcal{N}_{21} & 0 \\ \hline 0 & I \end{array}\right] < 0 \tag{2.31}$$

$$\left[\begin{array}{cc} R & I \\ I & S \end{array}\right] \geq 0 \tag{2.32}$$

The existence of an analytical solution to this problem is also considered, when the generalized plant in (2.29) satisfies the following conditions:

(1) (A, B_1) is controllable and (C_1, A) is observable.

(2) (A, B_2) is stabilizable, and (C_2, A) is detectable.

(3) $D_{12}^T \begin{bmatrix} C_1 & D_{12} \end{bmatrix} = \begin{bmatrix} 0 & I \end{bmatrix}$.

(4) $\begin{bmatrix} B_1 \\ D_{21} \end{bmatrix} D_{21}^T = \begin{bmatrix} 0 \\ I \end{bmatrix}$.

(5) $D_{11} = 0$ and $D_{22} = 0$.

In this case, the problem is called "*Simplified H_∞ problem*" [122]. This case is of interest since the solvability conditions are easy to check (compared with the LMI conditions in Theorem 2.1). Also, the solution can be obtained by solving standard Algebraic Riccati Equations, for which vast literature and software packages can be used. We will elaborate more on this issue in our discussion of Lipschitz observers in Chapter 3.

We will also develop results related to the so-called "Linear Unknown Input Observer (UIO)" problem, which is the state estimation problem for the following system:

$$\dot{x}(t) = Ax(t) + Bu(t) + Ed(t), \qquad A \in \mathbb{R}^{n \times n}, B \in \mathbb{R}^{n \times m}, E \in \mathbb{R}^{n \times r} \qquad (2.33)$$

$$y(t) = Cx(t), \qquad C \in \mathbb{R}^{p \times n} \qquad (2.34)$$

where $A \in \mathbb{R}^{n \times n}, B \in \mathbb{R}^{n \times m}, E \in \mathbb{R}^{n \times r}$ and $C \in \mathbb{R}^{p \times n}$. The matrix E is referred to as the *unknown input distribution matrix* and is assumed to be a known full column rank matrix (with $r \leq p$). In all the literature available for this problem, the observer proposed fall in the class of Luenberger-like observers, namely:

$$\dot{z}(t) = Fz(t) + Ly(t) + TBu(t) \qquad (2.35)$$

$$\hat{x}(t) = z(t) + Hy(t) \qquad (2.36)$$

where $F \in \mathbb{R}^{n \times n}, L \in \mathbb{R}^{n \times p}, T \in \mathbb{R}^{n \times n}$ and $H \in \mathbb{R}^{n \times p}$, and the objective is to get state estimates $\hat{x}$ that converge to the actual states x, and are totally decoupled from the uncertainty term $d(t)$. The following definition of a UIO is taken from [14].

Theorem 2.2 *The observer in (2.35)-(2.36) is said to be an Unknown Input Observer (UIO) for the system in (2.33)-(2.34) if the following matrix equations are satisfied:*

$$HCE = E \tag{2.37}$$

$$T = I - HC \tag{2.38}$$

$$F = A - HCA - L_1 C; \qquad \text{with } F \text{ stable} \tag{2.39}$$

$$L_2 = FH \tag{2.40}$$

$$L = L_1 + L_2 \tag{2.41}$$

The necessary and sufficient conditions for the existence of a UIO were developed in [14] as follows:

Theorem 2.3 *Necessary and sufficient conditions for (2.35)-(2.36) to be a UIO for the system (2.33)-(2.34) according to Theorem 2.2 are:*

(i) rank (CE) = rank(E).

(ii) $(\bar{A}, C)$ is detectable , where $\bar{A} = A - E\left[(CE)^T CE\right]^{-1}(CE)^T CA.$

Chapter 3

The Lipschitz Observer Design

Problem

In this chapter, we study the observer synthesis problem for a class of nonlinear systems known as Lipschitz systems. We introduce a new dynamic framework which is more general than classical Lipschitz observers and which also ensures asymptotic convergence of the state estimates. Moreover, the proposed sufficient condition for observer stability is shown to be equivalent to an H_∞ optimal control problem that satisfies the standard regularity assumptions in H_∞ optimization theory, laying the ground to a design procedure which is less restrictive than the existing ones. Finally, a simulation example is given to illustrate the observer design[1].

3.1 Background Results

As discussed in section 2.3, nonlinear state observer design has been an area of constant research for the last three decades and, despite important progress, many outstanding problems still remain unsolved. A class of nonlinear systems that has seen much attention in the literature about nonlinear observers, and for which many Lyapunov-like design techniques

---

[1]The results in this chapter have been published in the article: "A.M. Pertew, H.J. Marquez and Q. Zhao, H_∞ Observer Design for Lipschitz Nonlinear Systems," IEEE transactions on Automatic Control, Vol. 51, No. 7, pp. 1211-1216, July 2006.

have been proposed is the class of *Lipschitz* nonlinear systems of the form:

$$\dot{x}(t) = Ax(t) + \Gamma(u,t) + \Phi(x,u,t) \tag{3.1}$$

$$y(t) = Cx(t), \ A \in \mathbb{R}^{n \times n}, \ C \in \mathbb{R}^{p \times n} \tag{3.2}$$

and where the function $\Phi(x,u,t)$ satisfies a uniform Lipschitz condition globally in x, i.e,

$$\| \Phi(x_1,u,t) - \Phi(x_2,u,t) \| \leq \alpha \| x_1 - x_2 \| \tag{3.3}$$

$\forall u \in \mathbb{R}^m$, $t \in \mathbb{R}$ and $\forall x_1$, $x_2 \in \mathbb{R}^n$. Here $\alpha \in \mathbb{R}^+$ is referred to as the *Lipschitz constant* and is independent of x, u and t. Lipschitz systems constitute a very important class. Any nonlinear system $\dot{x} = g(x,u)$ can be expressed in the form of (3.1), at least locally, if $g(x,u)$ is continuously differentiable with respect to x. Many nonlinearities are locally Lipschitz. Examples include trigonometric nonlinearities occurring in robotics, nonlinearities which are square or cubic in nature, etc. The function Φ can also be considered as a perturbation affecting the system [100].

Observer design for Lipschitz systems was first considered by Thau in his seminal paper, [106], where he obtained a sufficient condition to ensure the asymptotic stability of the observer. Thau's condition is a very useful *analysis tool* but does not address the fundamental *design* problem. Encouraged by Thau's result, several authors studied the observer design problem for Lipschitz systems. In [121], Zak considered the use of Lyapunov functions and the Bellman-Gronwall lemma for this design problem, with application in feedback stabilization. In [91, 92], Raghavan formulated an iterative procedure to tackle this design problem based on solving an algebraic Riccati equation. Raghavan's technique was later extended by Garg and Hedrick, [42], to study fault detection in Lipschitz systems. Unfortunately, Raghavan's algorithm often fails to succeed even when the matrices (A, C) satisfy the usual observability assumptions. Moreover, it does not provide insight into what conditions must be satisfied by the observer gain to ensure stability. A rather complete solution of these problems was presented by Rajamani in [94, 93]. Rajamani obtained a sufficient condition which is directly related to the observer matrix and that ensures asymptotic stability of the observer. He formulated a design procedure based on the use of a gradient based optimization method. Rajamani also discussed the equivalence between the stability condition and the minimization of the H_∞ norm of a system in the standard form. However, he pointed out that the design is not solvable as a standard H_∞ optimization problem since the regularity assumptions required in the H_∞ framework are not satisfied.

In this chapter, we show that the condition in [93] is related to a modified H_∞ problem satisfying all of the regularity assumptions. Based on this result, we propose a new observer design for Lipschitz nonlinear systems. The observer synthesis is carried out using H_∞ optimization and can therefore be done using commercially available software packages. It is also less restrictive than the existing design techniques since it is directly related to the stability condition. Our formulation employs the input-output observer framework introduced in [76, 77] in which the static gain used in the classical observers is replaced with a dynamical filter.

In the remaining of this section we summarize some preliminary results on observer design for systems of the form (3.1)-(3.3) and where the pair (A, C) is detectable (see [122] for mathematical definition of "detectability"). The detectability condition ensures the existence of an observer for the linear part. This observer only guarantees local convergence when the nonlinear terms in Φ are considered, but it alleviates the need to test the observability condition discussed in Chapter 2 for this class of nonlinear systems.

In all the literature available for this class of nonlinear systems, the observer proposed falls in the class of *Luenberger-like* observers, namely:

$$\dot{\hat{x}} = A\hat{x} + \Gamma(u, t) + \Phi(\hat{x}, u, t) + L(y - \hat{y}), \quad L \in \mathbb{R}^{n \times p} \tag{3.4}$$

$$\hat{y} = C\hat{x} \tag{3.5}$$

The observer error dynamics is then given by

$$\dot{e} = (A - LC)\, e + \Phi(x, u, t) - \Phi(\hat{x}, u, t) \tag{3.6}$$

where $e = x - \hat{x}$. Thau was the first to introduce a sufficient condition for the asymptotic stability of the error in (3.6). His result was as follows:

Theorem 3.1 *[106] If the gain L is chosen s.t $\alpha < \frac{\lambda_{min}(Q)}{2\,\lambda_{max}(P)}$ with the Lyapunov equation $(A - LC)^T P + P(A - LC) = -Q$, then the estimation error in (3.6) is asymptotically stable.*

Theorem 3.1 provides a very important sufficient condition for the existence of an observer, but does not consider the design problem. Raghavan proposed a design algorithm based on the following theorem:

Theorem 3.2 *[92] If there exists an $\varepsilon > 0$ such that the Algebraic Riccati Equation (ARE) in (3.7) has a symmetric positive definite solution P, then the observer gain $L = \frac{1}{2\varepsilon} PC^T$*

stabilizes the error dynamics in (3.6) for all Φ with a Lipschitz constant α.

$$AP + PA^T + P(\alpha^2 I - \frac{1}{\varepsilon}C^T C)P + I + \varepsilon I = 0 \tag{3.7}$$

Based on this result, Raghavan proposed an iterative binary search procedure over ε, to obtain the observer gain. However, given a particular system of the form (3.1)-(3.3) with a specific Lipschitz constant α^*, this procedure may fail even if the pair of matrices (A, C) is observable. Moreover, Theorem 3.2 provides no insight into what conditions the matrix $(A - LC)$ must satisfy to ensure the observer's error stability. The answer to this puzzle was provided by Rajamani in the following theorem:

Theorem 3.3 *[93] The observer gain L stabilizes the error dynamics in (3.6) for all Φ with a Lipschitz constant α if L is chosen so as to ensure that $(A - LC)$ is stable and such that*

$$min_{\omega \in \mathbb{R}^+} \ \sigma_{min}(A - LC - j\omega I) > \alpha \tag{3.8}$$

Compared with Theorem 3.1, the beauty of this result is that it presents the condition for observer stability as a condition on the *observer matrix* itself. Besides, from the design perspective, it can be related to the H_∞ theory by rewriting (3.8) as [93]:

$$\| \ [sI - (A - LC)]^{-1} \ \|_\infty < \frac{1}{\alpha} \tag{3.9}$$

where the left hand side of (3.9) is equivalent to the H_∞ norm of the transfer function between τ and ζ in the following so-called standard form:

$$\dot{z} = \begin{bmatrix} A \end{bmatrix} z + \begin{bmatrix} I_n & -I_n \end{bmatrix} \begin{bmatrix} \tau \\ \nu \end{bmatrix} \tag{3.10}$$

$$\begin{bmatrix} \zeta \\ \varphi \end{bmatrix} = \begin{bmatrix} I_n \\ C \end{bmatrix} z + \begin{bmatrix} 0_n & 0_n \\ 0_{pn} & 0_{pn} \end{bmatrix} \begin{bmatrix} \tau \\ \nu \end{bmatrix} \tag{3.11}$$

where:

$$\tau = \tilde{\phi} = \Phi(x, u, t) - \Phi(\hat{x}, u, t), \ \zeta = e = x - \hat{x}, \ \nu = L\ (y - \hat{y}), \ \text{and} \ \varphi = y - \hat{y} \tag{3.12}$$

This can also be represented by *the standard setup figure* (i.e, Figure 2.2) where the plant G has the state space representation in (3.13) with the matrices in (3.10)-(3.11) and where the controller K is the static observer gain L.

$$\hat{G}(s) = \left[\begin{array}{c|cc} A & B_1 & B_2 \\ \hline C_1 & D_{11} & D_{12} \\ C_2 & D_{21} & D_{22} \end{array} \right] \tag{3.13}$$

Therefore, focusing on the design problem, several design approaches have been proposed to satisfy the stability condition in (3.8). In [93], Rajamani considered the use of a gradient based optimization method to continuously change the locations of the closed loop eigenvalues to minimize a performance index related to (3.8). The special case of A being Hurwitz has also been considered in [1, 95] introducing an analytical solution when a certain sufficient condition on the so called "*distance to unobservability*" of the pair (A, C) is satisfied. It can also be seen that the condition in Theorem 3.2 is a special form of (3.8). Moreover, the result in [93] has been used to design reduced-order observers in [123]. However, all these design approaches are restrictive in the sense that they only provide sufficient conditions to satisfy (3.8). Moreover, they only consider the use of the Luenberger structure in (3.4)-(3.5) and, hence, put another restriction on the observer gain order which may prevent the existence of a solution to the H_∞ problem in (3.9).

In this chapter, we focus on the design problem associated with the stability condition in (3.8). We first extend this condition to a more general dynamic framework making use of the input-output observer framework introduced in [76] where an observer gain is seen as a filter designed so that the error dynamics has some desirable frequency domain characteristics. We then prove that the new condition is equivalent to a standard H_∞ problem satisfying all the regularity assumptions (unlike (3.10)-(3.11)). Based on these results, we present a systematic design procedure (which is less restrictive than the existing design approaches) to compute the observer gain within the H_∞ framework. We also present a parameterization of all possible observer gains in this case. The same definitions and notation introduced in section 2.4 will be used throughout the chapter. We will also use the standard notation in the literature on H_∞ control [122], e.g. using $dom(Ric)$ to denote the domain that consists of all Hamiltonian matrices H with two properties, namely, H has no eigenvalues on the imaginary axis and the two related spectral subspaces are complementary. We will also use $Ric(H)$ to denote the unique solution to the Algebraic Riccati Equation (ARE) associated with H in this case.

3.2   Generalization to Dynamic Framework

In this section, following the approach in [76, 77], we present dynamical observers of the form:

$$\dot{\hat{x}}(t) = A\hat{x}(t) + \Gamma(u,t) + \Phi(\hat{x}, u, t) + \eta(t) \tag{3.14}$$

$$\hat{y}(t) = C\hat{x}(t) \tag{3.15}$$

where $\eta(t)$ is obtained by applying a dynamical compensator K of order k ("k" being arbitrary) on the output estimation error. In other words $\eta(t)$ is given from

$$\dot{\xi} = A_L\xi + B_L(y - \hat{y}), \quad A_L \in \mathbb{R}^{k \times k}, \quad B_L \in \mathbb{R}^{k \times p} \tag{3.16}$$

$$\eta = C_L\xi + D_L(y - \hat{y}), \quad C_L \in \mathbb{R}^{n \times k}, \quad D_L \in \mathbb{R}^{n \times p} \tag{3.17}$$

We will also write
$$K = \left[\begin{array}{c|c} A_L & B_L \\ \hline C_L & D_L \end{array} \right] \tag{3.18}$$

to represent the compensator in (3.16)-(3.17). It is straightforward to see that this observer structure reduces to the usual observer in (3.4)-(3.5) when $K = \left[\begin{array}{c|c} 0_k & 0_{kp} \\ \hline 0_{nk} & L \end{array} \right]$. The additional dynamics brings additional degrees of freedom in the design, something that will be exploited in the proposed H_∞ procedure. In this section, we generalize Theorem 3.3 to the dynamic framework as follows. First, note that the observer error dynamics in (3.6) is now given by

$$\dot{e} = A\,e + \Phi(x, u, t) - \Phi(\hat{x}, u, t) - \eta \tag{3.19}$$

which can also be represented by the standard setup in Figure 2.2 where G has the state space representation in (3.13) with the same matrices defined in (3.10)-(3.11) and with the same variables in (3.12) except for ν which is now given by

$$\nu = \eta = K(y - \hat{y}) \tag{3.20}$$

We denote by $\hat{T}_{\zeta\tau}$ the transfer function between τ and ζ for this setup. The following theorem is then the generalization of Theorem 3.3:

Theorem 3.4 *Given the Lipschitz system of equations (3.1)-(3.2), the state $\hat{x}$ of the observer (3.14)-(3.18) globally asymptotically converges to the system state x for all $\Phi(\cdot, \cdot, \cdot)$ satisfying (3.3) with a Lipschitz constant α if the dynamic observer gain K is chosen such that:*

$$sup_{\omega \in \mathbb{R}} \; \sigma_{max}[\hat{T}_{\zeta\tau}(j\omega)] < \frac{1}{\alpha} \tag{3.21}$$

Proof: Using the variable definitions in (3.12) along with ν in (3.20) and the matrices in (3.10), (3.11) and (3.18), $\hat{T}_{\zeta\tau}$ can be represented as:

$$\hat{T}_{\zeta\tau} = \hat{T}_{e\tilde{\phi}} = \left[\begin{array}{cc|c} A - D_L C & -C_L & I_n \\ B_L C & A_L & 0_{kn} \\ \hline I_n & 0_{nk} & 0_n \end{array} \right] \tag{3.22}$$

and is such that $\gamma(\hat{T}_{e\tilde{\phi}}) = \| \hat{T}_{e\tilde{\phi}} \|_\infty < \frac{1}{\alpha}$ according to (3.21). The proof follows from noting that the estimation error e is given from the feedback interconnection of $\hat{T}_{e\tilde{\phi}}$ and Δ as shown in Figure 3.1 where Δ is the static nonlinear time-varying operator defined as follows:

$$\Delta(t) : e \to \tilde{\phi} = \Phi(x, u, t) - \Phi(\hat{x}, u, t)$$

$$= \Phi(e + \hat{x}(t), u(t), t) - \Phi(\hat{x}(t), u(t), t)$$
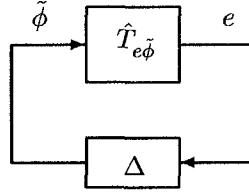
Figure 3.1: Feedback Interconnection.

In this loop, $\gamma(\hat{T}_{e\tilde{\phi}}) < \frac{1}{\alpha}$ as mentioned earlier and, although an exact expression for Δ is not available, we have $\gamma(\Delta) \le \alpha$ because from the Lipschitz condition in (3.3), it follows that:

$$\gamma(\Delta) = \sup_e \frac{\| \tilde{\phi} \|_{\mathcal{L}_2}}{\| e \|_{\mathcal{L}_2}} = \sup_e \frac{\sqrt{\int_0^\infty [\Phi(x, u, t) - \Phi(\hat{x}, u, t)]^T \, [\Phi(x, u, t) - \Phi(\hat{x}, u, t)] \, dt}}{\sqrt{\int_0^\infty [x - \hat{x}]^T \, [x - \hat{x}] \, dt}}$$

$$\le \frac{\sqrt{\int_0^\infty \alpha^2 \| x - \hat{x} \|^2 \, dt}}{\sqrt{\int_0^\infty \| x - \hat{x} \|^2 \, dt}} \le \alpha$$

Using the bounds on the $\mathcal{L}_2$ gains of the operators $\hat{T}_{e\tilde{\phi}}$ and Δ, we will make use of a dissipativity argument by noting that the following properties are satisfied for the feedback loop in Figure 3.1:

(a) Δ is a static nonlinearity (no internal states) and $\hat{T}_{e\tilde{\phi}}$ is the dynamic LTI system in (3.22).

(b) The mappings $\hat{T}_{e\tilde{\phi}} : \tilde{\phi} \to e$ and $\Delta : e \to \tilde{\phi}$ have finite $\mathcal{L}_2$ gains $\gamma(\hat{T}_{e\tilde{\phi}})$ and $\gamma(\Delta)$, and moreover they satisfy $\gamma(\hat{T}_{e\tilde{\phi}}).\gamma(\Delta) < 1$.

(c) $\hat{T}_{e\tilde{\phi}}$ and Δ are dissipative with the supply rates $\omega_1 = -e^T e + \gamma(\hat{T}_{e\tilde{\phi}})^2 \tilde{\phi}^T \tilde{\phi}$ and $\omega_2 = -\tilde{\phi}^T \tilde{\phi} + \alpha^2 e^T e$ respectively. We will denote by s_1 and s_2 the corresponding storage functions.

It is a direct application of Corollary 1 in [56] (see also [75], Chapter 9, for a comprehensive review of the subject) that $s_1 + as_2$, $a > 0$, is a Lyapunov function for this system, and that, since $\gamma(\hat{T}_{e\tilde{\phi}})\gamma(\Delta) < 1$, the system is asymptotically stable. This implies that $e \to 0$ as $t \to \infty$. $\qquad\qquad\square$

Corollary 3.1 *Under the conditions of Theorem 3.4, if condition (3.3) holds locally, then local asymptotic convergence of the observer is guaranteed (and in this case the observer (3.14)-(3.18) is a local one, i.e, it is local in "x" and in the estimation error "e").*

3.3 A new H_∞ Observer Design

In this section we present our main results by focusing on the design problem associated with the stability condition introduced in section 3.2. We first prove that the condition in (3.21) (and the one in (3.8) as a special case) is actually equivalent to a standard H_∞ problem satisfying all of the regularity assumptions. We then propose a systematic design procedure to compute the observer gain within the H_∞ framework. This design has the advantage of being directly related to the stability condition, and hence avoids much of the restrictions associated with the designs in [1, 92, 93, 95]. We finally present a parameterization of all possible observers in this case.

3.3.1 Problem Regularization

As mentioned earlier, the stability condition in (3.21) can be represented by the H_∞ norm of the setup in Figure 2.2 where G has the state space representation in (3.13) with the matrices defined in (3.10), (3.11). However, this H_∞ problem does not satisfy all the regularity assumptions in the H_∞ framework (notice that $D_{12}^T D_{12}$ and $D_{21} D_{21}^T$ are both singular). Although the LMI approach in [65], or the techniques in [99, 105] can be used to solve this singular problem, here we focus on the Riccati approach in [28] by showing that the problem is actually equivalent to the so-called "Simplified H_∞ problem" defined in [28, 122]. This helps to directly relate the stability condition to two Riccati equations (instead of the one in

(3.7)) and lays the ground to a systematic design procedure which is less restrictive than the existing design appoaches. This also has the advantage of classifying the set of all possible observer gains by using the standard parameterization of H_∞ controllers in [28, 122]. To this end, we adopt the following standard regularization procedure: By adding a "weighted" disturbance term in the output equation (3.2), now we tackle the problem of designing an observer for the system:

$$\dot{x}(t) = Ax(t) + \Gamma(u,t) + \Phi(x,u,t) \tag{3.23}$$

$$y(t) = Cx(t) + \epsilon\, d(t), \qquad \epsilon > 0 \tag{3.24}$$

where the function $\Phi(x,u,t)$ satisfies the Lipschitz condition. Using the same observer defined by (3.14)-(3.18), it can be seen that the standard form in (3.10)-(3.11) has now the following form:

$$\dot{z} = \begin{bmatrix} A \end{bmatrix} z + \begin{bmatrix} \begin{bmatrix} I_n & 0_{np} \end{bmatrix} & -I_n \end{bmatrix} \begin{bmatrix} \begin{bmatrix} \tau \\ d(t) \\ \nu \end{bmatrix} \end{bmatrix} \tag{3.25}$$

$$\begin{bmatrix} \zeta \\ \varphi \end{bmatrix} = \begin{bmatrix} I_n \\ C \end{bmatrix} z + \begin{bmatrix} \begin{bmatrix} 0_n & 0_{np} \\ 0_{pn} & \epsilon I_p \end{bmatrix} & \begin{matrix} 0_n \\ 0_{pn} \end{matrix} \end{bmatrix} \begin{bmatrix} \begin{bmatrix} \tau \\ d(t) \\ \nu \end{bmatrix} \end{bmatrix} \tag{3.26}$$

This can also be represented by the standard setup in Figure 2.2, except for redefining the matrices of $\hat{G}(s)$ in (3.13) and replacing τ by $\bar{\tau}$ defined as: $\bar{\tau} \overset{\Delta}{=} \begin{bmatrix} \tau & d(t) \end{bmatrix}^T$. This standard form, however, still does not satisfy the regularity assumptions since $D_{12}^T D_{12}$ is singular. Fortunately, regularization can be done by extending the external output ζ to include the "weighted" vector $\beta\nu$. This adds another change in the standard setup consisting of replacing ζ by $\bar{\zeta}$ defined as: $\bar{\zeta} = \begin{bmatrix} \zeta & \beta\nu \end{bmatrix}^T$. The entries of $\hat{G}(s)$ in (3.13) are then given by:

$$\dot{z} = \begin{bmatrix} A \end{bmatrix} z + \begin{bmatrix} \begin{bmatrix} I_n & 0_{np} \end{bmatrix} & -I_n \end{bmatrix} \begin{bmatrix} \begin{bmatrix} \tau \\ d \\ \nu \end{bmatrix} \end{bmatrix} \tag{3.27}$$

$$\begin{bmatrix} \begin{bmatrix} \zeta \\ \beta\nu \end{bmatrix} \\ \varphi \end{bmatrix} = \begin{bmatrix} \begin{bmatrix} I_n \\ 0_n \end{bmatrix} \\ C \end{bmatrix} z + \begin{bmatrix} \begin{bmatrix} 0_n & 0_{np} \\ 0_n & 0_{np} \\ 0_{pn} & \epsilon I_p \end{bmatrix} & \begin{bmatrix} 0_n \\ \beta I_n \\ 0_{pn} \end{bmatrix} \end{bmatrix} \begin{bmatrix} \begin{bmatrix} \tau \\ d \\ \nu \end{bmatrix} \end{bmatrix} \tag{3.28}$$

It is now straightforward to see that all the regularity assumptions below, [122], are now satisfied:

(1) (A, B_1) is controllable and (C_1, A) is observable (for any matrix A).

(2) (A, B_2) is stabilizable (for any matrix A), and (C_2, A) is detectable (iff (A, C) is detectable).

(3) $D_{12}^T \begin{bmatrix} C_1 & D_{12} \end{bmatrix} = \begin{bmatrix} 0 & \beta^2 I_n \end{bmatrix}$.

(4) $\begin{bmatrix} B_1 \\ D_{21} \end{bmatrix} D_{21}^T = \begin{bmatrix} 0 \\ \epsilon^2 I_p \end{bmatrix}$.

(5) $D_{11} = 0$ and $D_{22} = 0$.

It follows that the standard form in (3.27)-(3.28) satisfy the conditions of the so-called "*Simplified H_∞ problem*" (see [122], Chapter 14, for more details about this problem and its analytical solution). It is also important to note that all these conditions are satisfied here iff (A, C) is detectable, which does not impose any new design restrictions for the observer design. We now show the equivalence between the original problem and this "*Simplified H_∞ problem*" in the following sense:

Let T_1 be the setup in Figure 2.2 associated with (3.10)-(3.11), T_2 the one associated with (3.25)-(3.26) and T_3 the one associated with (3.27)-(3.28) where the three share the controller K in (3.18). And let $\hat{T}_1(s)$, $\hat{T}_2(s)$ and $\hat{T}_3(s)$ be their corresponding transfer matrices. The following lemmas demonstrate a certain equivalence relationships among these setups (see Appendix A.1 for the detailed proofs).

Lemma 3.1 *Consider a stabilizing controller K for the setups T_1 and T_2, then $\| \hat{T}_1(s) \|_\infty < \gamma$ if and only if $\exists\ \epsilon > 0$ such that $\| \hat{T}_2(s) \|_\infty < \gamma$.*

Lemma 3.2 *Given $\epsilon > 0$ and a stabilizing controller K for the setups T_2 and T_3, then $\| \hat{T}_2(s) \|_\infty < \gamma$ if and only if $\exists\ \beta > 0$ such that $\| \hat{T}_3(s) \|_\infty < \gamma$.*

3.3.2 Parameterization of All Observer Gains

We now present the main result of this chapter in the form of a theorem showing that the observer gain K needed to stabilize the observer error dynamics according to Theorem 3.4 must solve a "*Simplified H_∞ control problem*" according to the definition used in [122]. To this end, we define the regular continuous *Simplified H_∞ problem* "Problem 1" as follows:

Problem 1: *Given $\epsilon > 0$ and $\beta > 0$, find S, the set of admissible controllers K satisfying*

$\parallel \hat{T}_{\zeta\tilde{\tau}} \parallel_\infty < \gamma$ for the setup in Figure 2.2 with G having the state space representation in (3.13) along with the matrices in (3.27)-(3.28).

Defining the following two Hamiltonian matrices associated with Problem 1 (when $\gamma = \frac{1}{\alpha}$):

$$N_\infty = \begin{bmatrix} A & \alpha^2 I_n - \frac{1}{\beta^2} I_n \\ -I_n & -A^T \end{bmatrix}, \quad J_\infty = \begin{bmatrix} A^T & \alpha^2 I_n - \frac{1}{\epsilon^2} C^T C \\ -I_n & -A \end{bmatrix} \tag{3.29}$$
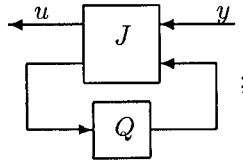
the main result is then summarized as follows:

Theorem 3.5 *There exists a gain K for the observer (3.14)-(3.18) (or a static gain L for (3.4)-(3.5)) that stabilizes the error dynamics according to Theorem 3.4 (or Theorem 3.3) if and only if $\exists\ \epsilon,\ \beta > 0$ such that:*

1) $N_\infty \in dom(Ric)$ and $X_\infty = Ric(N_\infty) > 0$.

2) $J_\infty \in dom(Ric)$ and $Y_\infty = Ric(J_\infty) > 0$.

3) $\rho(X_\infty Y_\infty) < \frac{1}{\alpha^2}$ (where $\rho(.)$ is the spectral radius defined as the maximum magnitude over all eigenvalues).

Proof: A direct result of Theorem 3.4, Lemmas 3.1 and 3.2.   □

Moreover, by using the result in [28], the set of all observer gains K can be represented by the set of all transfer matrices from y to u in Figure 3.2:

$$; \quad \hat{J}(s) = \left[\begin{array}{c|cc} \hat{A}_\infty & \frac{1}{\epsilon^2}(I_n - \alpha^2 Y_\infty X_\infty)^{-1} Y_\infty C^T & -\frac{1}{\beta}(I_n - \alpha^2 Y_\infty X_\infty)^{-1} \\ \hline \frac{1}{\beta^2} X_\infty & 0_{np} & \frac{1}{\beta} I_n \\ -\frac{1}{\epsilon} C & \frac{1}{\epsilon} I_p & 0_{pn} \end{array} \right]$$

Figure 3.2: Parameterization of All Observer Gains.

where $\hat{A}_\infty = A + (\alpha^2 - \frac{1}{\beta^2}) X_\infty - \frac{1}{\epsilon^2}(I_n - \alpha^2 Y_\infty X_\infty)^{-1} Y_\infty C^T C$, and Q is such that $\|Q\|_\infty < \frac{1}{\alpha}$.

3.3.3   A new H_∞ Design Procedure

Following the approach in [92], the following iterative "binary search" procedure is then proposed to evaluate the observer gain:

Design procedure:

Step 1 Set $\epsilon,\ \beta > 0$ and $\gamma \leftarrow \frac{1}{\alpha}$.

Step 2 Test solvability of Problem 1. If test fails then go to Step 3 ; otherwise solve the problem (using available software packages or the analytical results in [122]) and any $K \in \mathcal{S}$ is a candidate observer gain that globally stabilizes the error dynamics.

Step 3 Set $\epsilon \leftarrow \frac{\epsilon}{2}$, $\beta \leftarrow \frac{\beta}{2}$. If ϵ or $\beta <$ a threshold value then *stop* ; otherwise go to Step 2.

Remarks:

- This design procedure is less restrictive than the designs introduced in [1, 92, 93, 95], since it is directly related to the stability condition through the result in Theorem 3.5. This will be numerically demonstrated in Section 3.4.

- When the optimization problem can not be solved due to its infeasibility or due to limitations of the used software, one can increase γ which corresponds to a smaller Lipschitz constant α. The word *stop* in step 3 can then be replaced by: *decrease α and go to Step 1*. The algorithm is then guaranteed to work as $\alpha \to 0$. However, the region of convergence is decreased unlike if original α is used. The choice of the threshold in Step 3 is also important to avoid numerical instability of the used software.

- Same design can be used when the output is disturbed as in (3.24). The small gain theorem guarantees that the estimation error $e(t) \in \mathcal{L}_2$ if $d(t) \in \mathcal{L}_2$.

- Design of the H_∞ observer can also be done by including appropriate weightings to emphasize the performance requirements of the observer over specific frequency ranges. This will be considered in Chapter 4 when studying the sensor fault diagnosis problem.

- If some states are not affected by nonlinearities (i.e, if some entries of the Lipschitz function Φ are zeros), the corresponding 1's of the Identity matrix in the matrix B_1 of the setup (3.27)-(3.28) can be replaced by zeros. As long as (A, B_1) is controllable, the regularity assumptions will be satisfied, and the observer design is still equivalent to a "*Simplified H_∞ problem*".

3.4 Simulation Results

We consider the following example from [92] to show the advantages of using the proposed H_∞ design procedure. This is an example of a 2nd order system of the form (3.1)-(3.2) with $A = \begin{bmatrix} -2 & 3 \\ 3 & 1 \end{bmatrix}$, $\Gamma = \begin{bmatrix} 0 \\ 1 \end{bmatrix} u$, $\Phi = \begin{bmatrix} 0 \\ k \ sin(x_1) \end{bmatrix}$ and $C = \begin{bmatrix} 0 & 1 \end{bmatrix}$. The Lipschitz constant is $\alpha = |k|$.

The system is open loop unstable and therefore the design techniques in [1, 95] can not be used to design an observer of the form (3.4)-(3.5). In [92], the case of $\alpha = 1.5$ was considered and, although the design algorithm in Theorem 3.3 fails if the original system matrices are used, the static gain L was obtained *after using a state transformation* as $L = \begin{bmatrix} 2 & 4 \end{bmatrix}^T$.

Case study 1: We here show the improvement that can be achieved by using a dynamic observer, in terms of the maximum achievable α in (3.21). Using a static gain

$$L = \begin{bmatrix} a & b \end{bmatrix}^T \text{ in (3.22), we have } \hat{T}_{\zeta\tau} = \left[\begin{array}{c|c} \bar{A} & \bar{B} \\ \hline \bar{C} & \bar{D} \end{array} \right], \text{ with } \bar{A} = \begin{bmatrix} -2 & 3-a \\ 3 & 1-b \end{bmatrix}, \bar{B} = \bar{C} = I_2,$$

and $\bar{D} = 0_2$. It then follows, [122], that $\|\hat{T}_{\zeta\tau}\|_\infty < \gamma$ iff $\exists X = \begin{bmatrix} x_1 & x_3 \\ x_3 & x_2 \end{bmatrix} > 0$ such that

$$\begin{bmatrix} X\bar{A} + \bar{A}^T X & X\bar{B} & \bar{C}^T \\ \bar{B}^T X & -\gamma I_2 & \bar{D}^T \\ \bar{C} & \bar{D} & -\gamma I_2 \end{bmatrix} < 0. \text{ The term } X\bar{A} + \bar{A}^T X \text{ in the previous matrix inequality}$$

is $\begin{bmatrix} -4x_1 + 6x_3 & y_1 + 3x_2 \\ y_1 + 3x_2 & y_2 \end{bmatrix}$, where $y_1 = (3-a)x_1 - (b+1)x_3$, $y_2 = (6-2a)x_3 + (2-2b)x_2$.

We now use convex optimization as follows: by minimizing γ subject to the previous Linear Matrix Inequalities (LMIs), using the Matlab[2] command *"mincx"*, the optimal $\gamma = 0.2774$ which corresponds to $\alpha = 3.6055$. Therefore, the maximum possible α over all static observers satisfying the stability condition in (3.21) is $\alpha = 3.6055$. Using the H_∞ design algorithm of section 3.3.3 for $\alpha = 25$, a dynamic observer gain of order 2 can be obtained at $\epsilon = \beta = 0.015625$ as follows:

$$A_L = \begin{bmatrix} -64.114 & -4.803 \\ 0.256 & -146.361 \end{bmatrix}, B_L = \begin{bmatrix} 4.564 \\ 87.373 \end{bmatrix}, C_L = \begin{bmatrix} 62.114 & 3.239 \\ 3.239 & 70.79 \end{bmatrix} \& D_L = \begin{bmatrix} 0 \\ 0 \end{bmatrix} \quad (3.30)$$

This shows the advantage of using a dynamic observer gain in this case.

Case study 2: In this case we consider the case of $\alpha = 1.5$, comparing the dynamic observer with the static observer in [92], in a state feedback application. Using the H_∞ design algorithm of section 3.3.3 (starting with $\epsilon = \beta = 2$), *and without using any state transformations*, a candidate dynamic gain for the observer (3.14)-(3.18) is obtained after 4 iterations (at $\epsilon = \beta = 0.125$) as:

$$A_L = \begin{bmatrix} -8.644 & -8.5916 \\ 0.1753 & -21.5898 \end{bmatrix}, B_L = \begin{bmatrix} 8.7669 \\ 13.1211 \end{bmatrix}, C_L = \begin{bmatrix} 6.8861 & 2.9276 \\ 2.9276 & 9.8137 \end{bmatrix} \& D_L = \begin{bmatrix} 0 \\ 0 \end{bmatrix}$$

$$(3.31)$$

---

[2]The Matlab software used in this thesis is the MathWorks Inc MATLAB® Version 6.5 Release 13.

In the simulations, the system initial condition $x(0) = \begin{bmatrix} 1.6 & 2 \end{bmatrix}^T$, and the objective is to stabilize the equilibrium point at the origin by using an observer-based state feedback control law. To this end, the control law $u = \begin{bmatrix} 11 & 13 \end{bmatrix} x$, based on linearization, is proposed and Figure 3.3 (a), (b) compares the system performance for 3 different cases: (i) pure state feedback, (ii) observer-based state feedback with the static gain $L = \begin{bmatrix} 2 & 4 \end{bmatrix}^T$, (iii) observer-based state feedback with the dynamic gain in (3.31). The observers initial conditions is $\hat{x}(0) = \begin{bmatrix} 0 & 0 \end{bmatrix}^T$. The figures show the improvement in the state convergence rate when the dynamic observer is used.
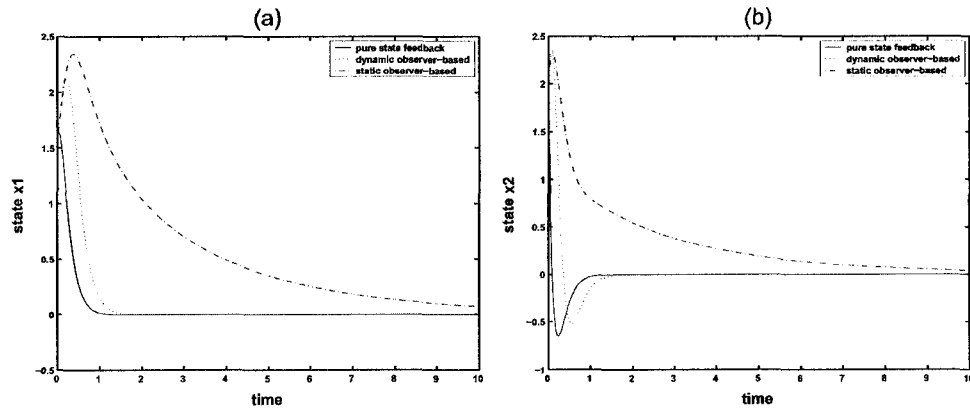
Figure 3.3: (a) Response of State x_1, (b) Response of State x_2 .

3.5 Conclusion

In this chapter, a new H_∞ observer design for Lipschitz nonlinear systems is proposed. It is first shown that the classical "Luenberger-like" observers are special cases of a more general dynamic framework, one that shows promise given the additional degrees of freedom. The equivalence between the observer design problem and a standard H_∞ control problem that satisfies all of the regularity assumptions is shown. A systematic design procedure which is less restrictive than the existing design approaches and that can be carried out using commercially available software is presented.

Chapter 4

Lipschitz Sensor Fault Diagnosis

In this chapter, we consider the sensor fault detection and identification problem for Lipschitz nonlinear systems, using the dynamic observer structure introduced in Chapter 3. We start by the LTI case showing that, unlike the classical observer structure, this problem is solvable with the additional dynamics by considering different frequency patterns for the sensor fault. The same approach is then extended to the Lipschitz case where the use of appropriate weightings to solve the problem in a standard convex optimization framework is demonstrated, and an LMI design procedure solvable using commercially available software is presented[1].

4.1 An investigation of the Effect of Dynamics in the LTI Case

As discussed in section 2.2, a widely accepted model for the Linear Time-Invariant (LTI) system with faults is the state-space model in (2.1)-(2.2) which can also be represented by

$$\dot{x}(t) = Ax(t) + Bu(t) + R_1 f(t) \tag{4.1}$$

$$y(t) = Cx(t) + Du(t) + R_2 f(t) \tag{4.2}$$

where $x(t) \in \mathbb{R}^n$ is the state vector, $u(t) \in \mathbb{R}^m$ is the control input, $y(t) \in \mathbb{R}^p$ is the measured output, and $f(t) \in \mathbb{R}^s$ is a single vector that represents all the faults in (2.1)-(2.2). In this

---

[1]The results for the LTI case have been published in the article: "A.M. Pertew, H.J. Marquez and Q. Zhao, H_∞ Dynamic Observer Design with Application in Fault Detection and Diagnosis," Proceedings of the 44th IEEE Conference on Decision and Control and European Control Conference (CDC-ECC 2005), Seville, Spain, pp. 7943-7948, December 2005. The results for the Lipschitz case have been submitted for publication: "A.M. Pertew, H.J. Marquez and Q. Zhao, LMI-based Sensor Fault Diagnosis for Nonlinear Lipschitz Systems," submitted to Automatica, December 2005.

model, A, B, C, D, R_1 and R_2 are known matrices of appropriate dimensions. In this case, the most famous technique used for residual generation (i.e, for the purpose of generating a signal $r(t)$ that can be used to detect faults) is the observer-based approach that uses the following *Luenberger* observer structure:

$$\dot{\hat{x}}(t) = A\hat{x}(t) + Bu(t) + L\left(y(t) - \hat{y}(t)\right) \tag{4.3}$$

$$\hat{y}(t) = C\hat{x}(t) + Du(t) \tag{4.4}$$

in addition to a weighting $Q(s)$ to generate the residual as:

$$r = Q(s)(y - \hat{y}); \qquad r(t) \in \mathbb{R}^q \tag{4.5}$$

The residual obtained from (4.5) is therefore the weighted output estimation error of the observer, and the residual generator (4.3)-(4.5) has two degrees of freedom, namely, the constant observer gain L and the post filter $Q(s)$. Within this context, the fault detection, isolation and identification objectives (which were discussed in section 2.2) can be defined as follows [13]: (note that in these definitions the transient period of the residuals is not considered)

Definition 4.1 *(Fault detection): The residual generator achieves fault detection (strong fault detection) if the following condition is satisfied:*

$$r_i(t) = 0 \; ; \quad for \; i = 1, \cdots, q \; ; \forall t \qquad if \; (if \; and \; only \; if) \qquad f_i(t) \; = 0 \; ; \quad for \; i = 1, \cdots, s \; ; \forall t$$

Definition 4.2 *(Fault isolation): The residual generator achieves fault isolation if the residual has the same dimension as $f(t)$ (i.e, $q = s$) and if the following condition is satisfied:*

$$(r_i(t) = \; 0 \; ; \quad \forall t \; \Longleftrightarrow \; f_i(t) = 0 \; ; \quad \forall t) \; ; \; for \; i = 1, \cdots, s$$

Definition 4.3 *(Fault identification): The residual generator achieves fault identification if the residual $r(t)$ has the same dimension as $f(t)$ and if the following condition is satisfied:*

$$(r_i(t) = \; f_i(t) \; ; \quad \forall t) \; ; \; for \; i = 1, \cdots, s$$

According to the previous definitions, in fault detection a binary decision could be made either that a fault occurred or not, while in fault isolation the location of the fault is determined and in fault identification the size of the fault is estimated. The relative importance of the three tasks is subjective and depends on the application, however it is

important to note that fault identification implies isolation and that fault isolation implies detection (but not the opposite). Necessary and sufficient conditions for fault detection and isolation have been developed in [34].

For the sensor faults diagnosis problem (which is our focus in this chapter), the system (4.1)-(4.2) is the special case where $R_1 = 0_{ns}$, $R_2 = I_p$ and $f(t) = f_s(t) \in \mathbb{R}^p$. Using the classical residual generator in (4.3)-(4.5), the observer error dynamics is given from:

$$\dot{e}(t) = (A - LC)e(t) - Lf_s(t) \tag{4.6}$$

$$\tilde{y}(t) = Ce(t) + f_s(t) \tag{4.7}$$

where $e = x - \hat{x}$, $\tilde{y} = y - \hat{y}$.

The fault vector f_s has direct effect on the output estimation error $\tilde{y}$, and hence on the residual. Therefore *sensor fault detection* according to definition 4.1 is achievable by this structure [13]. *Fault isolation* can also be achieved by using the dedicated observer scheme, where a bank of observers (4.3)-(4.4) is used to differentiate between different faults. However, for this approach, the number of sensor faults need to be known a priori, and also restrictive observability conditions need to be satisfied [108]. In this section we consider the multiple sensor faults identification problem for LTI-MIMO systems using a novel approach. Our methodology is based on the extension of the static observer structure in (4.3)-(4.4) to a more general dynamic framework similar to the one used in Chapter 3 for the Lipschitz observer design problem. We tackle the case when f_s is in a narrow frequency band by showing that the sensor fault identification problem is equivalent to an output zeroing problem which is solvable only with a dynamic observer. We further consider the cases of low and high frequency ranges showing that these two problems can be modeled as weighted H_∞ problems.

4.1.1 The Narrow Frequency Band Sensor Fault Diagnosis

For the sensor fault case (as seen in equations (4.6)-(4.7)), the observer's estimation error can be represented by Figure 4.1.

From this figure, it is clear that by minimizing "e", the output estimation error $\tilde{y}$ converges to f_s which guarantees fault identification in this case. In this subsection, we consider the solution of this minimization problem (when f_s is in a narrow frequency band around a nominal frequency ω_o) by using a dynamic observer structure, showing that the problem is not tractable for the static gain structure in (4.3)-(4.4).
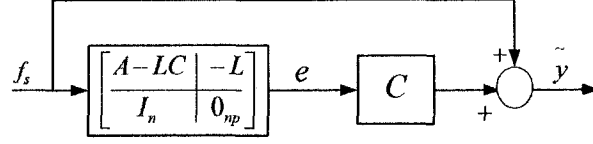
Figure 4.1: Error Dynamics of the Classical Observer Structure.

Same as in Chapter 3, we will make use of dynamical observers of the form:

$$\dot{\hat{x}}(t) = A\hat{x}(t) + Bu(t) + \eta(t) \tag{4.8}$$

$$\hat{y}(t) = C\hat{x}(t) + Du(t) \tag{4.9}$$

where $\eta(t)$ is obtained by applying a dynamical compensator on the output estimation error $(y - \hat{y})$, i.e $\eta(t)$ is given from

$$\dot{\xi} = A_L\xi + B_L(y - \hat{y}) \tag{4.10}$$

$$\eta = C_L\xi + D_L(y - \hat{y}). \tag{4.11}$$

We will also write

$$K = \left[\begin{array}{c|c} A_L & B_L \\ \hline C_L & D_L \end{array} \right] \tag{4.12}$$

to represent the compensator in (4.10)-(4.11). The additional degrees of freedom provided by this observer will be exploited in the minimization of the sensor faults effect. First, it can be seen that the observer error dynamics in (4.6) is now given by ($\dot{e} = Ae - \eta$) which can be represented by the following so-called standard form:

$$\dot{z} = \left[A \right] z + \left[0_{np} \quad -I_n \right] \left[\begin{array}{c} \tau \\ \nu \end{array} \right] \tag{4.13}$$

$$\left[\begin{array}{c} \zeta \\ \varphi \end{array} \right] = \left[\begin{array}{c} I_n \\ C \end{array} \right] z + \left[\begin{array}{cc} 0_{np} & 0_n \\ I_p & 0_{pn} \end{array} \right] \left[\begin{array}{c} \tau \\ \nu \end{array} \right] \tag{4.14}$$

where

$$\tau = f_s , \quad \nu = \eta = K(y - \hat{y})$$

$$\zeta = e = x - \hat{x} , \quad \varphi = y - \hat{y} \tag{4.15}$$

which can also be represented by *the standard setup figure* (i.e, Figure 2.2) where the plant G has the state space representation in (4.16) with the matrices in (4.13)-(4.14) and where

the controller K is given in (4.12).

$$\hat{G}(s) = \left[\begin{array}{c|cc} A & B_1 & B_2 \\ \hline C_1 & D_{11} & D_{12} \\ C_2 & D_{21} & D_{22} \end{array}\right] \tag{4.16}$$

All possible observer gains for the observer (4.8)-(4.12) (including the static case (4.3)-(4.4)) can then be parameterized by the set of "all stabilizing controllers" for the setup in Figure 2.2. This is a standard result (see [122]) and, for the problem considered in this section, it can be represented by the following theorem (as a special case of Theorem 11.4 in [122]):

Theorem 4.1 *Let F and L be such that $A + LC$ and $A - F$ are stable; then all possible observer gains K for the observer (4.8)-(4.12) can be parameterized as the transfer matrix from φ to ν in Figure 4.2 with any $\hat{Q}(s) \in RH_\infty$.*

$$; \quad \hat{J}(s) = \left[\begin{array}{c|cc} A - F + LC & -L & -I_n \\ \hline F & 0_{np} & I_n \\ -C & I_p & 0_{pn} \end{array}\right]$$
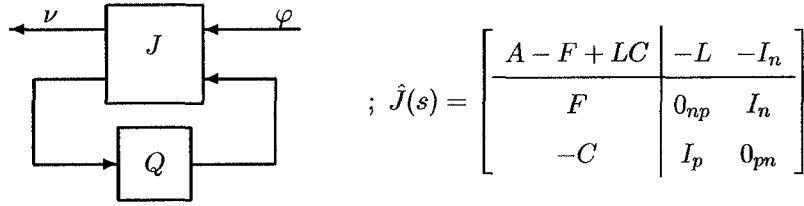
Figure 4.2: Parameterization of All Observer Gains.

As mentioned earlier, our objective is to minimize (in some sense) the effect of sensor faults (in a narrow frequency band around a nominal frequency ω_o) on the state estimation error in order to achieve sensor faults estimation. In this subsection, we consider the solution of this minimization problem in an $\mathcal{L}_2$ sense (when f_s is in a narrow frequency band around a nominal frequency ω_o) by using the dynamic observer structure introduced earlier, showing that the problem is not tractable for the classical structure in (4.3)-(4.4). Towards that goal, we will first assume that the fourier transform of the sensor fault $F_s(j\omega)$ have a frequency pattern restricted to the narrow band $\omega_o \pm \Delta\omega$ as described by equation (4.17):

$$\|F_s(j\omega)\| \leq \begin{cases} \Omega ; & |\omega - \omega_o| < \Delta\omega \\ \delta ; & \text{otherwise} \end{cases} \tag{4.17}$$

where δ is a small neglected number for the frequency magnitudes outside the region of interest. We will then define an observer gain K as optimal if $\| e \|_{\mathcal{L}_2}$ can be made arbitrarily small for all possible sensor faults satisfying (4.17). But by studying the gain of the error

dynamics in the standard setup, we have: $\|e\|_{\mathcal{L}_2} \leq \|\hat{T}_{ef_s}(s)\|_\infty \|f_s\|_{\mathcal{L}_2}$. And since (as $\Delta\omega \to$

0), $\hat{T}_{ef_s}(j\omega) \to \hat{T}_{ef_s}(j\omega_o)$ then we have $\|e\|_{\mathcal{L}_2} \leq \sigma_{max}\left(\hat{T}_{ef_s}(j\omega_o)\right) \|f_s\|_{\mathcal{L}_2}$, and therefore, it is

easy to see that an optimal gain K is one that satisfies $\hat{T}_{ef_s}(j\omega_o) = 0$.

The following theorem shows that a static observer gain can never be an optimal observer gain according to the previous discussion.

Theorem 4.2 *A static observer gain (such as the constant matrix L in (4.3)-(4.4)) can never be an optimal observer gain (i.e can not satisfy $\hat{T}_{ef_s}(j\omega_o) = 0$) for any nominal frequency ω_o.*

Proof: The proof follows by noting that the transfer matrix from f_s to e (as seen in (4.6)

and Figure 4.1) is $\hat{T}_{ef_s}(s) = \left[\begin{array}{c|c} A - LC & -L \\ \hline I_n & 0_{np} \end{array}\right]$. And since the gain L is chosen to stabilize

$(A - LC)$, then $(\forall\omega_o)$ $j\omega_o$ is not an eigenvalue of $(A - LC)$. Therefore, by using (2.28), we have

$\text{rank}\left(\hat{T}_{ef_s}(j\omega_o)\right) = \text{rank}\left[\begin{array}{cc} A - LC - j\omega_o I_n & -L \\ I_n & 0_{np} \end{array}\right] - n$. But rank $\left[\begin{array}{cc} A - LC - j\omega_o I_n & -L \\ I_n & 0_{np} \end{array}\right]$

$= \text{rank}\left[\begin{array}{cc} L & 0_n \\ 0_{np} & I_n \end{array}\right] = n + \text{rank}(L)$. Therefore, $\text{rank}\left(\hat{T}_{ef_s}(j\omega_o)\right) \neq 0$ unless $L = 0$. This

implies that no gain L can satisfy $\hat{T}_{ef_s}(j\omega_o) = 0$, and therefore a static observer gain can never be an optimal gain. $\square$

We now consider the case of the dynamic observer introduced in (4.8)-(4.12). As a result of the gain parametrization presented in theorem 4.1, the transfer matrix from f_s to e, achievable by an internally stabilizing gain K, is equal to the Linear Fractional Transformation (LFT) between T and Q as follows [122]:

$$\hat{T}_{ef_s}(s) \equiv LFT(T, Q) = \hat{T}_{11}(s) + \hat{T}_{12}(s)\hat{Q}(s)\hat{T}_{21}(s) \tag{4.18}$$

where $\hat{Q}(s) \in RH_\infty$ and where T is given from

$$\left[\begin{array}{cc} T_{11} & T_{12} \\ T_{21} & T_{22} \end{array}\right] = \left[\begin{array}{cc|cc} A - F & F & 0_{np} & -I_n \\ 0_n & A + LC & L & 0_n \\ \hline I_n & 0_n & 0_{np} & 0_n \\ 0_{pn} & C & I_p & 0_{pn} \end{array}\right] \tag{4.19}$$

We will denote $\hat{T}_{11}(s)$, $\hat{T}_{12}(s)$ and $\hat{T}_{21}(s)$ by $\hat{T}_1(s)$, $\hat{T}_2(s)$ and $\hat{T}_3(s)$ respectively. The following theorem presents a result on the invertibility of the transfer matrices $\hat{T}_2(s)$ and $\hat{T}_3(s)$ at a frequency ω_o (i.e, at $s = j\omega_o$).

Theorem 4.3 *The $(n \times n)$ and $(p \times p)$ matrices $\hat{T}_2(j\omega_o)$ and $\hat{T}_3(j\omega_o)$ are invertible if $j\omega_o$ is not an eigenvalue of A.*

Proof: By using (4.19), $\hat{T}_2(s) = \left[\begin{array}{cc|c} A-F & F & -I_n \\ 0_n & A+LC & 0_n \\ \hline I_n & 0_n & 0_n \end{array}\right] = \left[\begin{array}{c|c} A-F & -I_n \\ \hline I_n & 0_n \end{array}\right].$

Similarly, we have $\hat{T}_3(s) = \left[\begin{array}{c|c} A+LC & L \\ \hline C & I_p \end{array}\right]$. Therefore, using (2.28) the following two rank properties are satisfied:

1. $\mathrm{rank}\left(\hat{T}_2(j\omega_o)\right) = \mathrm{rank}\left[\begin{array}{cc} A-F-j\omega_o I_n & -I_n \\ I_n & 0_n \end{array}\right] - n$.

2. $\mathrm{rank}\left(\hat{T}_3(j\omega_o)\right) = \mathrm{rank}\left[\begin{array}{cc} A+LC-j\omega_o I_n & L \\ C & I_p \end{array}\right] - n$.

But $\mathrm{rank}\left[\begin{array}{cc} A-F-j\omega_o I_n & -I_n \\ I_n & 0_n \end{array}\right] = 2n$, $\forall\, \omega_o$. We also have, $\mathrm{rank}\left[\begin{array}{cc} A+LC-j\omega_o I_n & L \\ C & I_p \end{array}\right] =$

$\mathrm{rank}\left[\begin{array}{cc} A-j\omega_o I_n & L \\ 0_{pn} & I_p \end{array}\right] = n+p$; if $j\omega_o$ is not an eigenvalue of A.

Therefore, $\mathrm{rank}\left(\hat{T}_2(j\omega_o)\right) = n$ and $\mathrm{rank}\left(\hat{T}_3(j\omega_o)\right) = p$ (full ranks) if $j\omega_o$ is not eigenvalue of A, and the proof is completed. $\square$

Based on the results in theorem 4.3, it can be proven that, for $\hat{T}_{ef_s}(s)$ in (4.18), $\exists$ a transfer matrix $\hat{Q}(s) \in RH_\infty$ that satisfies $\hat{T}_{ef_s}(j\omega_o) = 0$ (see Appendix A.2 for details about computing $\hat{Q}(s)$). Therefore, for the dynamic observer in (4.8)-(4.12), an optimal gain can be found (unlike the static case). This shows the advantage of using the dynamic observer in this case. To summarize, based on the previous results, we will define an optimal residual generator as follows:

Theorem 4.4 *(Optimal residual for narrow frequency band): An observer of the form (4.8)-(4.12) along with $r = y - \hat{y}$ is an optimal residual generator for the sensor fault identification problem (with faults in a narrow frequency band around ω_o) if the dynamic gain K is chosen as the Linear Fractional Transformation $LFT(J,Q)$ in Figure 4.2 where $\hat{Q}(s) \in RH_\infty$ solves the problem $\hat{T}_{ef_s}(j\omega_o) = 0$ for the transfer matrix $\hat{T}_{ef_s}(s)$ in (4.18).*

Remarks

- According to the previous theorem, an optimal residual generator guarantees sensor faults estimation and at the same time state estimation (with minimum energy for the estimation errors). An advantage of having *state* estimation in presence of sensor faults is the possibility to use the observer in fault tolerant output feedback control (i.e, if a reconfiguration control action is involved).

- From the special cases of interest is the case of sensor bias, where the previous approach can be used to get an *exact* estimation of all sensor biases at the same time. A sufficient condition is that the matrix A has no eigenvalues at the origin.

4.1.2 Use of H_∞ in the Low and High Frequency Cases

We here consider two different cases: the low frequency range and the high frequency range. For the first case, we assume the system to be affected by sensor faults of low frequencies determined by a cutoff frequency ω_l, i.e the frequency pattern for $f_s(t)$ is confined to the region $[0, \omega_l]$. In the high frequency case, we assume these frequencies to be confined to the region $[\omega_h, \infty)$. Since the error dynamics can be represented by Figure 2.2 with the plant G in (4.16) having the matrices defined in (4.13)-(4.14) and with the controller K in (4.12), then these two cases can be solved by adding weightings to the setup in Figure 2.2 that emphasize the frequency range under consideration, and by solving these problems as weighted H_∞ problems. Moreover, it is important to note that, using a regularization procedure similar to the one introduced in section 3.3.1, the standard form in (4.13)-(4.14) can be regularized (by extending the external output ζ in Figure 2.2 to include the "scaled" vector $\beta\nu$; with $\beta > 0$), and hence observer synthesis can be carried out directly using the standard H_∞ solution. To this end, we replace (4.13)-(4.14) by the following augmented form:

$$\dot{z} = \begin{bmatrix} A \end{bmatrix} z + \begin{bmatrix} 0_{np} & -I_n \end{bmatrix} \begin{bmatrix} \tau \\ \nu \end{bmatrix} \tag{4.20}$$

$$\begin{bmatrix} \begin{bmatrix} e \\ \beta\nu \end{bmatrix} \\ \varphi \end{bmatrix} = \begin{bmatrix} \begin{bmatrix} I_n \\ 0_n \end{bmatrix} \\ C \end{bmatrix} z + \begin{bmatrix} \begin{bmatrix} 0_{np} \\ 0_{np} \end{bmatrix} & \begin{bmatrix} 0_n \\ \beta I_n \end{bmatrix} \\ I_p & 0_{pm} \end{bmatrix} \begin{bmatrix} \tau \\ \nu \end{bmatrix} \tag{4.21}$$

which satisfies the regularity assumptions. Similar to Lemmas 3.1 and 3.2, the following lemma demonstrates a certain equivalence relationships between the standard form in (4.13)-(4.14) and the regularized one in (4.20)-(4.21) (proof is omitted).

Lemma 4.1 *Let R_1 be the setup in Figure 2.2 associated with (4.13)-(4.14), R_2 be the one associated with (4.20)-(4.21) and consider a stabilizing controller K for both setups. Then $\| \hat{R}_1 \|_\infty < \gamma$ if and only if $\exists\ \beta > 0$ such that $\| \hat{R}_2 \|_\infty < \gamma$.*

We now consider faults of low frequencies determined by a cutoff frequency ω_l. The weighting $\hat{w}_l(s) = \frac{as+b}{s}$, [122], emphasizes this low frequency range with "b" selected as ω_l and "a" as an arbitrary small number for the magnitude of $\hat{w}_l(j\omega)$ as $\omega \to \infty$. Therefore, with a diagonal transfer matrix $\hat{W}(s)$ that consists of these weightings, the problem in Figure 2.2 can be modified to the weighted version in Figure 4.3.
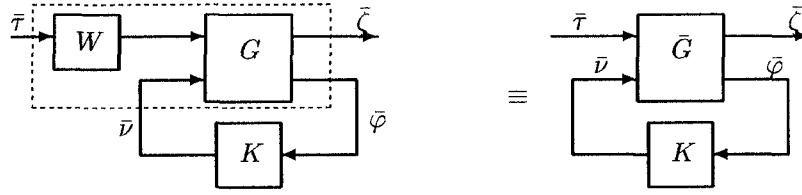
Figure 4.3: Weighted Standard Setup.

It can be seen that $\bar{G}$ is given by:

$$
\hat{\bar{G}}(s) = \left[
\begin{array}{c|c|c}
\left[\begin{array}{cc} A_w & 0_{pn} \\ 0_{np} & A \end{array}\right] & \left[\begin{array}{c} I_p \\ 0_{np} \end{array}\right] & \left[\begin{array}{c} 0_{pn} \\ -I_n \end{array}\right] \\
\hline
\left[\begin{array}{cc} 0_{np} & I_n \\ 0_{np} & 0_n \end{array}\right] & \left[\begin{array}{c} 0_{np} \\ 0_{np} \end{array}\right] & \left[\begin{array}{c} 0_n \\ \beta I_n \end{array}\right] \\
\hline
\left[\begin{array}{cc} C_w & C \end{array}\right] & D_w & 0_{pn}
\end{array}
\right]
\tag{4.22}
$$

where $A_w = 0_p$, $C_w = Diag_p(b)$ and $D_w = Diag_p(a)$. However, this standard form violates the regularity assumptions. Therefore, we introduce the modified weighting, [122], $\hat{w}_{lmod}(s) = \frac{as+b}{s+c}$; with arbitrary small positive "c". With this modification, the augmented plant $\bar{G}$ is the same as (4.22) except for A_w which is now given by the stable matrix $Diag_p(-c)$ and C_w which is given by $Diag_p(b - ac)$. Similar to the non weighted case, all the regularity assumptions are satisfied if and only if A has no eigenvalues on the imaginary axis. We define the regular H_∞ problem associated with the low frequency range as follows:

Definition 4.4 *(Low frequency H_∞): Given $\beta > 0$, find $\mathcal{S}$, the set of admissible controllers K satisfying $\| \hat{T}_{\bar{\zeta}\bar{\tau}} \|_\infty < \gamma$ for the setup in Figure 4.3 where $\bar{G}$ has the representation (4.22) with $A_w = Diag_p(-c)$, $C_w = Diag_p(b - ac)$ and $D_w = Diag_p(a)$.*

Based on the previous results, we now present the main result of this section in the form of the following definition for an optimal residual generator in $\mathcal{L}_2$ sense:

Theorem 4.5 *(Optimal residual for low frequencies): An observer (4.8)-(4.12) along with* $r = y - \hat{y}$ *is an optimal residual generator for the sensor faults identification problem (with faults of low frequencies below* ω_l*) if the dynamic gain* $K \in \mathcal{S}^*$ *(the set of controllers solving the* H_∞ *optimal control problem in Definition 4.4 with the minimum possible* γ*).*

Comments:

- A residual generator that is optimal in the sense of Theorem 4.5 can be found by using an iterative binary search algorithm over the constant β (in order to achieve the minimum possible γ for the problem in Definition 4.4). Existing software packages can be used to solve the regular H_∞ problem in Definition 4.4 for a given β.

- The constants a and c should be selected as arbitrary small positive numbers, while b must approximately be equal to ω_l (the cutoff frequency). Different weightings could also be used for the different sensor channels. In this case $A_w = Diag(-c_1, \cdots, -c_p)$, $C_w = Diag(b_1 - a_1c_1, \cdots, b_p - a_pc_p)$ and $D_w = Diag(a_1, \cdots, a_p)$.

The high frequency range case:

The SISO weighting $\hat{w}_{hmod}(s) = \frac{s+(a\times b)}{\epsilon s+b}$, [122], could be selected to emphasize the high frequency range $[w_h, \infty)$ with "b" selected as w_h and, "a" and "ϵ" > 0 as arbitrary small numbers. Similar to the low frequency range, a regular H_∞ problem related to this case can be defined. Also, an optimal residual generator can be defined in a similar way to Theorem 4.5 (details are omitted due to similarity).

4.1.3 Simulation Results on a Tank System

The PROCON Level/Flow/Temperature Process Control System (shown in Figure 4.4) includes two rigs which can be either controlled independently or by connecting them together to achieve simultaneous level and temperature control.

In these simulation experiments, we consider the configuration obtained by connecting the two modules in cascade as shown in Figure 4.5. In this case, there are two water circuits, namely, the hot water circuit and the cold water circuit. The water of both circuits flows into
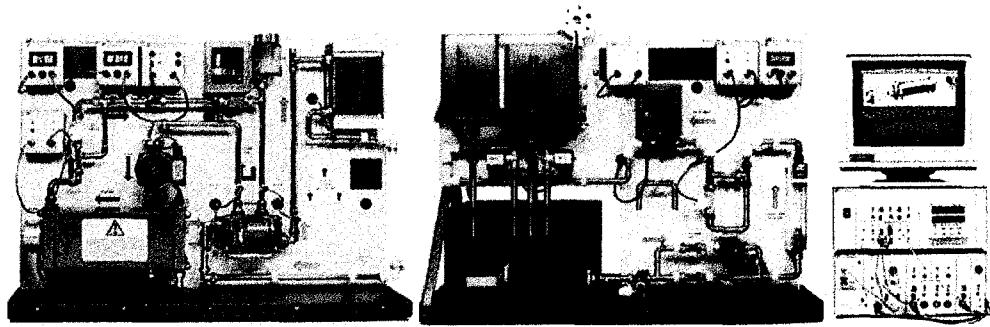
Figure 4.4: The Level/Flow/Temperature Process Control System.

a heat exchanger where the heat energy can be transferred from the hot water flow into the cold water flow. The hot water temperature is controlled manually by the on-off switch of the heater, while the flow rates of both circuits can be controlled through the two servo valves connected to the computer. A level sensor is used to measure the level of the cold water in the main upper tank, while the temperature (at exactly one position) can be measured through the transmitter. It is important to note that there are 5 available positions for temperature measurement: T_1 (T_2) for the hot water input flow to (output flow from) the heat exchanger, T_3 (T_4) for the cold water input (output) flow, and T_5 for the cold water output flow from the cooling radiator. In this experiment, our objective is to control the water level and the temperature of the hot water circuit by controlling the flow rates of the valves. According to this configuration, the process has two inputs (the cold water and hot water servo valves) and two outputs (the level of the water in the upper tank and the temperature T_2). The inputs will be denoted u_1 and u_2 respectively and they both have the same operating range of 0 to 4 litres/min. The operating ranges for the outputs y_1 and y_2 are (0, 14 cm) and (0, 100 Celsius) respectively. The heater set point (i.e, T_1) is chosen as 80 Celsius, while the cold water in the reservoir is at the room's temperature (i.e, $T_3 \cong 23$ Celsius).

Using the first principle physical laws, a model of the process can be developed. However, this model is highly nonlinear and many of its parameters are unknown. Therefore, identification experiments are conducted, and based on the operating point ($u_1 = 2.8$ litres/min, $u_2 = 0.8$ litres/min, $y_1 = 6.35$ cm and $y_2 = 35$ Celsius) a 5th order state space model of the form ($\dot{x} = Ax + Bu$; $y = Cx + Du$) is identified, where $u = \begin{bmatrix} u_1 & u_2 \end{bmatrix}^T$ and $y = \begin{bmatrix} y_1 & y_2 \end{bmatrix}^T$ (see Appendix B.1 for the system matrices). This model is used to demonstrate the proposed sensor faults identification schemes. Towards that goal, the system is controlled to stabilize
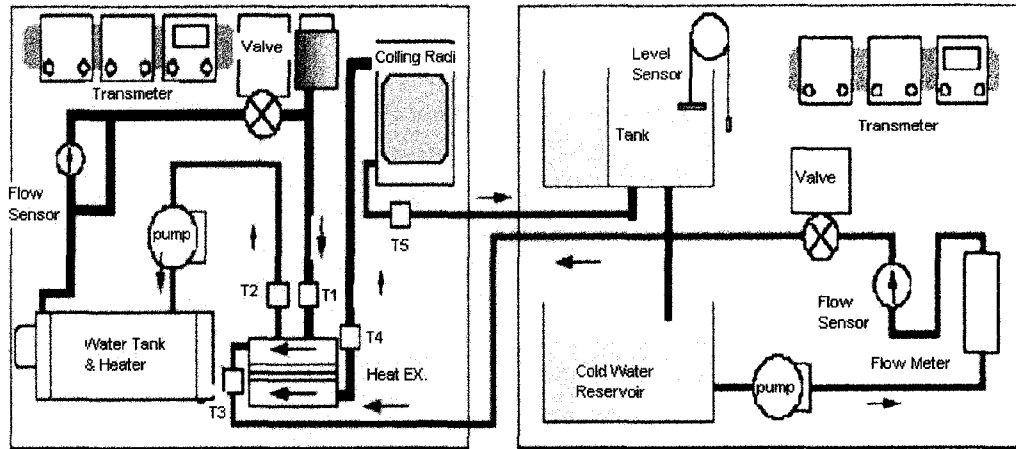
Figure 4.5: Structure of the Connected Rigs.

the output at $y_1 = 8$ cm and $y_2 = 40$ Celsius as seen in Figure 4.6 .
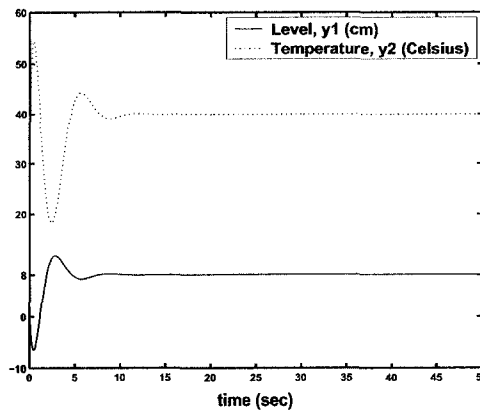
Figure 4.6: Actual System Outputs for the Controlled Process.

Case study 1: In this case, the system is assumed to be affected by sensor biases, where both measured outputs are affected by piecewise constant faults. This is the special case where $\omega_o = 0$ for the problem in section 4.1.1, and since the matrix A in Appendix B.1 has no eigenvalues on the origin, an optimal observer gain that can estimate both sensor biases simultaneously can be designed. This optimal gain K, in our case, is the LFT in Figure 4.2 with $\hat{Q}(s)$ (computed using the algorithm in Appendix A.2) as follows:

$$\hat{Q}(s) = \hat{Q}(0) = \begin{bmatrix} 104.9570 & -116.5842 \\ -75.2350 & -356.1628 \\ -6.8637 & 783.5496 \\ -74.8358 & -694.0620 \\ 36.3072 & 112.4389 \end{bmatrix}$$

(4.23)

Using this observer gain with the observer initial conditions as $\begin{bmatrix} 0 & 0 & 0.1 & 0 & 0.005 \end{bmatrix}^T$, two biases simultaneously changing with time are successfully estimated as seen in Figure 4.7.
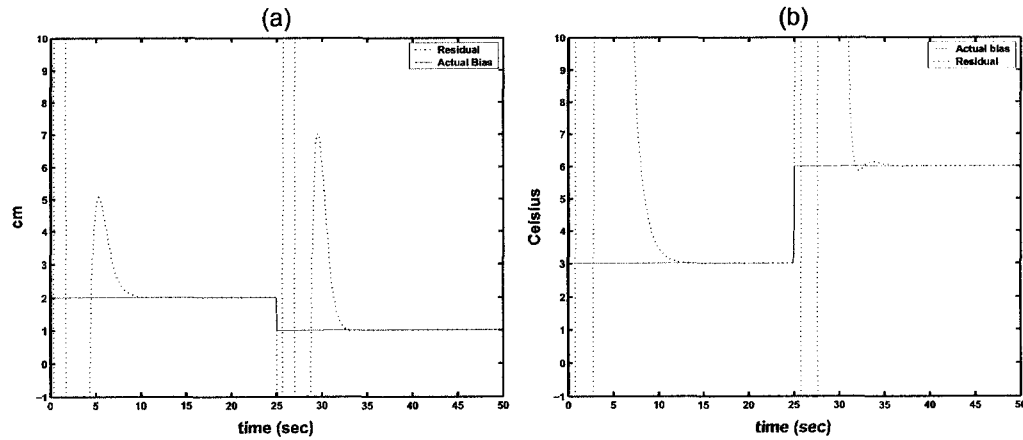
Figure 4.7: (a) Bias Estimation for y_1, (b) Bias Estimation for y_2 .

The state and output estimation errors also converge to zero in this case (Figure 4.8 shows the exact output estimation).

Case study 2: In this case, we consider the case of low frequency sensor faults (in the range [0, 5 rad/sec]). Using the H_∞ design introduced in section 4.1.2 for the low frequency case (and with the weighting selections as $a = 0.01$, $b = 5$ and $c = 0.001$), the optimal observer gain is obtained by solving the H_∞ problem in Definition 4.4 using the command *hinfsyn* in MATLAB, with minimum γ as 0.1 and with $\beta = 1$. Using this observer for the faulty outputs in Figure 4.9, a correct estimation of the low frequency sensor faults is shown in Figure 4.10. The maximum error in that case was 0.0839 for the first fault estimation, and 0.2787 for the second fault estimation.
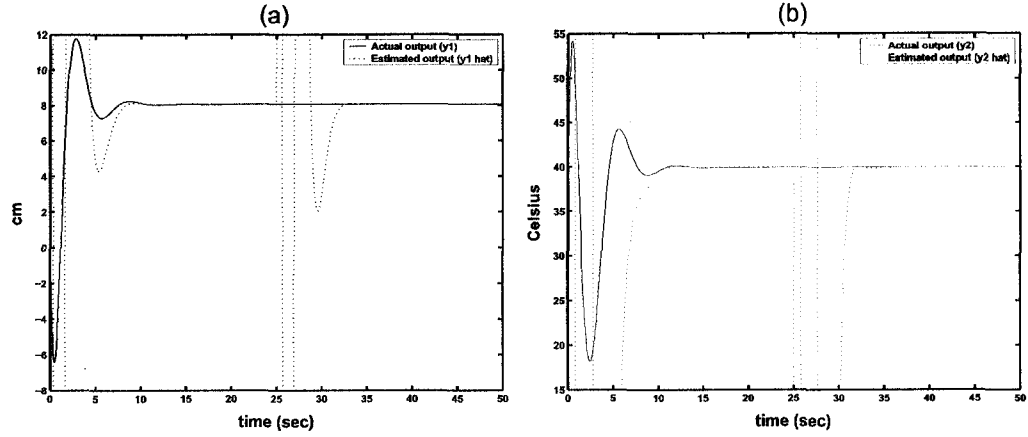
Figure 4.8: (a) Output Estimation for y_1, (b) Output Estimation for y_2.
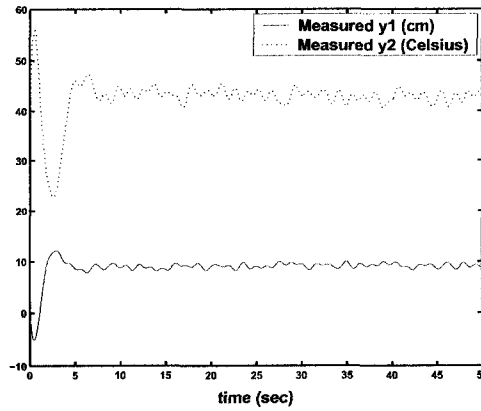
Figure 4.9: Outputs y_1 and y_2 Affected by Low Frequency Sensor Faults.

4.2 Extension to the Lipschitz Case

The same approach that showed promise in the LTI case is now adopted for the case of nonlinear Lipschitz systems, namely systems defined by equations (3.1)-(3.3) and subject to the faulty output:

$$y(t) = Cx(t) + f_s(t) \tag{4.24}$$

At this point, general sensor faults are assumed (i.e, no assumptions are made on the time-domain or frequency-domain properties of the faults). The dynamic observer in (3.14)-(3.18), with the residual:

$$r = y - \hat{y} \tag{4.25}$$
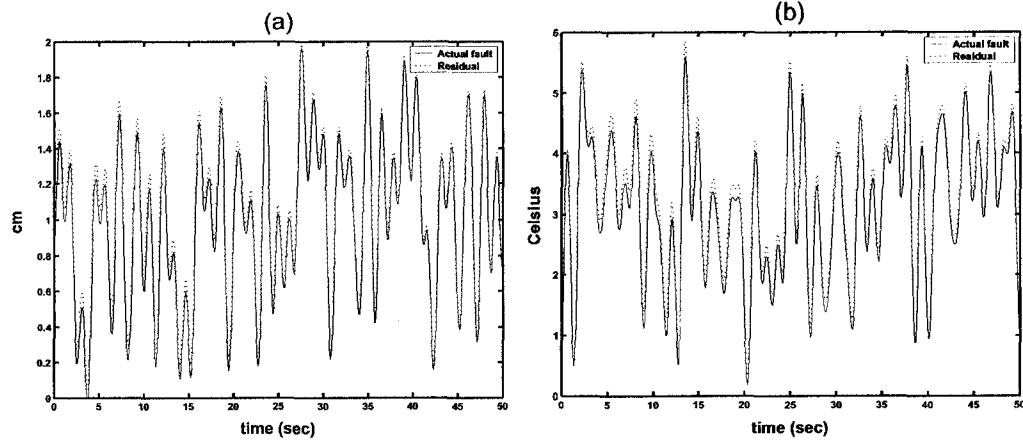
Figure 4.10: (a) Fault Estimation for y_1, (b) Fault Estimation for y_2 .

is used as the residual generator, and the objective is to develop conditions on the observer gain K that guarantee fault detection according to Definition 4.1. To this end, it can be seen that the residual dynamics are given by:

$$\dot{e}(t) = Ae(t) - \eta(t) + \tilde{\phi}(t) \tag{4.26}$$

$$r(t) = Ce(t) + f_s(t) \tag{4.27}$$

where $e = x - \hat{x}$ is the observer estimation error, and $\tilde{\phi} = \Phi(x, u, t) - \Phi(\hat{x}, u, t)$.

By defining the variables:

$$\tau \triangleq \begin{bmatrix} \tau_1 \\ \tau_2 \end{bmatrix} = \begin{bmatrix} \tilde{\phi} \\ f_s \end{bmatrix}$$

$$\nu = \eta = K \ (y - \hat{y}) \tag{4.28}$$

$$\zeta = e = x - \hat{x}$$

$$\varphi = y - \hat{y} = Ce + f_s$$

Then, the error dynamics in (4.26) can still be represented by Figure 2.2 (same as the LTI case) but with the following equations:

$$\dot{z} = \begin{bmatrix} A \end{bmatrix} z + \begin{bmatrix} \begin{bmatrix} I_n & 0_{np} \end{bmatrix} & -I_n \end{bmatrix} \begin{bmatrix} \tau \\ \nu \end{bmatrix} \tag{4.29}$$

$$\begin{bmatrix} \zeta \\ \varphi \end{bmatrix} = \begin{bmatrix} I_n \\ C \end{bmatrix} z + \begin{bmatrix} \begin{bmatrix} 0_n & 0_{np} \end{bmatrix} & 0_n \\ \begin{bmatrix} 0_{pn} & I_p \end{bmatrix} & 0_{pn} \end{bmatrix} \begin{bmatrix} \tau \\ \nu \end{bmatrix} \tag{4.30}$$

The following theorem is an extension of the observer asymptotic convergence result (obtained in Chapter 3) to the fault detection problem. It uses the previous standard form to give the sufficient condition for achieving fault detection according to Definition 4.1. The proof is similar to Theorem 3.4, and is hence omitted.

Theorem 4.6 *Given the nonlinear system of equations (3.1)-(3.3), the residual generator (3.14)-(3.18), (4.25) achieves fault detection (according to Definition 4.1) for the sensor faults in (4.24) for all $\Phi(\cdot, \cdot, \cdot)$ satisfying (3.3) with a Lipschitz constant α if the observer gain K is chosen s.t:*

$$sup_{\omega \in \mathbb{R}} \ \sigma_{max}[\hat{T}_{\zeta \tau_1}(j\omega)] < \frac{1}{\alpha} \tag{4.31}$$

4.2.1 A Multiobjective Optimization Problem

Throughout the rest of this chapter, we will assume the fault detection objective (i.e, the condition stated in Theorem 4.6) to be satisfied for the residual generator (3.14)-(3.18),(4.25). We will further consider the fault identification problem (according to Definition 4.3) with the objective to make the residual converge to the sensor fault vector achieving detection and estimation at the same time. In this section, we focus on the case when the sensor faults are in a narrow frequency band around a nominal frequency ω_o. Existence conditions for solving this problem are provided, and a numerical LMI design procedure is presented using the dynamic observer structure.

Since the residual "r" is given from equation (4.27), it is then clear that the observer estimation error "e" constitutes an important part of the residual response, and that by minimizing "e" the residual converges to f_s which guarantees fault identification in this case. In fact, the estimation error e can be represented by the feedback interconnection in Figure 4.11 (which is the modified version of Figure 3.1 introduced in Chapter 3), where f_s is the sensor fault vector that affect the system. Hence, minimizing "e" is equivalent to minimizing the effect of f_s on the feedback interconnection of Figure 4.11.

In this section, we consider the solution of this minimization problem in an $\mathcal{L}_2$ sense (when f_s is in a narrow frequency band around a nominal frequency ω_o) by using the dynamic observer structure introduced in Chapter 3. It is easy to show (same as for the LTI case in section 4.1.1) that the problem is not tractable for the classical structure in (3.4)-(3.5).

Towards that goal, same as in section 4.1.1, we will first assume that the Fourier
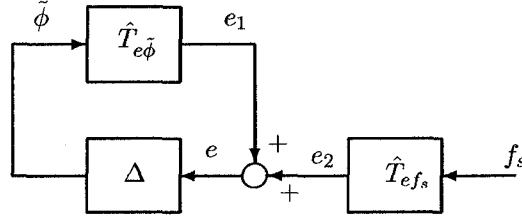
Figure 4.11: Feedback Interconnection: the Sensor Fault Case.

transform of the sensor fault $F_s(j\omega)$ has a frequency pattern restricted to the narrow band $\omega_o \pm \Delta\omega$ as follows:

$$\|F_s(j\omega)\| \leq \begin{cases} \Omega \; ; & |\omega - \omega_o| < \Delta\omega \\ \delta \; ; & \text{otherwise} \end{cases} \tag{4.32}$$

where δ is a small neglected number for the frequency magnitudes outside the region of interest, and where Ω is a positive upper bound on these magnitudes inside the considered domain. We will then define an observer gain K as optimal if $\| e \|_{\mathcal{L}_2}$ can be made arbitrarily small for all possible sensor faults satisfying (4.32). But by applying the small gain theorem to Figure 4.11 when fault detection is satisfied (i.e, when K satisfies $\| \hat{T}_{e\tilde{\phi}} \|_\infty = \mu < \frac{1}{\alpha}$) we have: $\|e\|_{\mathcal{L}_2} \leq \frac{1}{1-\mu\alpha} \|e_2\|_{\mathcal{L}_2}$. And since (as $\Delta\omega \to 0$), $\hat{T}_{ef_s}(j\omega) \to \hat{T}_{ef_s}(j\omega_o)$ then we have $\|e_2\|_{\mathcal{L}_2} \leq \sigma_{max}\left(\hat{T}_{ef_s}(j\omega_o)\right) \|f_s\|_{\mathcal{L}_2}$, and therefore, it is easy to see that an optimal gain K is one that satisfies $\hat{T}_{ef_s}(j\omega_o) = 0$. By assuming that the fault detection objective is satisfied (as stated in Theorem 4.6), it follows that *fault identification* according to Definition 4.3 is satisfied if the following two conditions are satisfied: (i) $\| \hat{T}_{e\tilde{\phi}} \|_\infty < \frac{1}{\alpha}$. (ii) $\hat{T}_{ef_s}(j\omega_o) = 0$, where the first one is a necessary condition in order to achieve *fault detection*.

Based on the previous discussion, we will define an optimal residual generator as follows:

Theorem 4.7 *(Lipschitz optimal residual generator for narrow frequency band): An observer of the form (3.14)-(3.18),(4.25) is said to be an optimal residual generator for the sensor faults identification problem (with faults in a narrow frequency band around ω_o) if the observer gain K satisfies $\| \hat{T}_{e\tilde{\phi}} \|_\infty < \frac{1}{\alpha}$ and $\hat{T}_{ef_s}(j\omega_o) = 0$, for the standard setup in Figure 2.2 where the plant G has the state space representation in (4.16) with the matrices defined in (4.29)-(4.30).*

The same theorem used in the LTI case (Theorem 4.2) can be used to show that the

classical observer structure in (3.4)-(3.5) can never be an optimal residual generator according to Theorem 4.7, which shows the importance of having a dynamic observer gain in this case.

In section 4.1.1, we showed that for the special case $\alpha = 0$ (the LTI case), an analytical solution exists by using the dynamical framework. In the following section (section 4.2.2), we provide a numerical approach based on Linear Matrix Inequalities (LMI) for the more general case of α by modeling the problem as a convex multiobjective optimization problem using the dynamic observer structure introduced in Chapter 3.

4.2.2   LMI Design Procedure

After defining the *fault identification problem* as the two-objective problem in Theorem 4.7, we now show that the second objective, i.e $\hat{T}_{ef_s}(j\omega_o) = 0$, can also be modeled as a weighted H_∞ problem. To this end, we first note that for an observer gain K that satisfies the fault detection condition (as stated in Theorem 4.6), the following two statements are equivalent:

   (i) $\hat{T}_{ef_s}(j\omega_o) = 0$.

   (ii) $W(s)\hat{T}_{ef_s}(s) \in RH_\infty$.

where $W(s) = Diag_p(\frac{1}{s})$ if $\omega_o = 0$ and $W(s) = Diag_p(\frac{1}{s^2+\omega_o^2})$ if $\omega_o \neq 0$.

The equivalence of the previous two statements can be seen by first noting that the condition in Theorem 4.6 implies that $\| \hat{T}_{e\tilde{\phi}} \|_\infty < \frac{1}{\alpha}$ and hence that $\hat{T}_{e\tilde{\phi}} \in RH_\infty$. It then follows that $\hat{T}_{ef_s}(s) \in RH_\infty$ since $\hat{T}_{ef_s}$ and $\hat{T}_{e\tilde{\phi}}$ both have the same state transition matrix. Finally, since $\hat{T}_{ef_s}(j\omega_o) = 0$ corresponds to $j\omega_o$ being a system zero of $\hat{T}_{ef_s}(s)$ (which is equivalent to cancelling the poles of $W(s)$ on the imaginary axis), it is then easy to see that $\hat{T}_{ef_s}(j\omega_o) = 0$ is equivalent to having $W(s)\hat{T}_{ef_s}(s) \in RH_\infty$.

According to the previous discussion, it follows that the objective $\hat{T}_{ef_s}(j\omega_o) = 0$ can be restated as follows:

$$\exists \epsilon > 0 \text{ such that } \left\{ \epsilon \parallel W(s)\hat{T}_{ef_s}(s) \parallel_\infty < \frac{1}{\alpha} \right\}$$

where the scalar ϵ is used for compatibility with the first objective (i.e, $\| \hat{T}_{e\tilde{\phi}} \|_\infty < \frac{1}{\alpha}$). It then follows that the two objectives can be combined in the unified framework in Figure 4.12, where the plant G has the state space representation in (4.16) with the matrices defined in (4.29)-(4.30), and with the weighting W defined above.
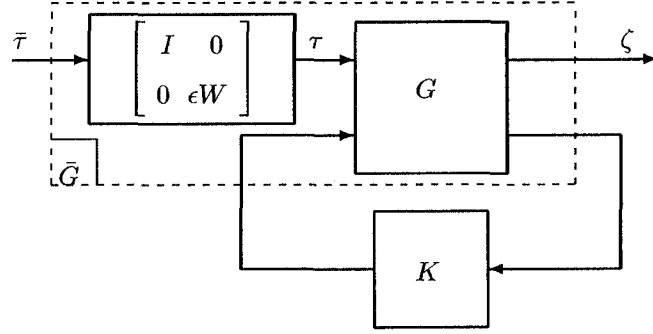
Figure 4.12: Weighted Standard Setup: the Lipschitz Case.

It can be seen that the augmented plant $\bar{G}$ in Figure 4.12 is given by:

$$
\hat{\bar{G}}(s) = \left[\begin{array}{c|cc} \bar{A} & \bar{B}_1 & \bar{B}_2 \\ \hline \bar{C}_1 & \bar{D}_{11} & \bar{D}_{12} \\ \bar{C}_2 & \bar{D}_{21} & \bar{D}_{22} \end{array} \right] = \left[\begin{array}{c|cc} \left[\begin{array}{cc} A_\theta & 0_{\ell n} \\ 0_{n\ell} & A \end{array} \right] & \left[\begin{array}{cc} 0_{\ell n} & B_\theta \\ I_n & 0_{np} \end{array} \right] & \left[\begin{array}{c} 0_{\ell n} \\ -I_n \end{array} \right] \\ \hline \left[\begin{array}{cc} 0_{n\ell} & I_n \end{array} \right] & \left[\begin{array}{cc} 0_n & 0_{np} \end{array} \right] & \left[\begin{array}{c} 0_n \end{array} \right] \\ \left[\begin{array}{cc} \epsilon C_\theta & C \end{array} \right] & \left[\begin{array}{cc} 0_{pn} & 0_p \end{array} \right] & 0_{pn} \end{array} \right] \quad (4.33)
$$

where

$$
\left\{ \begin{array}{l} \ell{=}p, \quad A_\theta{=}0_p, \quad B_\theta{=}I_p, \quad C_\theta{=}I_p \ ; \qquad \text{if } \omega_o{=}0 \\ \ell{=}2p, \quad A_\theta{=}Diag_p \left(\left[\begin{array}{cc} 0 & 1 \\ -\omega_o^2 & 0 \end{array} \right] \right), B_\theta{=}Diag_p \left(\left[\begin{array}{c} 0 \\ 1 \end{array} \right] \right), C_\theta{=}Diag_p \left(\left[\begin{array}{cc} 1 & 0 \end{array} \right] \right) ; \quad \omega_o \neq 0 \end{array} \right.
$$

$$(4.34)$$

Based on the previous results, the following theorem redefines the identification problem in Theorem 4.7 as follows:

Theorem 4.8 *Given the nonlinear system of equations (3.1)-(3.2), there exists an optimal residual according to Theorem 4.7, for all $\Phi(\cdot, \cdot, \cdot)$ satisfying (3.3) with a Lipschitz constant α if and only if $\exists \epsilon > 0$ and a controller K satisfying $\| \hat{T}_{\zeta \bar{\tau}} \|_\infty < \frac{1}{\alpha}$ for the setup in Figure 4.12 where $\bar{G}$ has the state space representation in (4.33).*

Proof: a direct result of Theorem 4.7 and of the discussion preceding (4.33). □

However, standard H_∞ tools can not be directly applied for the H_∞ problem defined in Theorem 4.8. For instance the Riccati approach in [122] can not be implemented since

the augmented plant $\bar{G}$ in (4.33) does not satisfy the needed regularity assumptions. Moreover, the LMIs in equation (2.30)-(2.32) are not feasible due to the poles that $\bar{G}$ has on the imaginary axis, making the use of the LMI approach in [40] impossible.

In the following, we propose a numerical approach to solve this problem by replacing the weightings $W(s)$ by the modified weightings $\bar{W}(s)$ where $\bar{W}(s) = Diag_p(\frac{1}{s+\lambda})$ if $\omega_o = 0$ and $\bar{W}(s) = Diag_p(\frac{1}{s^2+2\lambda\omega_o s+\omega_o^2})$ if $\omega_o \neq 0$, with $\lambda \in \mathbb{R}^+$. With this change, the augmented plant $\bar{G}$ in Figure 4.12 is still given by equation (4.33), but where A_θ is now given by:

$$A_\theta = \begin{cases} Diag_p(-\lambda) \quad ; \quad \omega_o = 0 \\ Diag_p\left(\begin{bmatrix} 0 & 1 \\ -\omega_o^2 & -2\lambda\omega_o \end{bmatrix}\right); \quad \omega_o \neq 0 \end{cases} \qquad (4.35)$$

which has no poles on the imaginary axis.

Using this modified augmented plant and the result in Theorem 2.1, we then propose the following *convex optimization problem* to solve the problem defined in Theorem 4.8:

$$min_{R,S} \ \lambda$$

subject to " the 3 LMIs in (2.30)-(2.32) with $\gamma = \frac{1}{\alpha}$ "

where the matrices in (2.30)-(2.32) are replaced by the corresponding matrices in (4.33), (4.34) and (4.35).

The set of all admissible observer gains K for a given λ can then be parameterized using R, S by using the result in [40]. It can also be seen, that these LMIs are feasible for all $\lambda > 0$, and that minimizing λ in this case is equivalent to minimizing $\sigma_{max}\left(\hat{T}_{ef_s}(j\omega_o)\right)$. This guarantees that the proposed optimization problem converges to the existing solution as $\lambda \to 0$.

Comments

- From the special cases of interest is the case of sensor bias, where the previous approach can be used to get an *exact* estimation of all sensor biases at the same time. An important advantage over the adaptive approaches used to diagnose sensor faults in nonlinear systems, such as [22, 32, 109, 111] is the ability to diagnose piecewise constant biases with the same observer. This will be shown in simulation in section 4.3. Moreover, unlike adaptive techniques, the proposed approach is not limited to sensor biases and can be used to diagnose faults of any harmonics.

- In case of multiple frequency bands, a bank of observers can be used where each one estimates the faults vector in a specific range as in Figure 4.13. These multiple estimates can then be used to restore the original fault vector.
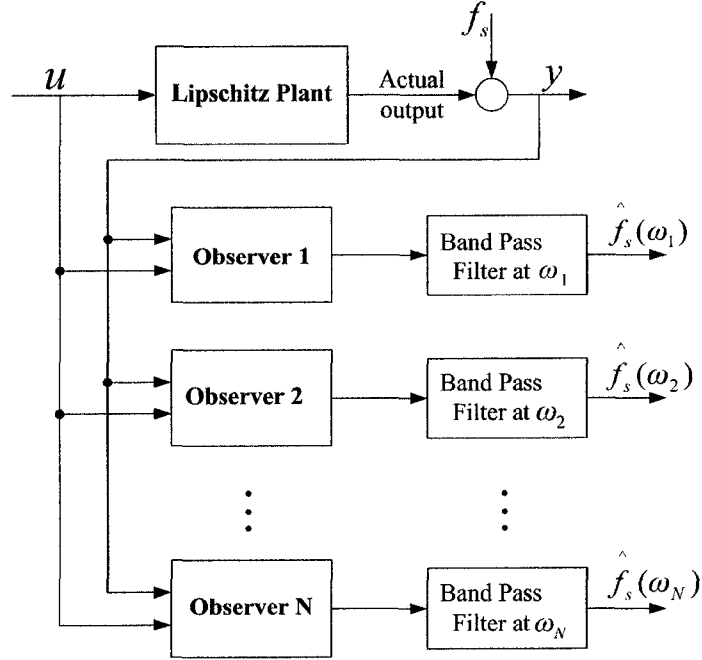
Figure 4.13: Residual Set over a Frequency Range.

4.2.3   The Low and High Frequency Ranges

These two cases are very similar to the narrow frequency band, except that appropriate weightings should be used to emphasize the considered frequency range. For the low frequency range, using the same approach in section 4.1.2, we introduce the weighting $\hat{w}_{lmod}(s) = \frac{as+b}{s+\lambda}$ (see section 4.1.2 for guidelines on the selection of the parameters a, b and λ).

It is easy to see that, with this weighting, the augmented plant $\bar{G}$ in Figure 4.12 can be represented as follows (compare with (4.33) in the narrow frequency band case):

$$
\hat{\bar{G}}(s) = \left[\begin{array}{c|cc} \bar{A} & \bar{B}_1 & \bar{B}_2 \\ \hline \bar{C}_1 & \bar{D}_{11} & \bar{D}_{12} \\ \bar{C}_2 & \bar{D}_{21} & \bar{D}_{22} \end{array} \right] = \left[\begin{array}{c|cc} \left[\begin{array}{cc} A_\theta & 0_{pn} \\ 0_{np} & A \end{array}\right] & \left[\begin{array}{cc} 0_{pn} & B_\theta \\ I_n & 0_{np} \end{array}\right] & \left[\begin{array}{c} 0_{pn} \\ -I_n \end{array}\right] \\ \hline \left[\begin{array}{cc} 0_{np} & I_n \\ \epsilon C_\theta & C \end{array}\right] & \left[\begin{array}{cc} 0_n & 0_{np} \\ 0_{pn} & \epsilon D_\theta \end{array}\right] & \left[\begin{array}{c} 0_n \\ 0_{pn} \end{array}\right] \end{array} \right] \tag{4.36}
$$

where $A_\theta = Diag_p(-\lambda)$, $B_\theta = I_p$, $C_\theta = Diag_p(b - a\lambda)$ and $D_\theta = Diag_p(a)$.

Similar to the narrow frequency band case, the assumptions of Theorem 2.1 are now satisfied and the LMI approach in [40] can then be used to solve the associated H_∞ problem. To this end, we define the continuous H_∞ problem associated with the low frequency range as follows:

Definition 4.5 *(Lipschitz low frequency H_∞): Given $\lambda > 0$, $\epsilon > 0$, find S, the set of admissible controllers K satisfying $\| \hat{T}_{\zeta\bar{r}} \|_\infty < \gamma$ for the setup in Figure 4.12 where $\bar{G}$ has the state space representation (4.36).*

Based on the previous results, we now present the main result of this section in the form of the following definition for an optimal residual generator in $\mathcal{L}_2$ sense:

Theorem 4.9 *(Lipschitz optimal residual for low frequencies): An observer of the form (3.14)-(3.18), (4.25) is an optimal residual generator for the sensor fault identification problem (with low frequency faults below the cutoff frequency ω_l) if the dynamic gain $K \in S^*$ (the set of controllers solving the H_∞ problem in Definition 4.5 with $\gamma = 1/\alpha$ and with the minimum possible λ).*

Comments

- Definition 4.5 and Theorem 4.9 can be viewed as the extensions of Definition 4.4 and Theorem 4.5 to the Lipschitz case.

- A residual generator that is optimal in the sense of Theorem 4.9 can be found by solving a convex optimization problem similar to the one presented in section 4.2.2. Existing software packages can be used to solve this optimization problem.

- In the high frequency case, where sensor faults are confined to the region $[\omega_h, \infty)$, the weighting $\hat{w}_{hmod}(s) = \frac{s+(a\times b)}{\lambda s+b}$, with "$b$" selected as w_h and "a" as an arbitrary small number for $|\hat{w}_h(j\omega)|$ as $\omega \to 0$, and with an arbitrary small $\lambda > 0$. Similar to the low frequency case, the augmented $\bar{G}$ is also given from (4.36) but with A_θ, B_θ, C_θ and D_θ as $Diag_p(-\frac{b}{\lambda})$, I_p, $Diag_p(\frac{a\times b}{\lambda} - \frac{b}{\lambda^2})$ and $Diag_p(\frac{1}{\lambda})$ respectively. An optimal residual generator can be defined in a similar way to Theorem 4.9 (details are omitted due to similarity).
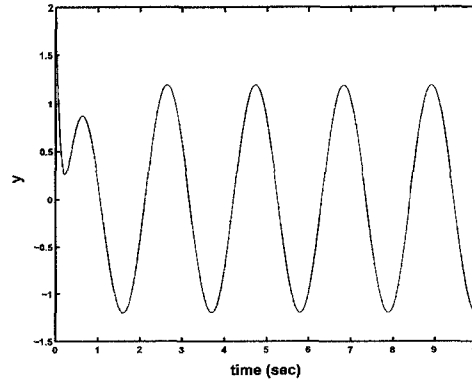
Figure 4.14: Actual System Output for the Controlled Process.

4.3   A Design Example

We reconsider the numerical example introduced in Chapter 3. We assume $k = 1.5$, and hence the Lipschitz constant is $\alpha = 1.5$ (see section 3.4 for more details about the model). In section 3.4, the objective of pure state estimation (without any faults or disturbances affecting the system) was considered. We here consider the sensor fault diagnosis problem. To this end, we first assume the system initial condition as $x(0) = \begin{bmatrix} 1.6 & 2 \end{bmatrix}^T$, and we use a state feedback control law to make the output track a sinusoidal input as shown in Figure 4.14. In [92], the design algorithm fails if the original system matrices are used, and the gain matrix L needed to use the observer (3.4)-(3.5) was obtained (after using a state transformation) as $L = \begin{bmatrix} 2 & 4 \end{bmatrix}^T$. Using the LMI approach to solve the design problem in theorem 4.6, and *without using any state transformation*, the dynamic gain for the observer (3.14)-(3.18) is obtained as:

$$A_L = \begin{bmatrix} -11.7202 & 3.3452 \\ -9.8614 & -12.0657 \end{bmatrix}, B_L = \begin{bmatrix} -6.5969 \\ -12.0657 \end{bmatrix}, C_L = \begin{bmatrix} -2.6961 & -7.4884 \\ -7.3739 & -3.9456 \end{bmatrix} \text{ and } D_L = \begin{bmatrix} 0 \\ 0 \end{bmatrix}.$$

Figure 4.15 show the observers performance, where the initial condition for both observers is taken as $\hat{x}(0) = \begin{bmatrix} 0 & 0 \end{bmatrix}$. This figure shows the improvement in the transient response by using the dynamic observer gain. This is an important advantage for the fault detection objective presented in theorem 4.6.

We now consider the fault identification problem. In this case, the system is assumed to be affected by sensor biases, where the measured output is affected by a piecewise constant fault. This is the special case where $\omega_o = 0$ for the problem in section 4.2.1, and using the LMI design discussed in section 4.2.2, the dynamic gain for the observer (3.14)-(3.18) that
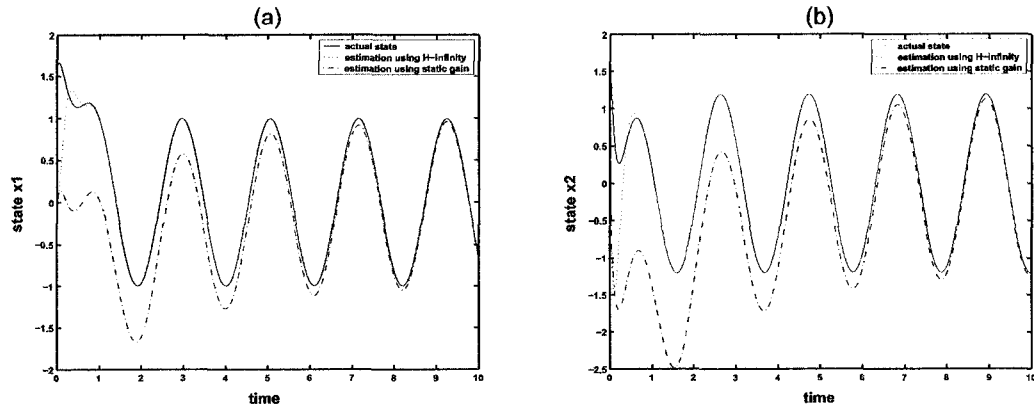
Figure 4.15: (a) Estimation of State x_1, (b) Estimation of State x_2.

achieves fault identification is obtained (at $\lambda = 10^{-15}$) as:

$$A_L = \begin{bmatrix} -2.3056 & -0.8143 & -4.3747 \\ 2.4066 & -4.9397 & 2.3329 \\ -8.1999 & -2.3151 & -9.8718 \end{bmatrix}, B_L = \begin{bmatrix} 1.6009 \\ -1.7743 \\ 5.8222 \end{bmatrix}, C_L = \begin{bmatrix} 0.2305 & -1.2755 & 8.4409 \\ 0.4083 & 0.7954 & 13.6105 \end{bmatrix}$$

and $D_L = \begin{bmatrix} 0 & 0 \end{bmatrix}^T$. Using this observer, a time varying sensor bias is successfully estimated as seen in Figure 4.16.
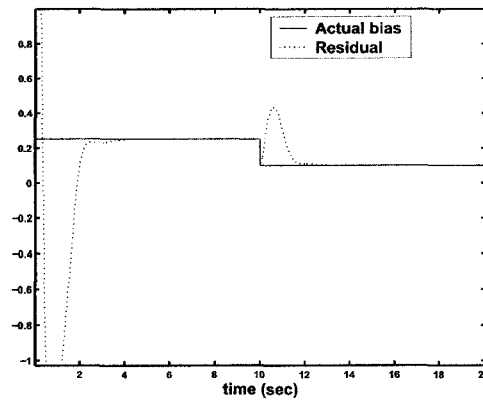
Figure 4.16: Bias Estimation.

The state and output estimation errors also converge to zero by using this observer. Figure 4.17 shows the state estimation errors in this case.
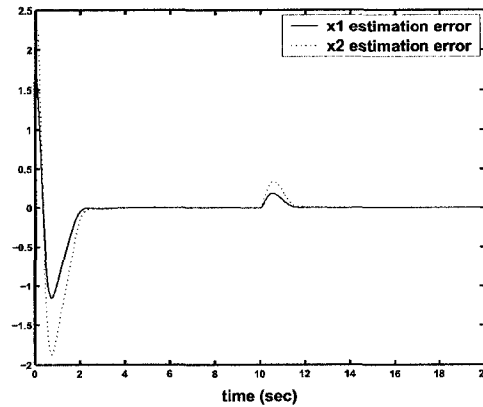
Figure 4.17: State Estimation Errors.

4.4 Conclusion

In this chapter, a new LMI observer design for Lipschitz nonlinear systems is proposed and is applied in the fault diagnosis problem. This design offers extra degrees of freedom over the classical static gain structure and we show how this freedom can be used for the sensor faults and state estimations problems. For the narrow frequency band case, the problem is shown to be equivalent to an output zeroing problem for which a dynamic gain is necessary. The use of appropriate weightings, for different frequency patterns, to transform these problems into standard H_∞ optimal control problems is also demonstrated. A systematic design procedure that can be carried out using commercially available software products is presented.

Chapter 5

Robustness using Unknown Input Observers

In this chapter, we consider the robustness problem associated with the fault diagnosis schemes developed in Chapter 4. We start by generalizing the standard Unknown Input Observer (UIO) approach (used to deal with additive uncertainties in LTI systems) to the Lipschitz case. The proposed observer is then applied to the robust sensor fault diagnosis problem, by modelling the problem as a two-objectives optimization problem similar to the one introduced in Chapter 4, and which is solvable using numerical techniques. A discussion on the applicability of the previous results to more general system faults is also presented[1].

5.1 Background Results

As discussed in section 1.2, the robustness problem, which is the problem of considering the effect of uncertainties in the FDI system, is of crucial importance in all model-based FDI techniques (including the observer-based approach adopted in this thesis). This is due to the fact that any discrepancies between the actual process and its model (such as modelling errors, plant disturbances and sensor noise) corrupt the state reconstruction given by the observer and constitute a source of false and missed alarms which can corrupt the FDI system performance. Therefore, for successful operation of the observer-based FDI system,

---

[1]The results in this chapter have been published in the article: "A.M. Pertew, H.J. Marquez and Q. Zhao, H_∞ Synthesis of Unknown Input Observers for Non-linear Lipschitz Systems," International Journal of Control, Vol. 78, No. 15, pp. 1155-1165, October 2005.

certain measures of robustness need to be introduced in the observer design problem.

One of the most successful robust observer design techniques is the use of the disturbance decoupling principle, in which the estimation error is designed to be insensitive to unknown additive uncertainties. This problem deals with the model in (2.33)-(2.34), where the vector "d" represents the uncertainty terms and where "E" is referred to as the *unknown input distribution matrix* and is assumed to be a known full column rank matrix. This problem is also referred to as the *unknown input observer (UIO)* design and it dates back to 1975 where Wang [110] proposed a minimal order UIO structure for linear systems with both known and unknown inputs. After this important work, several approaches for designing reduced order and full order UIOs have been proposed, including the geometric approach of Bhattacharyya [8], the inversion algorithm of Kobayashi and Nakamizo [69], the matrix algebra method of Watanabe and Himmelblau [113], the singular value decomposition technique of Fairman [30] and the algebraic approaches of Hou and Müller in [60] and Patton, Chen and Zhang in [14] (see also [21, 51, 61, 70] for different UIO design techniques). Achieving less restrictive existence conditions and more direct design procedures has always been a challenge in this area. The UIO application in fault diagnosis has also attracted many researchers. Watanabe and Himmelblau introduced the concept of UIO for robust sensor fault diagnosis in systems with modeling uncertainty [113]. Their approach was later extended in a series of papers by Wünnenberg and Frank (see [39, 118] and references therein) and also by Patton and Chen (see [13, 14, 87]) to the detection of both sensor and actuator faults in which case the unknown input appears both in the state and output equations.

Despite these success stories, most of the previous results are restricted to linear systems and results on nonlinear UIO are scarce. A direct extension of the linear results to the nonlinear case was considered by Wünnenberg in [117]. His approach was referred to as the NUIO (Nonlinear UIO) and considered a class of nonlinear systems with nonlinearities that are functions of inputs and outputs. However, this class of nonlinear systems is rather limited and many physical systems can not be modelled in this way. Another limitation is the difficulty of transforming a general nonlinear system into the required form. An alternative approach referred to as the DDNO (Disturbance Decoupling Nonlinear Observer) was presented in a series of papers by Seliger and Frank [38, 101, 102]. The class of nonlinear systems considered by the DDNO is more general and the basic idea is the use of a nonlinear state transformation to satisfy the decoupling condition. However, the existence conditions for such a transformation are derived from the Frobenius theorem and are rather restrictive.

Another drawback of the DDNO is that the transformation leads to another nonlinear system for which a nonlinear observer design is not a straightforward and tractable problem. It is also important to note that much work has been done on estimating the unknown input distribution matrix (the matrix E in (2.33)) when it is not fully known (see for example [12, 29, 46, 47, 87, 88, 89]).

In this chapter, we consider the UIO design problem for nonlinear Lipschitz systems and its application to the fault diagnosis problem that we studied in Chapter 4. In other words, we consider the extension of the model in (2.33)-(2.34) to the following:

$$\dot{x}(t) = Ax(t) + \Gamma(u,t) + \Phi(x,u,t) + Ed(t), \quad E \in \mathbb{R}^{n \times r} \tag{5.1}$$

$$y(t) = Cx(t) + f_s(t), \quad A \in \mathbb{R}^{n \times n}, \quad C \in \mathbb{R}^{p \times n} \tag{5.2}$$

where Φ satisfies the Lipschitz condition in (3.3), and where the term $d(t)$ represents unknown additive disturbances and/or modelling uncertainties. Our main objective is to extend the fault diagnosis results in section 4.2 to this case. We will show that, with the same necessary and sufficient conditions of Theorem 2.3, the Lipschitz UIO design problem is solvable and can be used to diagnose different sensor faults using the numerical approach introduced in Chapter 4. The application of the proposed structure to more general system faults will also be discussed.

5.2 Lipschitz Unknown Input Observer

Consider the system in (5.1)-(5.2). We first consider the case of no sensor faults (i.e, $f_s = 0$). We propose the following dynamical observer structure to achieve globally asymptotically convergent state estimates (i.e, $\hat{x} \to x$ as $t \to \infty$) which are decoupled from the uncertainty term $d(t)$ in this case:

$$\dot{z}(t) = w_1(t) + w_2(t) + T\,\Gamma(u,t) + T\Phi(\hat{x},u,t) \tag{5.3}$$

$$\hat{x}(t) = z(t) + H\,y(t) \tag{5.4}$$

$$\hat{y}(t) = C\hat{x}(t) \tag{5.5}$$

where $w_1(t)$ and $w_2(t)$ are obtained by applying dynamical compensators of arbitrary orders on the vectors z and y respectively. In other words, w_1 and w_2 are given by :

$$\dot{\xi}_1 = A_F\,\xi_1 + B_F\,z \tag{5.6}$$

$$w_1 = C_F\,\xi_1 + D_F\,z \tag{5.7}$$

and

$$\dot{\xi}_2 = A_L\ \xi_2 + B_L\ y \tag{5.8}$$

$$w_2 = C_L\ \xi_2 + D_L\ y \tag{5.9}$$

This can be represented by the structure in Figure 5.1.
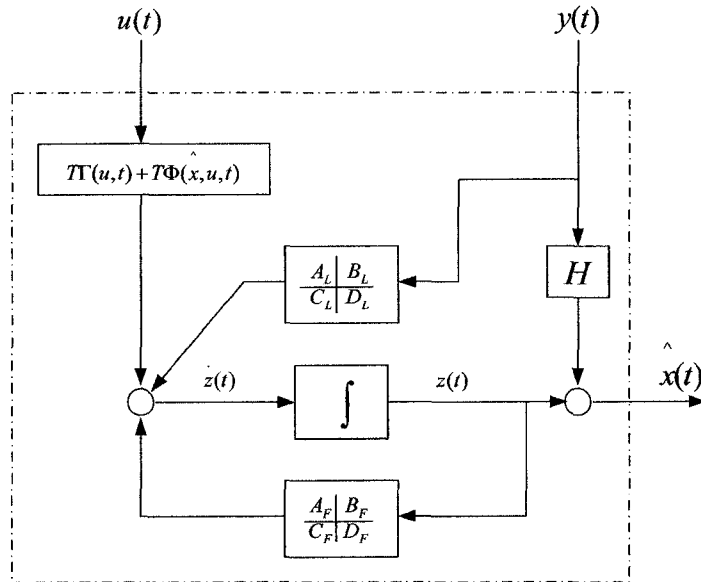
Figure 5.1: Dynamic Structure of the UIO.

Compare this structure to the one in (2.35)-(2.36) where it can be seen that the new structure offers more dynamics (F and L are replaced with dynamic compensators). This will be used in this section to tackle the Lipschitz UIO (LUIO) design problem.

As a step towards that goal, we consider first its use to achieve "local" asymptotic convergence of the state estimates. The following lemma develops conditions that guarantee the observer stability in this case (see Appendix A.3 for the detailed proof):

Lemma 5.1 *The error dynamics of (5.3)-(5.9) as an observer for (5.1)-(5.2) (with $f_s = 0$) is locally asymptotically stable and decoupled from the uncertainty term $d(t)$ if the following*

conditions are satisfied:

$$HCE = E \tag{5.10}$$

$$T = I_n - HC \tag{5.11}$$

$$\begin{bmatrix} A_F & B_F \\ C_F & D_F \end{bmatrix} stable;\ with \begin{cases} A_F = & A_L \\ B_F = & B_{L1}C \\ C_F = & -C_L \\ D_F = & A - HCA - D_{L1}C \end{cases} \tag{5.12}$$

$$D_{L2} = D_F H \tag{5.13}$$

$$B_{L2} = -B_F H \tag{5.14}$$

$$B_L = B_{L1} + B_{L2} \tag{5.15}$$

$$D_L = D_{L1} + D_{L2} \tag{5.16}$$

In the following theorem, we show that same conditions of theorem 2.3 (which were necessary and sufficient to satisfy (2.37)-(2.41)) are still necessary and sufficient for (5.10)-(5.16).

Theorem 5.1 *There exists a dynamic UIO for the system (5.1)-(5.2) (according to the conditions of Lemma 5.1) if and only if :*

(i) rank $(CE) = rank\ (E)$ \hfill (5.17)

(ii) $(\bar{A}, C)$ is a detectable pair, where $\bar{A} = A - E\left[(CE)^T CE\right]^{-1}(CE)^T CA.$ \hfill (5.18)

Proof: The proof is constructive (i.e, shows the steps needed to design a dynamic UIO). It is a direct result of the proof of theorem 2.3 and of the interpretation of conditions (5.12)-(5.16) as follows. It was proved in [13] that (5.10) is solvable if and only if (5.17) is satisfied and that the general solution is

$$H = E(CE)^+ + H_0 \left[I_p - CE(CE)^+\right] \tag{5.19}$$

where $H_0 \in \mathbb{R}^{n \times p}$ is an arbitrary matrix and $(CE)^+$ is the left inverse of (CE) which is:

$$(CE)^+ = \left[(CE)^T CE\right]^{-1}(CE)^T$$

The rest of the proof follows by noting that satisfying (5.12) is equivalent to finding A_L, C_L, B_{L1} and D_{L1} such that $\begin{bmatrix} A_L & B_{L1}C \\ -C_L & A - HCA - D_{L1}C \end{bmatrix}$ is stable. This is equivalent to the stabilization problem in Figure 5.2 which is solvable if and only if $(A - HCA, C)$ is detectable.

Plant "G"

$$\left[\begin{array}{c|c} A - HCA & -I_n \\ \hline C & 0_{pn} \end{array}\right]$$

Controller "K"

$$\left[\begin{array}{c|c} A_L & B_{L1} \\ \hline C_L & D_{L1} \end{array}\right]$$
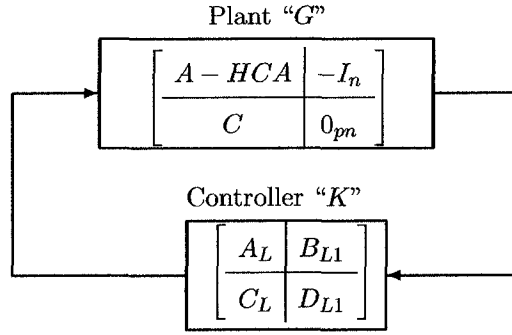
Figure 5.2: Stabilization Problem.

Finally, notice that for any H that satisfies (5.19), $(A - HCA, C)$ is detectable iff $(\bar{A}, C)$ is detectable (as proven in [13]) where $\bar{A}$ is given by (5.18). Therefore, conditions (i) and (ii) are necessary and sufficient to satisfy (5.10)-(5.16) and the proof is complete. $\qquad\square$

As a conclusion, with the same existence conditions of the UIO in [14], the locally stable LUIO design problem is reduced to the stabilization problem in Figure 5.2. The advantage of the dynamic framework is now evident since the solution to this stabilization problem is a *set* of controllers [122]. Therefore, disturbance decoupling is satisfied with extra degrees of freedom. We will make use of this freedom to solve the original problem of "global" observer stability as follows. It can be seen that the error dynamics of the observer (5.3)-(5.9) is given from (see proof of Lemma 5.1 in Appendix A.3):

$$\dot{\xi} = A_F \xi + B_F e \tag{5.20}$$

$$\dot{e} = C_F \xi + D_F e + T \left(\Phi(x, u, t) - \Phi(\hat{x}, u, t) \right) \tag{5.21}$$

This can also be represented (using (5.12)) by the transfer function between τ and ζ in the following standard form:

$$\dot{\psi} = \left[A - HCA \right] \psi + \left[T \quad -I_n \right] \begin{bmatrix} \tau \\ \nu \end{bmatrix} \tag{5.22}$$

$$\begin{bmatrix} \zeta \\ \varphi \end{bmatrix} = \begin{bmatrix} I_n \\ C \end{bmatrix} \psi + \begin{bmatrix} 0_n & 0_n \\ 0_{pn} & 0_{pn} \end{bmatrix} \begin{bmatrix} \tau \\ \nu \end{bmatrix} \tag{5.23}$$

where

$$\tau = \tilde{\phi} = \Phi(x, u, t) - \Phi(\hat{x}, u, t)$$

$$\nu = K\,(y - \hat{y}) \tag{5.24}$$

$$\zeta = e = x - \hat{x}$$

$$\varphi = y - \hat{y}$$

and where K is the dynamic controller

$$K = \left[\begin{array}{c|c} A_L & B_{L1} \\ \hline C_L & D_{L1} \end{array} \right] \tag{5.25}$$

This can also be represented by the standard setup figure (Figure 2.2) where the operator G has the state space representation shown in (5.26) with the matrices defined in (5.22)-(5.23) and where the controller K is given from (5.25).

$$\hat{G}(s) = \left[\begin{array}{c|cc} A & B_1 & B_2 \\ \hline C_1 & D_{11} & D_{12} \\ C_2 & D_{21} & D_{22} \end{array} \right] \tag{5.26}$$

We denote by $\hat{T}_{\zeta\tau}$ the transfer function between τ and ζ for this setup. The following theorem is the main result of this section. The proof is similar to Theorem 3.4 (hence omitted).

Theorem 5.2 *Given the Lipschitz system of equations (5.1)-(5.2) (with $f_s = 0$), the state $\hat{x}$ of the observer (5.3)-(5.9) (satisfying conditions (5.10)-(5.16)) globally asymptotically converges to the system state x for all Φ satisfying (3.3) with Lipschitz constant α if K in (5.25) satisfies*

$$sup_{\omega \in \mathbb{R}}\ \sigma_{max}\left[\hat{T}_{\zeta\tau}(j\omega)\right] < \frac{1}{\alpha} \tag{5.27}$$

It is important to note that the same discussion in section 3.3 applies to the LUIO presented in Theorem 5.2: a regular H_{∞} problem similar to the one in section 3.3.1 can be defined, a parametrization of all possible observers can be derived, and a design procedure similar to the one in section 3.3.3 can also be developed. Moreover, if condition (3.3) holds locally, then local asymptotic convergence of the observer is guaranteed. Details are omitted due to similarity.

5.3 Lipschitz Robust Fault Diagnosis

We will now consider the application of the LUIO to the fault diagnosis problem. We will first study the sensor fault effect on the observer's error dynamics in (5.20)-(5.21). It can be seen that the error dynamics of the observer will be as follows (see Appendix A.4 for the derivation of this model)

$$\dot{\xi} = A_F \xi + B_F e + B_{L1} f_s \tag{5.28}$$

$$\dot{e} = C_F \xi + D_F e + T\left(\Phi(x, u, t) - \Phi(\hat{x}, u, t)\right) - D_{L1} f_s - H \dot{f}_s \tag{5.29}$$

Similar to (5.20)-(5.21), this model can be represented by a standard form similar to the one in (5.22)-(5.25) if we augment the external input τ to include both f_s and $\dot{f}_s$. However, to avoid dealing with f_s and $\dot{f}_s$ as two different inputs in the following design, we consider a state augmentation in which only $\dot{f}_s$ is added to the external input, and the state ψ is augmented accordingly, thus obtaining the following model for the error dynamics in (5.28)-(5.29):

$$\dot{\psi} = \begin{bmatrix} A - HCA & 0_{np} \\ 0_{pn} & 0_p \end{bmatrix} \psi + \left[\begin{bmatrix} T & -H \\ 0_{pn} & I_p \end{bmatrix} \quad \begin{bmatrix} -I_n \\ 0_{pn} \end{bmatrix} \right] \begin{bmatrix} \tau \\ \nu \end{bmatrix} \tag{5.30}$$

$$\begin{bmatrix} \zeta \\ \varphi \end{bmatrix} = \begin{bmatrix} I_n & 0_{np} \\ C & I_p \end{bmatrix} \psi + \left[\begin{bmatrix} 0_n & 0_{np} \\ 0_{pn} & 0_p \end{bmatrix} \quad \begin{matrix} 0_n \\ 0_{pn} \end{matrix} \right] \begin{bmatrix} \tau \\ \nu \end{bmatrix} \tag{5.31}$$

where

$$\tau = \begin{bmatrix} \tilde{\phi} \\ \dot{f}_s \end{bmatrix} \tag{5.32}$$

while ν, ζ, φ, and K are same as (5.24)-(5.25).

Comments:

(1) The advantage of the model (5.30)-(5.31) over (5.28)-(5.29) is that first it is in the standard "Plant-Controller" form where the dynamic observer gain "K" is the design freedom in our case. Besides, the fault effect is manifested through a single external input "$\dot{f}_s$": assuming a certain frequency pattern for the fault f_s, the frequency information of $\dot{f}_s$ can be determined a priori, and we can then use (5.30)-(5.31) to proceed with a fault diagnosis design similar to the one adopted in Chapter 4 for the deterministic case.

(2) Model (5.30)-(5.31) is also a natural generalization of the models considered in Chapter 4 (as (4.13)-(4.14) for the LTI case, and (4.29)-(4.30) for the Lipschitz case)

to the unknown input case. Generally speaking, by considering all the different possibilities of uncertainty/nonlinearity we get the following cases:

- Case of no uncertainty/no nonlinearity: $H = 0$, $T = 0$. The model reduces to (4.13)-(4.14), and the problem is equivalent to the one considered in section 4.1.

- Case of no uncertainty/nonlinearity: $H = 0$, $T = I$. The model reduces to (4.29)-(4.30), and the problem is equivalent to the one considered in section 4.2.

- Case of uncertainty/no nonlinearity: $H \neq 0$, $T = 0$.

- Case of uncertainty/nonlinearity: $H \neq 0$, $T \neq 0$.

Our focus in the following is on the last two cases, with particular emphasis on the design problem associated with the last one.

The uncertainty/nonlinearity case

We here adopt the same approach of section 4.2 by modeling the design problem associated with the error dynamics in (5.30)-(5.31) as a two-objective optimization problem in which:

- First objective is to minimize the effect of $\dot{f}_s$ on the estimation error when the sensor fault f_s has a known frequency pattern.

- Second objective is to cancel the effect of the nonlinearity by designing the observer gain such that $\|\hat{T}_{e\tilde{\phi}}\| < \frac{1}{\alpha}$, with α as the Lipschitz constant for the nonlinearity in equation (5.1).

It is easy to see that the solution of this problem guarantees fault detection and estimation at the same time (the residual for this general case being $y - \hat{y} = Ce + f_s$). It is also clear that the second objective is a standard H_∞ problem similar to the one in section 5.2, and unaffected by the state augmentation. Weighting functions can then be introduced to combine these two objectives into a single H_∞ framework that can be solved using LMI techniques as was done in Chapter 4 (details are omitted due to similarity).

It is also important to note that one case of interest is the case of sensor bias (where $\omega_o = 0$). The direct effect of $\dot{f}_s$ on the error dynamics in (5.29) is cancelled, and the model

(5.30)-(5.31) reduces to:

$$\dot{\psi} = \begin{bmatrix} A - HCA \end{bmatrix} \psi + \begin{bmatrix} \begin{bmatrix} T & 0_{np} \end{bmatrix} & -I_n \end{bmatrix} \begin{bmatrix} \tau \\ \nu \end{bmatrix} \tag{5.33}$$

$$\begin{bmatrix} \zeta \\ \varphi \end{bmatrix} = \begin{bmatrix} I_n \\ C \end{bmatrix} \psi + \begin{bmatrix} \begin{bmatrix} 0_n & 0_{np} \\ 0_{pn} & I_p \end{bmatrix} & \begin{bmatrix} 0_n \\ 0_{pn} \end{bmatrix} \end{bmatrix} \begin{bmatrix} \tau \\ \nu \end{bmatrix} \tag{5.34}$$

which is similar to (4.29)-(4.30), except for $A - HCA$ replacing A and the appearance of T instead of I_n in (4.29).

General system fault diagnosis

The case of faults affecting the state equation can be represented by the following model

$$\dot{x}(t) = Ax(t) + \Gamma(u,t) + \Phi(x,u,t) + Ed(t) + Ff(t), \tag{5.35}$$

$$y(t) = Cx(t) + f_s(t), \quad A \in \mathbb{R}^{n \times n}, \quad C \in \mathbb{R}^{p \times n} \tag{5.36}$$

where the vector $f(t)$ can represent more general system faults (as actuator faults or component faults) that may affect the system. The problem in this case can be solved using the same approach by augmenting the two-objective problem to include the transfer function from $f(t)$ to $e(t)$ as an additional design parameter. A complete study of the solvability of this problem is suggested as a future work.

5.4 Design Example

To illustrate the benefit of the LUIO design introduced in section 5.2, we consider the following example of a 2nd order system with modelling uncertainties:

$$\begin{bmatrix} \dot{x}_1 \\ \dot{x}_2 \end{bmatrix} = \begin{bmatrix} -2 & 3 \\ 3 & a \end{bmatrix} \begin{bmatrix} x_1 \\ x_2 \end{bmatrix} + \begin{bmatrix} 0 \\ 1 \end{bmatrix} u + \begin{bmatrix} 0.4\ sin(x_1) \\ 0 \end{bmatrix}$$

$$y = x_2$$

where a is an unknown parameter. The system can be represented in the form (5.1)-(5.2) with:

$$A = \begin{bmatrix} -2 & 3 \\ 3 & 0 \end{bmatrix}, \quad \Gamma = \begin{bmatrix} 0 \\ u \end{bmatrix}, \quad \Phi = \begin{bmatrix} 0.4\ sin(x_1) \\ 0 \end{bmatrix}, \quad E = \begin{bmatrix} 0 \\ 1 \end{bmatrix}, \text{ and } C = \begin{bmatrix} 0 & 1 \end{bmatrix}.$$

The Lipschitz constant is $\alpha = 0.4$. Using the design procedure introduced in section 5.2, the matrices for the observer (5.3)-(5.4) are obtained as follows:

$$H = \begin{bmatrix} 0 \\ 1 \end{bmatrix} \text{ and } T = \begin{bmatrix} 1 & 0 \\ 0 & 0 \end{bmatrix}.$$

$$A_L = \begin{bmatrix} -2.9805 & -4.1928 \\ -5.3338 & -24.6602 \end{bmatrix}, \ B_L = \begin{bmatrix} 0 \\ 0 \end{bmatrix}, \ C_L = \begin{bmatrix} 2.3525 & 8.1687 \\ 8.1687 & 33.2083 \end{bmatrix} \text{ and } D_L = \begin{bmatrix} 3 \\ 0 \end{bmatrix}.$$

$$A_F = A_L, \ B_F = \begin{bmatrix} 0 & 1.3145 \\ 0 & 1.0934 \end{bmatrix}, \ C_F = -C_L \text{ and } D_F = \begin{bmatrix} -2 & 3 \\ 0 & 0 \end{bmatrix}.$$

Figures 5.3 and 5.4 show the performance of this LUIO when applied to an actual plant with $a = 1$ and with initial conditions $x_1(0) = 1.6$ and $x_2(0) = 2$.
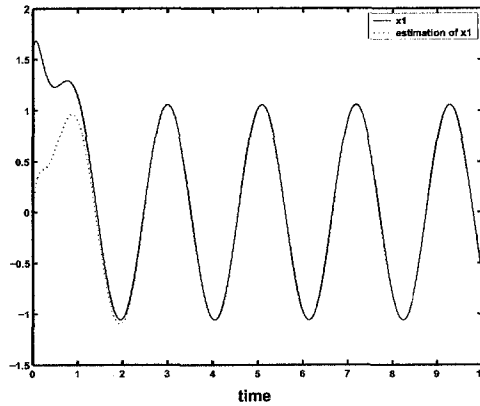
Figure 5.3: Estimation of State x_1.
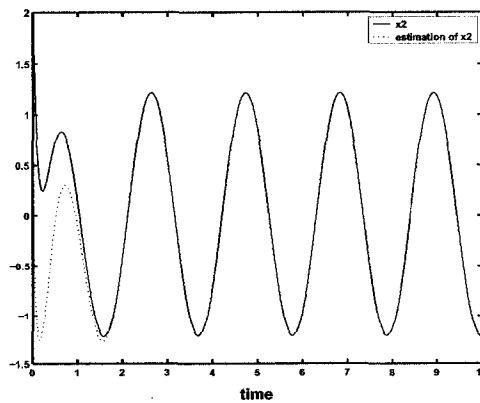
Figure 5.4: Estimation of State x_2.

5.5 Conclusion

In this chapter, the robust FDI problem for Lipschitz nonlinear systems is considered by studying the case of additive uncertainties. Firstly, the standard *Unknown Input Observer* (UIO) approach (used to deal with additive uncertainties in linear systems) is generalized to Lipschitz systems. The new observer is then applied to the robust sensor fault diagnosis problem. The error dynamics of the proposed observer are affected by the time derivatives of the faults. An augmentation of the dynamics is proposed to avoid dealing with the faults and their derivatives as two separate inputs. The problem is then modelled as a two-objectives optimization problem similar to the one introduced in Chapter 4, and is solvable using numerical techniques. The applicability of the proposed results to more general system faults is briefly discussed, laying the ground for future research in this area.

Chapter 6

Experimental Results and Application in Robotics

In this chapter, we consider an application of the results of previous chapters to the *Quanser* rotary inverted pendulum (ROTPEN) available in the Control Systems Lab, Electrical and Computer Engineering department, University of Alberta. Our intention is the application of the proposed approaches to Lipschitz observer design and sensor fault diagnosis to robotic systems. Towards that goal, the ROTPEN model as a special case of robot manipulators models, is represented in two forms: (i) a linear model around an operating point of interest, (ii) a nonlinear model in the Lipschitz form. Different observer design and sensor fault diagnosis strategies are applied in real-time for these two cases. The experimental results assess the validity of the proposed techniques in a physical example, and illustrate the advantages of using the Lipschitz design in this case.

6.1 Robot Manipulator as Lipschitz System

The dynamic equations of a robot manipulator can be represented by the following structure [98]:

$$u = M(\theta) \, \ddot{\theta} + V(\theta, \dot{\theta}) \tag{6.1}$$

where θ, $\dot{\theta}$ and $\ddot{\theta} \in \mathbb{R}^n$ are vectors representing the position, velocity and acceleration of the n robot joints respectively, $u \in \mathbb{R}^n$ represent the actuator torques applied at these joints, $M(\theta)$ is referred to as the inertia matrix, and $V(\theta, \dot{\theta})$ is a vector representing the centrifugal,

75

coriolis, gravity and friction terms. It is important to note that sensors are usually available to measure the joints positions and velocities. Therefore, θ and $\dot{\theta}$ are assumed measurable for control and trajectory generation purposes (it will be seen, however, that for the ROTPEN model discussed in section 6.2 not all velocities are measurable).

By defining the state variables as $x_1 = \theta$, $x_2 = \dot{\theta}$ (note that here x_1, x_2 represent n-dimensional vectors) we get the state space model:

$$\dot{x} = f(x) + g(x)u \tag{6.2}$$

where $f(x) = \begin{bmatrix} x_2 \\ -M^{-1}(x_1)V(x_1, x_2) \end{bmatrix}$, $g(x) = \begin{bmatrix} 0_n \\ M^{-1}(x_1) \end{bmatrix}$, which can also be represented as:

$$\dot{x} = Ax + \Phi(x, u) \tag{6.3}$$

where $A = \begin{bmatrix} 0_n & I_n \\ 0_n & 0_n \end{bmatrix}$, $\Phi = \begin{bmatrix} 0_n \\ M^{-1}(x_1)u - M^{-1}(x_1)V(x_1, x_2) \end{bmatrix}$. It is important to note that the nonlinear terms in Φ are locally Lipschitz, and an upper bound on the Lipschitz constant can be found by computing $\|\Phi(x, u)\|$ over the operating range. Another representation of (6.2) is:

$$\dot{x} = Ax + Bu + \Phi(x, u) \tag{6.4}$$

where $A = \left(\frac{\partial f}{\partial x} \right) |_{x^*}$, $B = \left(\frac{\partial g}{\partial x} \right) |_{x^*}$, $\Phi = (f(x) - Ax + g(x)u - Bu)$.

It is also important to note that (6.3) and (6.4) are both exact models of (6.2). By neglecting the terms in Φ in (6.4), one gets the approximate linearization around the operating point x^*, i.e:

$$\dot{x} = Ax + Bu \tag{6.5}$$

where $A = \left(\frac{\partial f}{\partial x} \right) |_{x^*}$, $B = \left(\frac{\partial g}{\partial x} \right) |_{x^*}$, which is an approximate model of (6.2).

6.2 The ROTPEN: Models and Assumptions

The *Quanser* rotary inverted pendulum (ROTPEN) is shown schematically in Figure 6.1, [72]. The angle that the perfectly rigid link of length l_1 and inertia J_1 makes with the x-axis of an inertial frame is denoted θ_1 (degrees). Also, the angle of the pendulum (of length l_2 and mass m_2) from the z-axis of the inertial frame is denoted θ_2 (degrees).
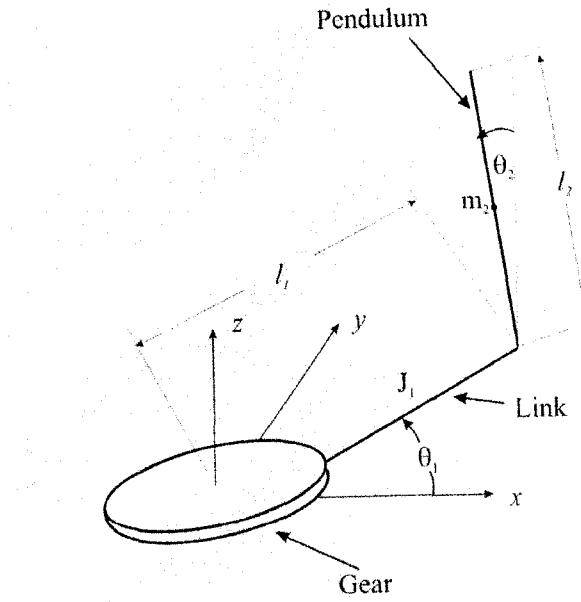
Figure 6.1: The Rotary Inverted Pendulum (ROTPEN).

The system has one input which is the scalar servomotor voltage input (Volt). Therefore, the system is a special case of the robot manipulator model discussed in section 6.1: a planar robot manipulator with two links ($n = 2$), with only one torque applied at the first joint, while the second joint is subject to the gravitational force. In fact, the ROTPEN has a state space model of the form $\dot{x} = f(x) + g(x)u$, where $x = [\theta_1\ \theta_2\ \dot{\theta}_1\ \dot{\theta}_2]^T$ is the state vector, and u is the scalar servomotor voltage input (Volt). More details about this model and its parameters can be found in Appendix B.2.

The system has an infinite number of equilibrium points, representing the following two equilibrium points:

1) Pendant position: $x_1 = 0$ (rad), $x_2 = \pi$ (rad), $x_3 = x_4 = 0$ (rad/sec).

2) Inverted position: $x_1 = x_2 = 0$ (rad), $x_3 = x_4 = 0$ (rad/sec).

By separating the nonlinear terms, the model can be put in the form $\dot{x} = Ax + \Phi(x, u)$, where:

$$A = \begin{bmatrix} 0 & 0 & 1 & 0 \\ 0 & 0 & 0 & 1 \\ 0 & -25.14 & -17.22 & 0.2210 \\ 0 & 68.13 & 16.57 & -0.599 \end{bmatrix}, \ \Phi(x, u) = \begin{bmatrix} 0 \\ 0 \\ \phi_1(x, u) \\ \phi_2(x, u) \end{bmatrix}.$$ The nonlinear terms in Φ are

mainly trigonometric terms, and using the symbolic MATLAB toolbox, an upper bound on

$\|\Phi(x, u)\|$ is found as 44.45, and hence the Lipschitz constant for the ROTPEN is $\alpha = 44.45$. This follows from the fact that if $\Phi : \mathbb{R}^n \times \mathbb{R} \to \mathbb{R}^m$ is continuously differentiable on a domain D and the derivative of Φ with respect to the first argument satisfies $\|\frac{\partial \Phi}{\partial x}\| \le \alpha$ on D, then Φ is Lipschitz continuous on D with constant α, i.e.:

$$\|\Phi(x, u) - \Phi(y, u)\| \le \alpha \|x - y\|, \ \forall \ x, \ y \ \in \ D \tag{6.6}$$

There are two encoders to measure the angle of the servomotor output shaft (θ_1) and the angle of the pendulum (θ_2). An encoder is also available to measure the motor velocity $\dot{\theta}_1$, but no one is available to measure the pendulum velocity $\dot{\theta}_2$. In our experiments, we use linear as well as nonlinear control schemes to stabilize the pendulum at the inverted position $(\theta_2 = 0)$, while tracking a step input of 30 degrees for the motor angle.

6.3   Experiment A - Linear Observer Design and Fault Diagnosis

In this experiment, the results in section 4.1 are assessed on the linearized model around the inverted position. A small operating range for the pendulum is guaranteed by using a linear state feedback controller and a feedforward gain as follows:

$$u = -F\ x + p\ r \tag{6.7}$$

where "r" is the reference motor angle to be tracked. First, the linear model is obtained as (see Appendix B.3):

$$\dot{x} = Ax + Bu \tag{6.8}$$

The control parameters in (6.7) are computed by placing the poles of $(A - BF)$ at $\{-18 + 18i, \ -18 - 18i, \ -1.5 + 1.5i, \ -1.5 - 1.5i\}$ (see Appendix B.3). In this experiment, different fault scenarios are assumed to affect the pendulum sensor. The linear design technique is used to diagnose these faults, and their effect on the tracking performance is also considered.

6.3.1   Case Study 1

In this case study, sensor bias faults are assumed, and the design procedure in section 4.1.1 is used to accurately estimate and tolerate these faults. The faults are assumed to affect

the pendulum measurement, and therefore the reduced LTI model is used for the design (see Appendix B.3 for all models and parameters of this case study). Two observers are compared in this case study:

1) A high gain Luenberger observer of the form (4.3)-(4.4). The static gain L_1 is computed by placing the poles of $(A - L_1 C)$ at $\{-70, \quad -20 + 5i, \quad -20 - 5i\}$.

2) A dynamic observer of the form (4.8)-(4.12). The dynamic gain K_1 is computed using the design procedure in section 4.1.1 for the special case $\omega_o = 0$.

Figure 6.2[1] compares the two observers with respect to one sensor bias that results from the error in the initial condition of the pendulum. As can be seen in the figure, the dynamical observer outperforms the static observer in the bias estimation. This shows an important application of the dynamic observer in the problem of estimating the initial condition of the pendulum (this problem will be discussed in more details in section 6.5 using the Lipschitz observer design). In Figure 6.3, a sensor bias of 10 degrees is added to the pendulum measurement at the time 10 seconds. The two observers are used in observer-based control. The effect that the correct fault estimation has on the tracking performance is clear in the case of the dynamic observer. This is also illustrated in Figure 6.4 for a different fault scenario (a time-varying bias of 5 degrees that starts at 10 seconds, then increases to 10 degrees at 40 seconds, and decreases back to 0 degrees at 70 seconds).

6.3.2   Case Study 2

We consider the case of low frequency sensor faults (in the range [0, 1 rad/sec]). Using the design in section 4.1.2 (and with $a = 0.1$, $b = 1$ and $c = 0.001$), the optimal observer gain K_2 is obtained by solving the H_∞ problem in Definition 4.4 using the command $hinfsyn$ in MATLAB, with minimum γ as 10 and with $\beta = 1$. Using this observer for fault diagnosis, a correct estimation of a low frequency sensor fault is shown in Figure 6.5. Figure 6.6 compares the response of the dynamic observer-based controller with the Luenberger-based controller in this case. The improvement in the tracking performance is clear in this figure.

---

[1] All remaining figures of this chapter can be found in section 6.7

6.4   Experiment B - Lipschitz Observer Design

In this experiment, we focus on the nonlinear state estimation problem when no faults are affecting the system. We consider situations in which the operating range of the pendulum is either close or far from the equilibrium point, comparing the Luenberger observer with the Lipschitz observer in these cases. For the purpose of applying the Lipschitz observer design, the nonlinear model discussed in section 6.2 is used. We also compare the dynamic Lipschitz observer of Chapter 3 with the static design method in References [91, 92]. In this experiment the full-order linear and Lipschitz models are used for observer design, where the output is assumed as $y = [x_1 \ x_2]^T$ (all observer parameters used in this experiment can be found in Appendix B.4).

6.4.1   Case Study 3

In this case study, the same controller in Experiment A (6.7) is used with a small operating range around the inverted position. Three observers are compared:

1) Observer 1: A Luenberger observer of the form (4.3)-(4.4), where the observer gain is obtained by placing the poles of $(A - LC)$ at $\{-24, \ -3.8, \ -4.8, \ -12.8\}$ (see $L_{3-small}$ in Appendix B.4).

2) Observer 2: A high gain Luenberger observer, which has the same form of Observer 1 but with the poles placed at $\{-200, \ -70, \ -20 + 15i, \ -20 - 15i\}$ (see $L_{3-large}$ in Appendix B.4).

3) Observer 3: A Lipschitz observer of the form (3.14)-(3.18), based on the full-order Lipschitz model of the ROTPEN. The dynamic gain is computed using the design procedure in section 3.3.3, for $\alpha = 44.45$ (see K_3 in Appendix B.4).

The three observers run successfully with stable estimation errors. Table 6.1 shows the maximum estimation errors in this case. It can be seen that both the Luenberger observer (large poles) and the Lipschitz observer achieve comparable performance, which is much better than the Luenberger observer with small poles. The three observers are also tested in observer-based control, and their tracking performance is compared in Table 6.2. We conclude that, due to the small operating range considered in this case study, a high-gain Luenberger observer achieves a good performance in terms of the state estimation errors and the tracking errors.

Table 6.1: Case study 3 - Estimation errors "e_1" and "e_2" in degrees

	Small-gain Luenberger	High-gain Luenberger	Lipschitz
$max \ |e_1|$	3.6485	0.4323	0.1716
$max \ |e_2|$	1.5681	0.0925	0.1865

Table 6.2: Case study 3 - Tracking performance in degrees

	pure state feedback	High-gain Luenberger	Lipschitz
Percentage of overshoot	20.3613%	12.7440%	48.4863%
$|steady \ state \ error \ |$	2.5635	3.4424	3.7939

6.4.2 Case Study 4

We here consider a large operating range by using a nonlinear control scheme that stabilizes the pendulum angle at the pendant position (see Appendix B.4 for more details about the controller used in this case study). Using this controller, a large operating range is obtained as seen in Figure 6.7.

The same observers (Observers 2 and 3 of Case study 3) are used in parallel with this control scheme, and the resulting estimation errors are compared in Figure 6.8.

The two observers are also compared in observer-based control, and the Luenberger observer fails in this case, causing total system instability. The Lipschitz observer, on the other hand, runs successfully and its performance (as compared to the pure state feedback control) is shown in Figure 6.9. This case study illustrates the importance of the Lipschitz observer in large operating regions, where the linear observer normally fails.

6.4.3 Case Study 5

In this case study, we conduct a comparison between static and dynamic Lipschitz observers, namely the observer (3.4)-(3.5) and the one in (3.14)-(3.18). Our comparison is based on the new design proposed in Chapter 3 and the one in References [91, 92]. First, the design algorithm in Theorem 3.2 is tested for different values of α and ε. It fails for all values of $\alpha > 1$, and the maximum attainable value is $\alpha = 1$ (see L_5 in Appendix B.4), while the

Lipschitz constant of the ROTPEN model is 44.45 as mentioned earlier. This observer is then compared with the dynamic Lipschitz observer successfully computed in Case study 3, and the estimation errors are compared in Figure 6.10. It is also important to note that the static Lipschitz observer fails in stabilizing the system, when used in observer-based control, for both the small and large operating range experiments. This illustrates the importance of the dynamic Lipschitz observer in this case.

6.5   Experiment C - Lipschitz Sensor Fault Diagnosis

In this experiment, the results in section 4.2 are assessed on the nonlinear Lipschitz model. A large operating range is considered by using a nonlinear, switching, LQR control scheme (with integrator) that stabilizes the pendulum at the inverted position (starting from the pendant position) while tracking a step input of 30 degrees for the motor angle as seen in Figure 6.11 (the no-bias case). More details about the control scheme can be found in Appendix B.5.

In the first part of this experiment, an important fault that affects the ROTPEN in real-time is considered. This is a sensor fault introduced by the pendulum encoder. The encoder returns the pendulum angle relative to the initial condition, assuming this initial condition to be $\theta_2 = 0$. This constitutes a source of bias, as shown in Figure 6.11(b), when the pendulum initial condition is unknown or is deviated from the inverted position. The effect of this fault on the tracking performance is also illustrated in Figure 6.11(a) for two different bias situations.

The dynamic Lipschitz observer (developed in section 4.2) is applied to diagnose and tolerate this fault. In addition to this bias fault, the observer is also applied for a 2 rad/sec fault introduced in real-time, as well as for the case of a low frequency fault in the range [0, 1 rad/sec].

6.5.1   Case Study 6

In this case study, we use the design procedure in section 4.2.2 to accurately estimate and tolerate the bias faults shown in Figure 6.11(b). This is the special case where $\omega_o = 0$ for this problem. Using the reduced-order Lipschitz model with $\alpha = 44.45$ (see Appendix B.5) and using the LMI design, the dynamic gain for the observer (3.14)-(3.18),(4.25) that achieves fault identification is obtained as K_6 (see Appendix B.5).

Using this observer, the biases affecting the system in Figure 6.11 are successfully estimated as seen in Figure 6.12. Moreover, by using this observer in an observer-based control scheme, the tracking performance in the large bias case is illustrated in Figure 6.13. The performance is much improved over the one with no fault tolerance as seen in Figure 6.13(b). It also gives less overshoot than the no bias case, as seen in Figure 6.13(a). Similar results are obtained for the small bias case.

6.5.2 Case Study 7

We here consider the case of a sensor fault in the form of harmonics having a frequency of 2 rad/sec. The dynamic gain for the observer (3.14)-(3.18),(4.25) is computed using the design in section 4.2.2. This is the special case where $\omega_o = 2$ for this problem. The gain is obtained at $\lambda = 10^{-12}$ as K_7 (see Appendix B.5). Using this observer, Figure 6.14 shows the correct estimation of a sensor fault of amplitude 20 degrees and frequency 2 rad/sec.

6.5.3 Case Study 8

We consider the case of low frequency sensor faults (in the range $[0, 1 \text{ rad/sec}]$). Using the design in section 4.2.3 (and with $a = 0.1$, $b = 1$ and $\epsilon = 0.1$), the optimal observer gain is obtained by solving the H_∞ problem in Definition 4.5 using the command *hinflmi* in MATLAB, with minimum λ as 10^{-12} (see K_8 in Appendix B.5). Using this observer for fault diagnosis, a correct estimation of a low frequency sensor fault (generated using the MATLAB command *idinput*) is shown in Figure 6.15.

6.6 Conclusion

In this chapter, the rotary inverted pendulum (ROTPEN) is used as a demonstration for the dynamic Lipschitz observer design techniques in a practical example. First, the linear model is considered in Experiment A, and the system is controlled over a small operating range. It is shown that adding more dynamics to the *linear* observer offers better fault detection capabilities with respect to sensor faults affecting the system.

In Experiments B and C, the operating region is much increased, showing the importance of using the dynamic Lipschitz design either for the state estimation or the sensor fault diagnosis applications. The dynamic Lipschitz design is also compared to the static design

technique in Experiment B. It is shown that, unlike the dynamic approach, the static method fails when applied to the ROTPEN due to the large Lipschitz constant that the system has.

The dynamic Lipschitz design is also very efficient in dealing with an important fault that affects the ROTPEN. This is illustrated in Experiment C, where the pendulum bias (that results from error in the initial conditions of the encoder) is successfully estimated in real-time. The effect on the control response is also tested in different bias situations, and it is shown that better tracking performances are achieved in this case.

6.7 Figures of Experiments A, B and C
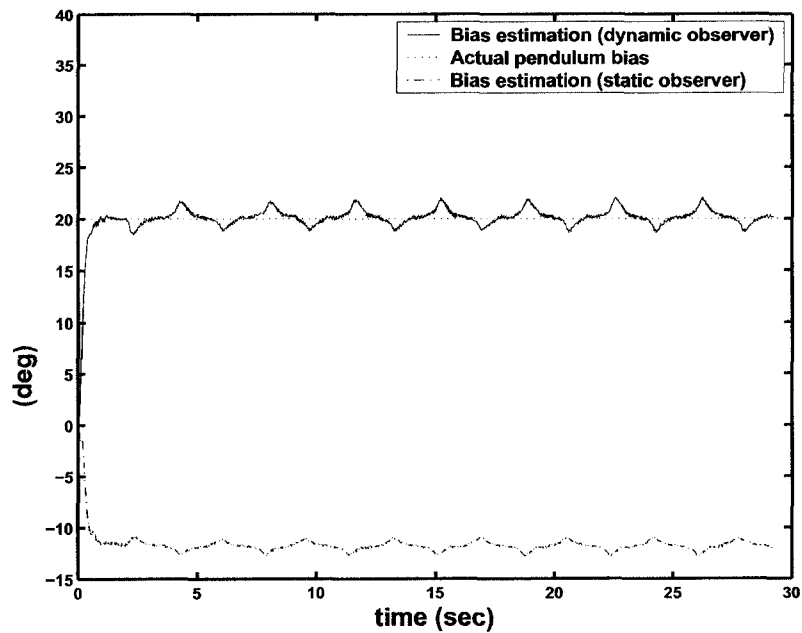
Figure 6.2: Case 1 - Sensor Bias Estimation.
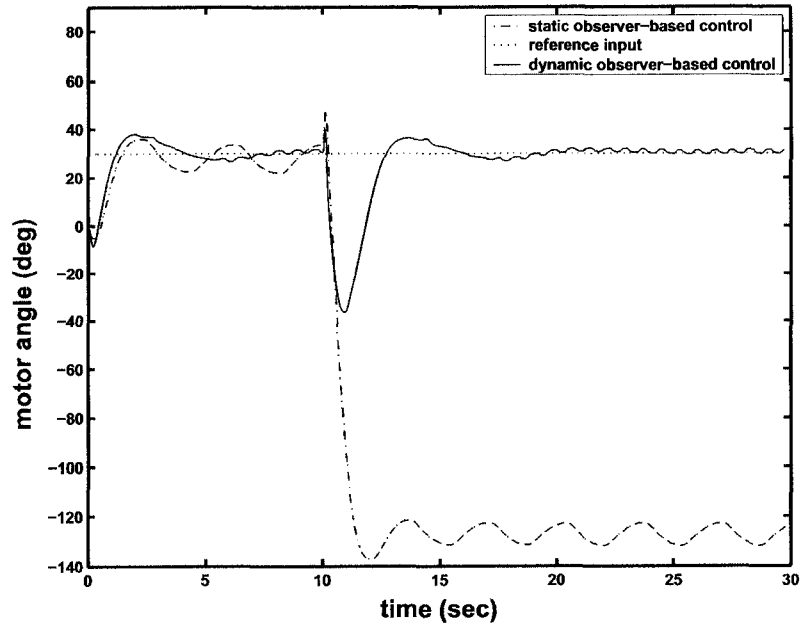
Figure 6.3: Case 1 - Observer-based Response.
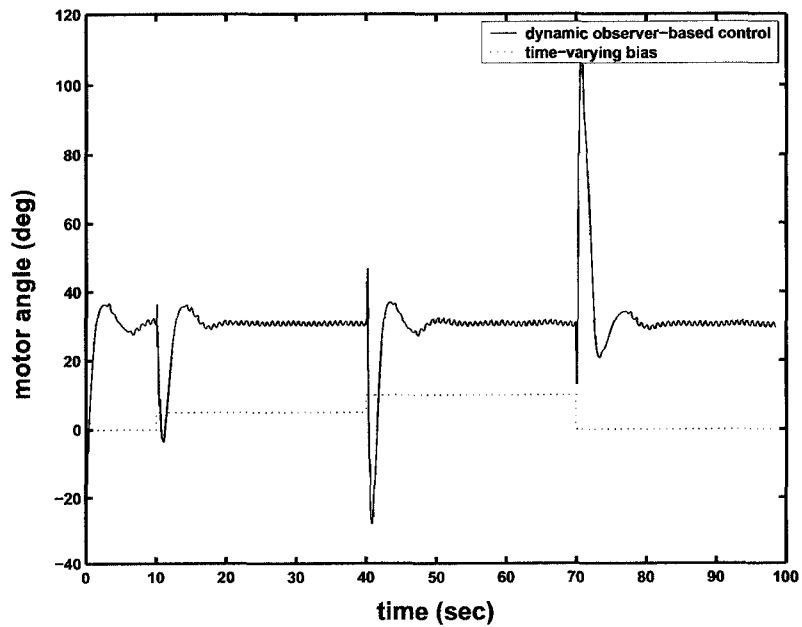
Figure 6.4: Case 1 - Observer-based Response (Time-varying Bias).
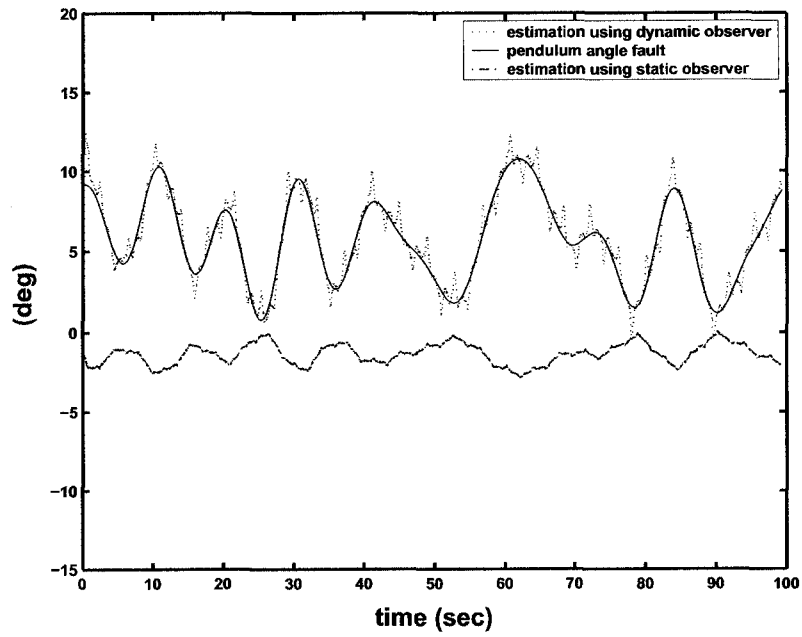
Figure 6.5: Case 2 - Low Frequency Estimation.
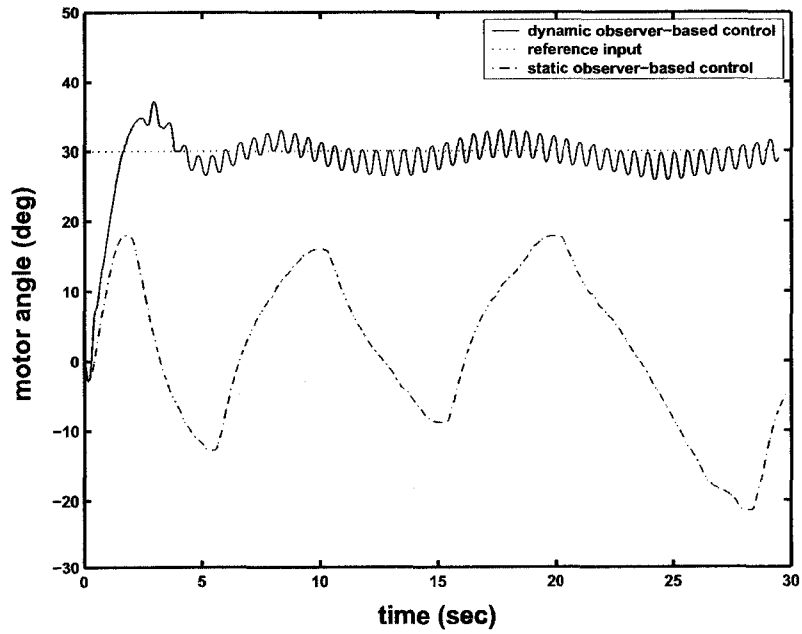
Figure 6.6: Case 2 - Observer-based Response.
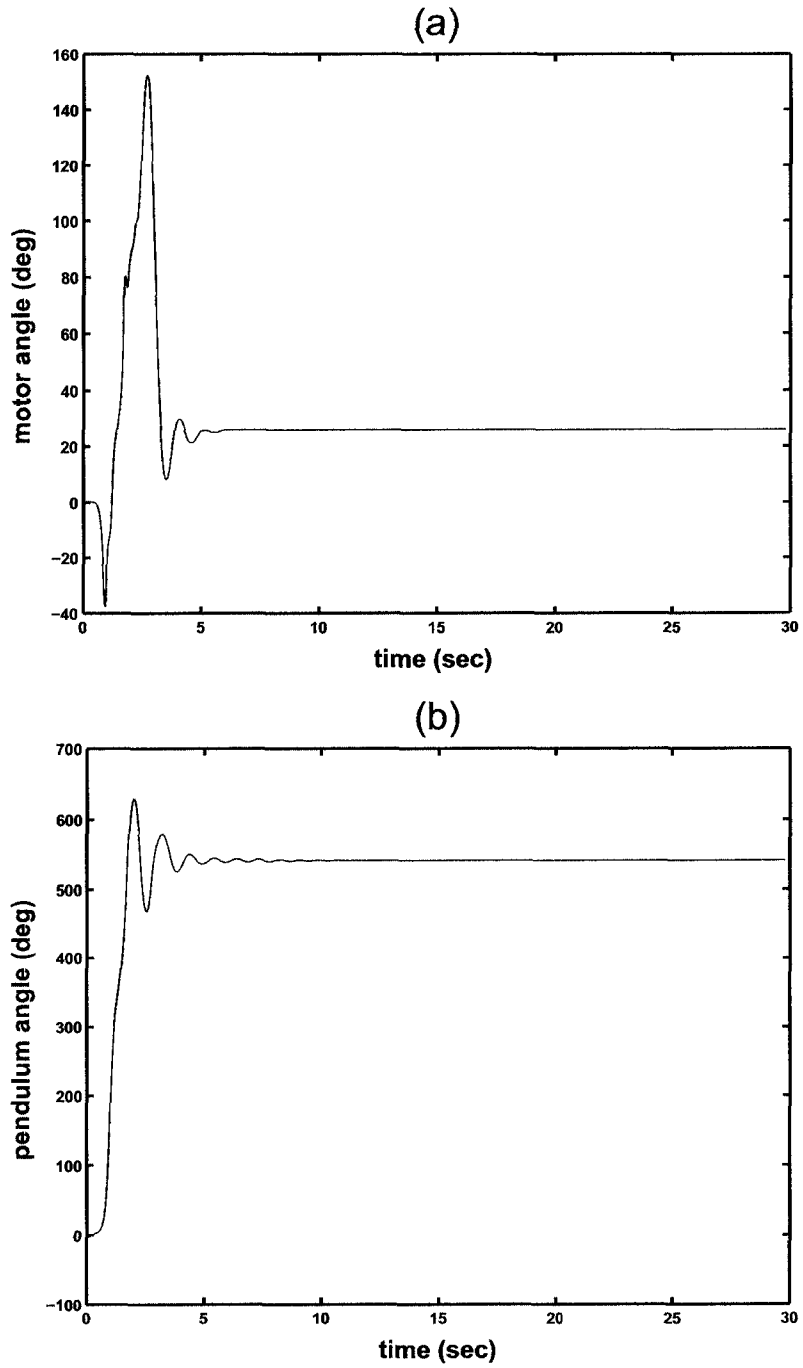
Figure 6.7: Case 4 - (a) Motor Response, (b) Pendulum Response.
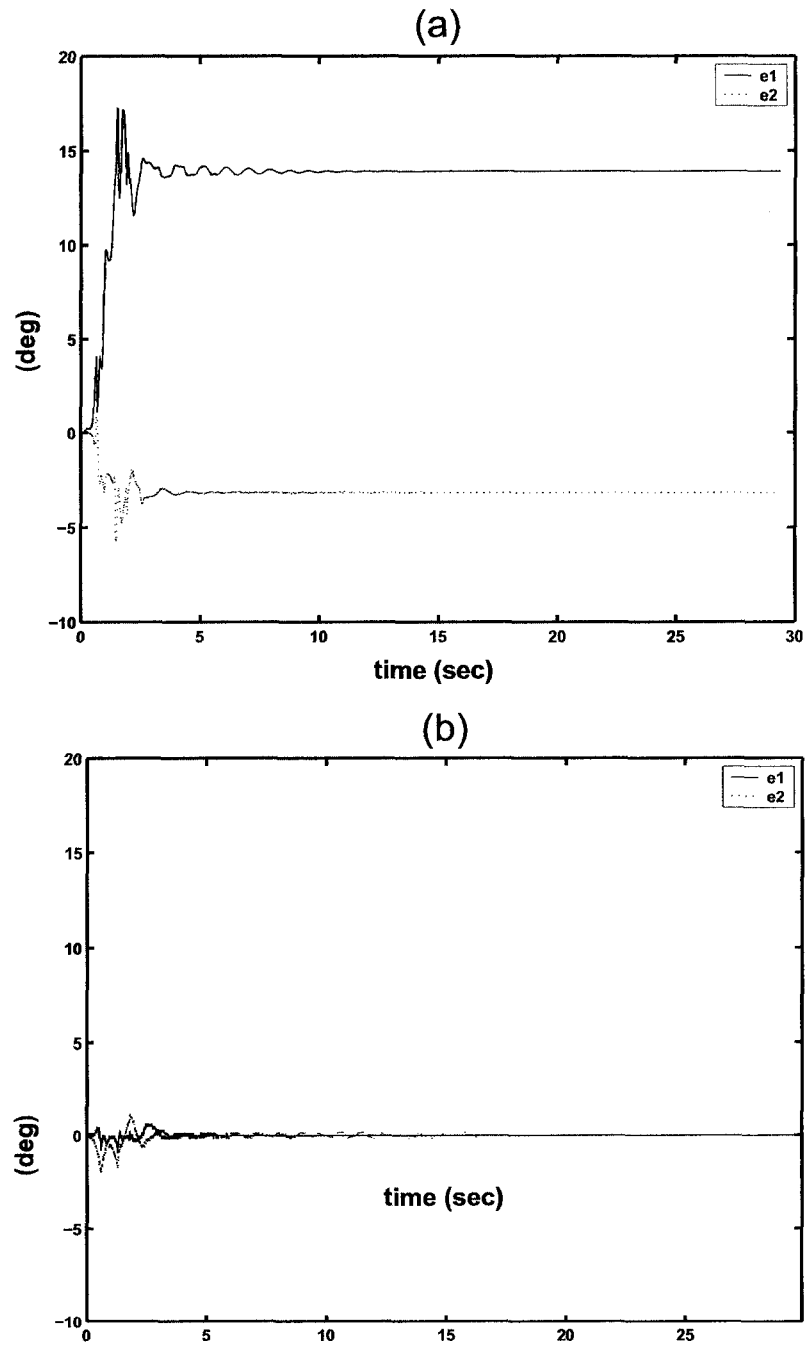
Figure 6.8: case 4 - (a) High-gain Luenberger Errors, (b) Dynamic Lipschitz Errors.

(a)

(b)
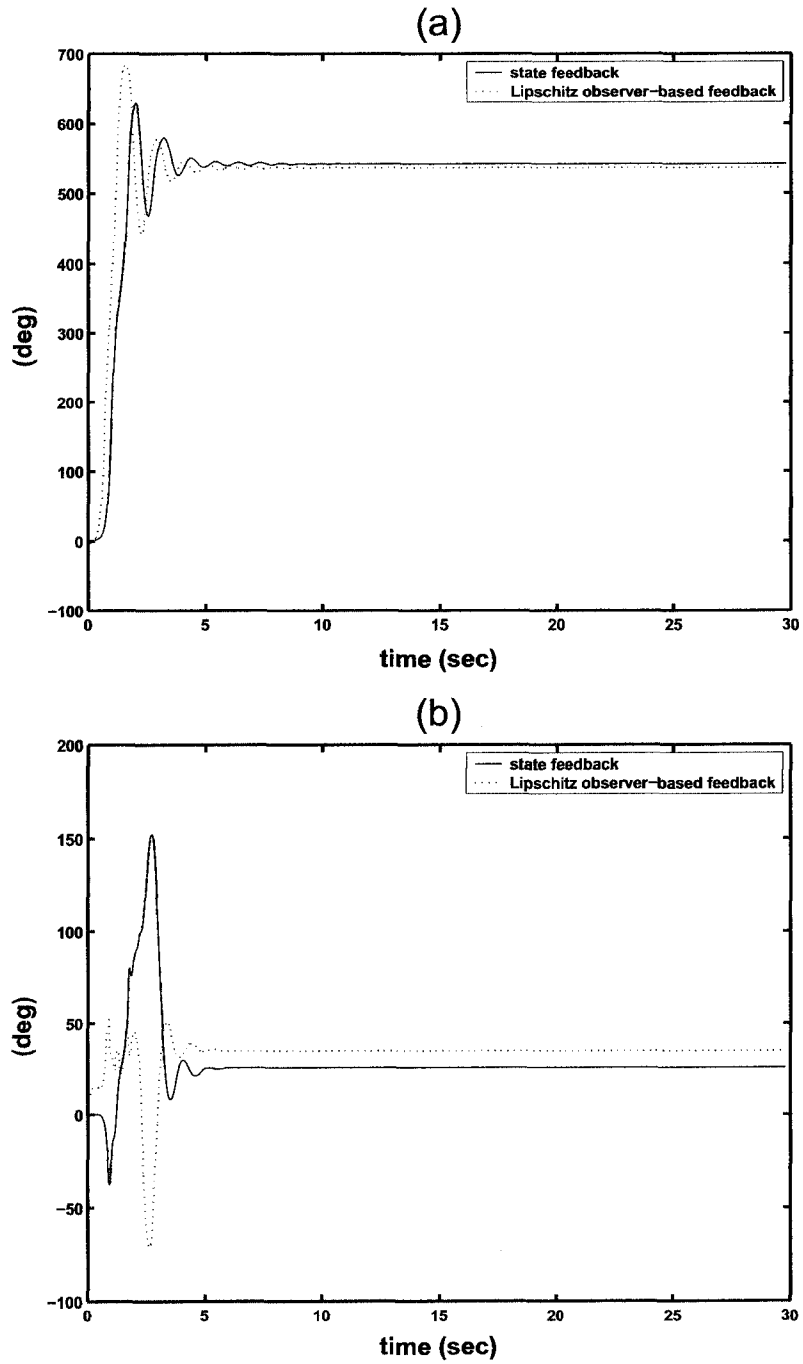
Figure 6.9: Case 4 - (a) Pendulum Angle, (b) Motor Angle.
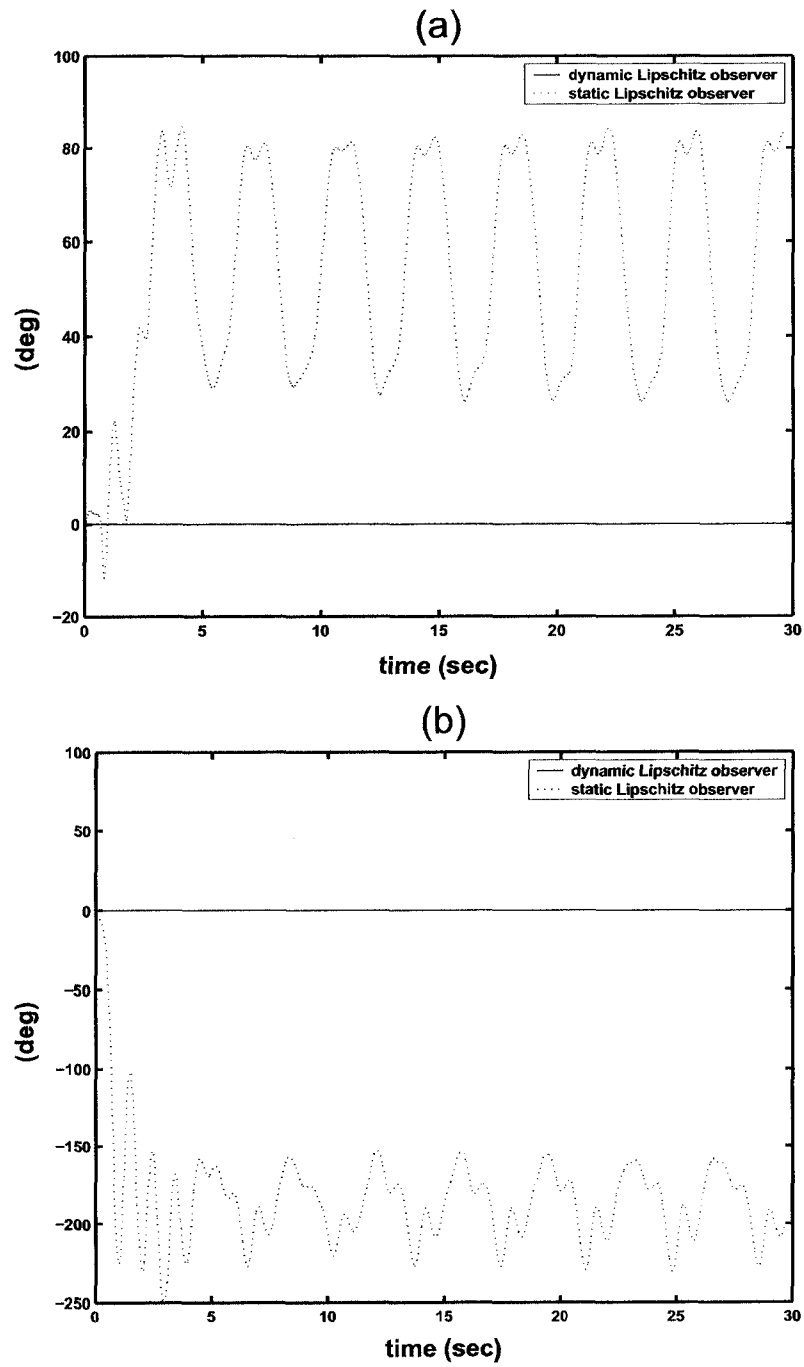
Figure 6.10: Case 5 - (a) Estimation Error "e_1", (b) Estimation Error "e_2".
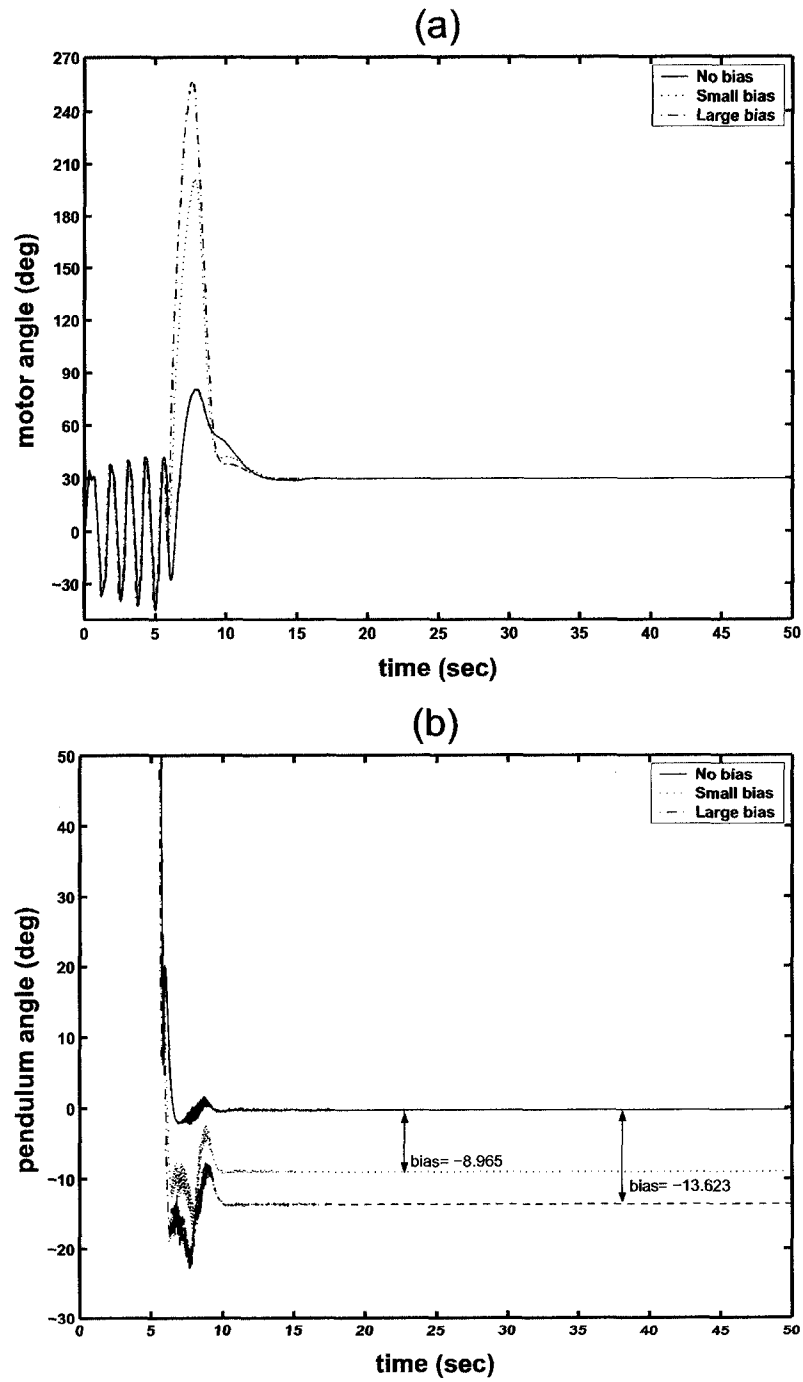
Figure 6.11: Case 6 - (a) Tracking Performance, (b) Pendulum Angle.
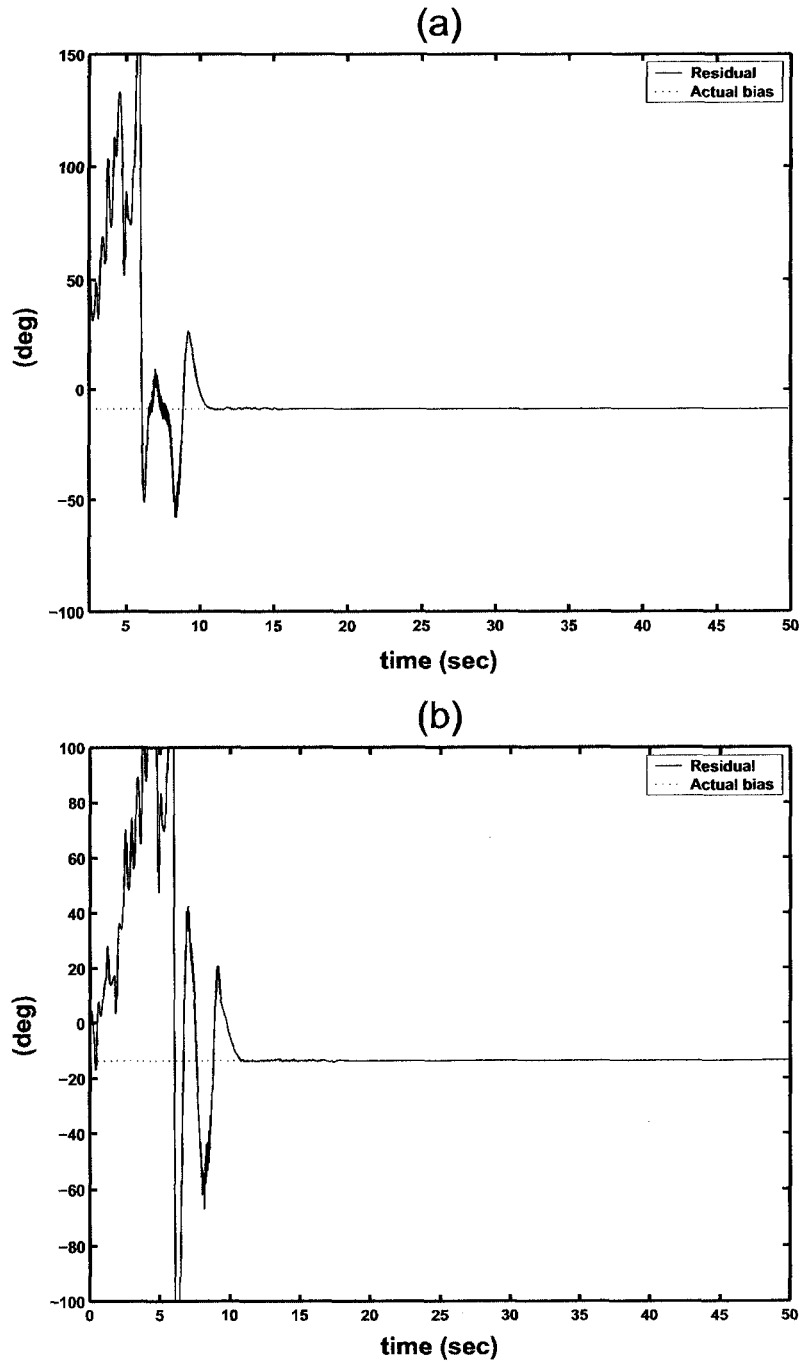
Figure 6.12: Case 6 - (a) Estimation of the Small Bias, (b) Estimation of the Large Bias.
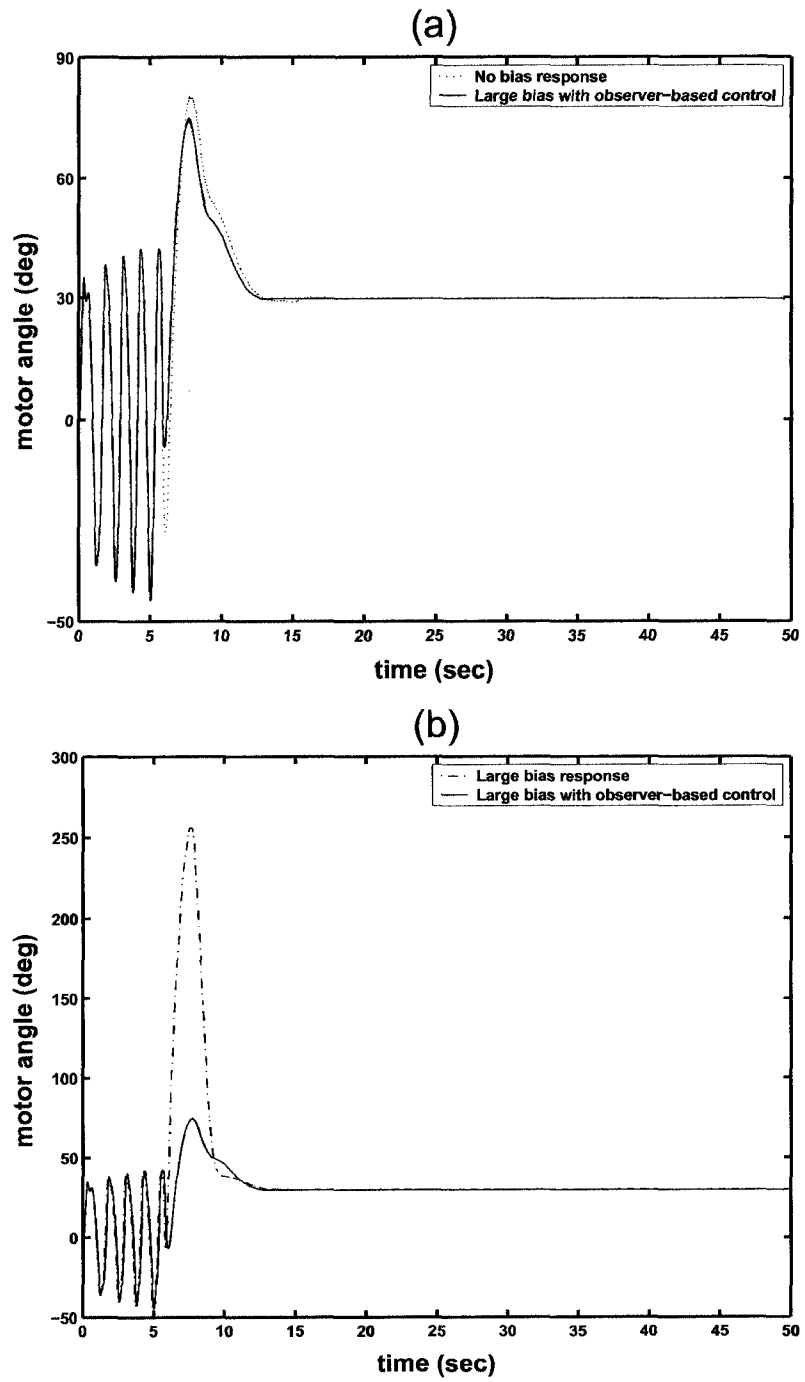
Figure 6.13: Case 6 - (a) No-bias versus Observer-based, (b) Large Bias versus Observer-based.
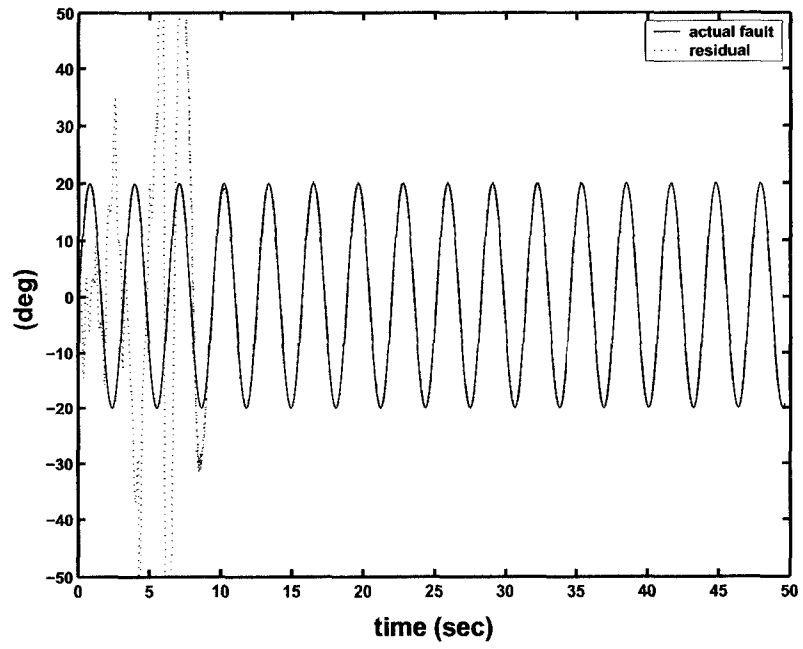
Figure 6.14: Case 7 - Frequency Band Estimation.
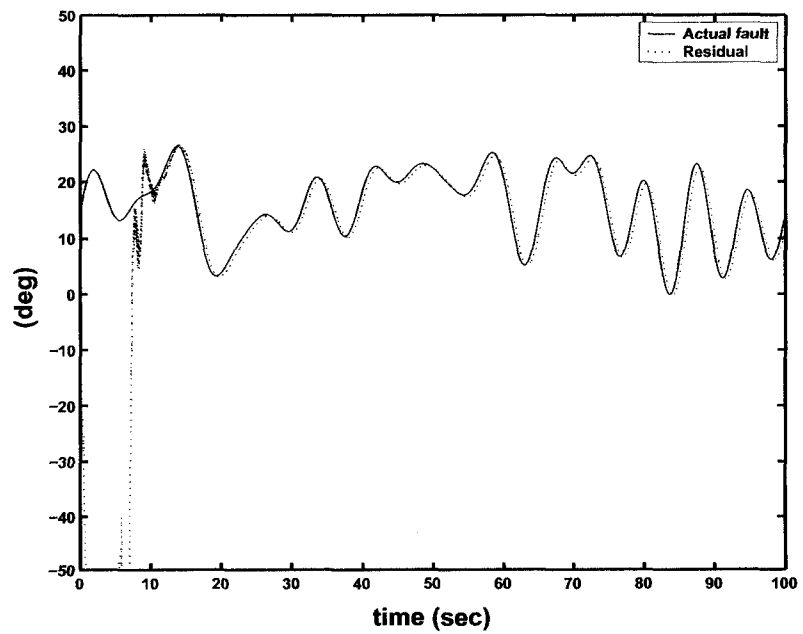
Figure 6.15: Case 8 - Diagnosis of Low Frequency Sensor Fault.

Chapter 7

Some Related Sampled-data

Results

In this chapter, the problem of sampled-data state reconstruction in linear time invariant systems is considered. A new full order observer structure that can generate intersample state estimation is introduced. The observer synthesis is carried out using the H_∞ framework and is shown to have some important advantages over the classical lifting technique that has been used to study similar problems. A simulation example illustrates the application of the proposed design in the fast rate fault detection problem[1].

7.1 Problem Definition

In this chapter, our interest is the sampled-data observer (SDO) design problem. It is the problem of reconstructing the states of a continuous-time plant using a discrete-time observer, which can operate with a rate higher than the sample and hold devices connected to the plant because of the fact that the digital computer speed is normally very high compared with these devices. This is different from most linear and nonlinear observer designs discussed throughout the thesis that consider the continuous-time problem in which a continuous-time observer is designed to observe the state of a continuous-time plant. An important advantage of the sampled-data framework is the possibility to provide intersample estimation

---

[1]The results in this chapter have been published in the article: "A.M. Pertew, H.J. Marquez and Q. Zhao, H_∞ Optimal Sampled-data State Observer Design," IEE Proceedings - Control Theory and Applications, Vol. 153, No. 4, pp. 453-461, July 2006.

and, therefore, better piecewise approximate reconstruction of the continuous-time states of interest. Such information is very useful for observer applications specially in system monitoring and fault detection where critical decisions should be taken within relatively short periods of time. However, obtaining this information is a challenge given the fact that the output information (needed for observer design) is only available at the slow rate of the sample device.

A classical approach used for the SDO design problem mainly in control applications is the so-called *inferential control* approach. In this technique, selected (primary) measurements of both process inputs and outputs are used to estimate the effect of secondary measurements (these may include unmeasured states, disturbances affecting the system, etc.) and then a standard control system is used to adjust the fast rate control effort [115]. The most important part of this technique is the design of an estimator that minimizes the estimation error of inferred measurements at fast sampling points where an actual measurement is unavailable [97]. In most cases, however, inferential control methods are restricted to specific types of control schemes or processes. Besides, the issues of practical importance (such as model uncertainty, system dynamics, unmeasured disturbances/noise, restrictions on the controller structure) are not incorporated [71].

This encouraged much research to be done in the area of sampled-data control and one of the successful approaches that has been introduced is the *lifting technique* [15, 80]. The main idea of the lifting technique is to generate slow rate control inputs that depend on fast rate information of the reference input, using this additional information to control an augmented output which represents the fast rate error signal. Design of the controller in this case can be done within the multirate digital control framework [79]. This technique can also be used for the dual SDO design problem. In this chapter, we apply the dynamical observer approach to solve the SDO design problem, comparing it to a design based on Lifting. An observer design based on the fast rate plant model is introduced. In order to achieve intersample state estimation using this observer, we proceed as follows: two signals are fed to the observer; namely, the plant input and the plant output. The plant input is constant during the intersample, owing to the hold device and is therefore fed to the observer at the fast rate. The plant output, on the other hand, is only available at the sampling instants and is therefore fed at the slow rate of the sample device connected to the plant. In order to obtain a robust estimate with respect to this unknown intersample output information, we formulate the problem as an H_∞ optimal control problem, making use of the dynamic

observer structure introduced in this case. Similar to the Lipschitz case, we show that the proposed SDO-H_∞ problem is equivalent to a modified H_∞ optimal control problem which satisfies the standard regularity assumptions in the discrete H_∞ optimization theory. The proposed H_∞ approach is also compared to the classical lifting approach through a set of simulation experiments conducted on the ROTPEN and is shown to have some important advantages over the lifting technique when applied to a fast rate fault detection problem.

7.1.1 Preliminaries and Notation

Our attention is focused on the sampled-data observer (SDO) design design problem for sampled-data systems such as the one shown in Figure 7.1 where the sample and hold devices are both operating with the speed $1/h_s$ (h_s being the sampling time). The objective of the SDO as seen in Figure 7.1 is to provide state estimates at a faster rate $1/h_f$ using the available input-output information.
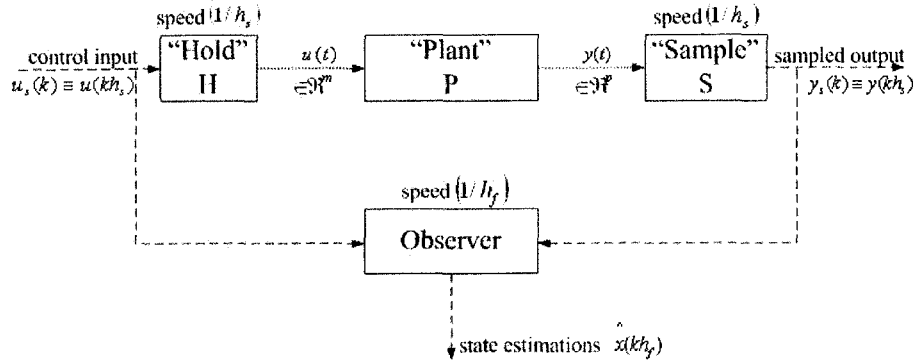
Figure 7.1: The Sampled-data Observer (SDO) Design Problem.

Given the fact that most physical systems of interest in systems and control are naturally continuous-time, in the sequel we consider the model of the plant P to be a known LTI system Σ of the form:

$$\Sigma : \begin{cases} \dot{x}(t) = A\,x(t) + B\,u(t), & A \in \mathbb{R}^{n\times n}, B \in \mathbb{R}^{n\times m} \\ y(t) = C\,x(t) + D\,u(t), & C \in \mathbb{R}^{p\times n}, D \in \mathbb{R}^{p\times m} \end{cases} \tag{7.1}$$

where the pair (A, C) is observable.

Knowing h_s and h_f, it follows that the two systems Σ_s and Σ_f (seen as the exact discretizations of the system Σ at the sampling rates $1/h_s$ and $1/h_f$ respectively) are known

and can be represented by the following *step-invariant transformations* [15]:

$$\Sigma_{\mathbf{s}} : \begin{cases} x_s(k+1) = A_s\ x_s(k) + B_s\ u_s(k) \\ \\ y_s(k) = C\ x_s(k) + D\ u_s(k) \end{cases} \tag{7.2}$$

$$\Sigma_{\mathbf{f}} : \begin{cases} x_f(k+1) = A_f\ x_f(k) + B_f\ u_f(k) \\ \\ y_f(k) = C\ x_f(k) + D\ u_f(k) \end{cases} \tag{7.3}$$

where for $i = (s, f)$: $A_i = e^{h_i A}$, $B_i = \int_0^{h_i} e^{\tau A} d\tau B$ and where $x_i(k) \triangleq x(kh_i)$, $u_i(k) \triangleq u(kh_i)$ and $y_i(k) \triangleq y(kh_i)$.

The sampling times h_s and h_f are assumed to satisfy the following:

(i) h_f is strictly less than h_s and the ratio between them is an integer number, i.e:

$$r = \frac{h_s}{h_f}, \qquad \text{where } r \in \mathbb{Z}^+ \text{ and } r > 1 \tag{7.4}$$

(ii) The sampling time h_f is *non-pathological*, i.e, no two eigenvalues of A differ by $(j.k\frac{2\pi}{h_f})$, $k \in \mathbb{Z}$, $k \neq 0$, and j being the imaginary number.

Assumption (i) is a technical assumption that guarantees that the slow rate data is a proper subset of the fast rate data. Assumption (ii) implies that the observability assumption is preserved for the pair (A_f, C) [15].

Luenberger observers for $\Sigma_{\mathbf{s}}$ and $\Sigma_{\mathbf{f}}$ will be denoted by $\Psi_{\mathbf{s}}$ and $\Psi_{\mathbf{f}}$ respectively and have the following structure:

$$\Psi_{\mathbf{i}},\ i = (s, f) : \begin{cases} \hat{x}_i(k+1) = A_i\ \hat{x}_i(k) + B_i\ u_i(k) + L_i\ [y_i(k) - \hat{y}_i(k)],\ L_i \in \mathbb{R}^{n \times p} \\ \\ \hat{y}_i(k) = C\ \hat{x}_i(k) + D\ u_i(k) \end{cases} \tag{7.5}$$

where L_i (the observer gain) is a static matrix designed to ensure that all of the eigenvalues of the matrix $(A_i - L_i C)$ lie in the open unit circle of the complex plane.

Throughout this chapter, we will also make use of the same definitions and notations introduced in Chapter 2 (section 2.4) but for discrete-time signals and systems, with the main differences as:

- **Definition 7.1** *(ℓ_2 Space): The space ℓ_2 consists of all Lebesgue measurable functions* $u : \mathbb{Z}^+ \to \mathbb{R}^q$, *having a finite ℓ_2 norm* $\|u\|_{\ell_2}$, *where* $\|u\|_{\ell_2} \triangleq \sqrt{\sum_{k=0}^{\infty} \|u(k)\|^2}$, *with* $\|u(k)\|$ *as the Euclidean norm of the vector $u(k)$.*

- In the case of a linear time-invariant system $G : \ell_2 \to \ell_2$ with a stable transfer matrix $\hat{G}(z)$, $\gamma(G)$ is equivalent to the H_∞ norm of $\hat{G}(z)$ defined as follows:

$$\gamma(G) \overset{\Delta}{=} \parallel \hat{G}(z) \parallel_\infty = \max_{\theta \in [0, 2\pi]} \sigma\mathrm{max}(\hat{G}(e^{-j\theta})).$$

where $\sigma_{\mathrm{max}}(.)$ represents the maximum singular value of $\hat{G}(e^{-j\theta})$.

- The partitioned matrix K:

$$K = \left[\begin{array}{c|c} A & B \\ \hline C & D \end{array} \right]$$

(when used as an operator from y to u, i.e, $u = Ky$) represents the state space representation:

$$\xi(k+1) = A \ \xi(k) + B \ y(k)$$
$$u(k) = C \ \xi(k) + D \ y(k)$$

and in that case the transfer matrix is $\hat{K}(z) = C(zI - A)^{-1}B + D$.

- In all block diagrams used in this chapter, solid and dashed lines represent continuous-time and discrete-time signals respectively.

7.2 Lifting Formulation for SDO Design

To solve the SDO design problem introduced in section 7.1 and represented by Figure 7.1, it is necessary to find a model that captures the fast rate states that we need to estimate (i.e, $x_f(k)$) and which is, at the same time, function of an available set of input/output information. The model Σ_s in (7.2) (which is an exact model of SPH) is a slow rate model though, and the Luenberger observer Ψ_s in (7.5) (or any other observer designed for Σ_s) would just give a state estimation for the slow rate states $x_s(k)$. On the other hand, using the model Σ_f in (7.3) to design an observer such as Ψ_f in (7.5) is not a feasible solution for the SDO design problem, since it assumes the complete knowledge of the fast rate output information $y_f(k)$ (which is not available in real-time). The multirate system SPH_f, however, maps the fast rate input $u_f(k)$ into the slow rate output $y_s(k)$ where both are measured "known" signals. In this subsection, we will use the Lifting technique to find a model for SPH_f that also captures the fast rate states $x_f(k)$. To this end, we will first give a brief introduction to the Lifting technique, then we will present how it can be used to design a SDO for the system in Figure 7.1. It will be shown that the Lifting solution is equivalent to

a trivial design which consists of fast rate open loop estimations that are updated by a slow rate classical Luenberger observer.

7.2.1 Lifting Technique

The Lifting technique is one of the classical approaches used in multirate digital control. It relies on the use of a linear, time-varying, non-causal operator $\mathbf{L}_\mu$, which operating on a discrete signal $v(k) \equiv \{v(0), v(1), v(2), \ldots\}$ gives another discrete signal referred to as the lifted signal $\underline{v}(k)$ where:

$$\underline{v}(k) \stackrel{\Delta}{=} \mathbf{L}_\mu v(k) \equiv \left\{ \begin{bmatrix} v(0) \\ v(1) \\ \vdots \\ v(\mu-1) \end{bmatrix}, \begin{bmatrix} v(\mu) \\ v(\mu+1) \\ \vdots \\ v(2\mu-1) \end{bmatrix}, \ldots \right\} \tag{7.6}$$

Here $\mu \in \mathbb{Z}^+$ is referred to as the Lifting order. The Lifting operator transforms a fast rate signal into a slow rate signal that contains the same information. This is clear by noting that if $v(k)$ is a discrete-time signal of vectors of order "q" sampled every "h" seconds, $\underline{v}(k)$ can be considered as a signal of vectors of order "μq" (sampled every "μh" seconds) and that store the same information in $v(k)$. According to the previous discussion on the Lifting operator, the two signals $x_s(k) \in \mathbb{R}^n$ and $x_f(k) \in \mathbb{R}^n$ (defined in (7.2) and (7.3)) are two discrete signals of different sampling times (h_s and h_f respectively), while $x_s(k) \in \mathbb{R}^n$ and $\underline{x_f}(k) \in \mathbb{R}^{rn}$ ($\stackrel{\Delta}{=} \mathbf{L}_r x_f(k)$) have the same sampling time and are related by:

$$x_s(k) = \begin{bmatrix} I_n & 0_n & \ldots & 0_n \end{bmatrix}_{1 \times r} \underline{x_f}(k)$$

The inverse of $\mathbf{L}_\mu$ is denoted by $\mathbf{L}_\mu{}^{-1}$ and is also a linear, time varying (but causal) operator. Both $\mathbf{L}_\mu$ and $\mathbf{L}_\mu{}^{-1}$ preserve the ℓ_2 norms [15].

In addition to lifting signals, the Lifting operators are also used to lift systems as follows:

Consider G_d; a discrete-time, LTI, single rate system (inputs and outputs are discrete signals sampled every "h" seconds) that has n states, m inputs and p outputs, and that is represented as:

$$G_d \stackrel{\Delta}{=} \left[\begin{array}{c|c} A & B \\ \hline C & D \end{array} \right]$$

where A, B, C and D are matrices of appropriate dimensions. The lifted system $\underline{G_d}$ is defined as the system $\underline{G_d} \stackrel{\Delta}{=} \mathbf{L}_\mu G_d \mathbf{L}_\mu{}^{-1}$. It can be shown that the representation of $\underline{G_d}$ is as

follows [15]:

$$\underline{G_d} \equiv \left[\begin{array}{c|cccc} A^\mu & A^{\mu-1}B & A^{\mu-2}B & \ldots & B \\ \hline C & D & 0_{pm} & \ldots & 0_{pm} \\ CA & CB & D & \ldots & 0_{pm} \\ \vdots & \vdots & \vdots & \vdots & \vdots \\ CA^{\mu-1} & CA^{\mu-2}B & CA^{\mu-3}B & \ldots & D \end{array}\right] \tag{7.7}$$

The system $\underline{G_d}$ is also a discrete-time, LTI, single rate system. But it has μm inputs and μp outputs and all these inputs and outputs are sampled every "μh" seconds. Therefore, $\underline{G_d}$ is considered as a slow rate representation of G_d. Lifting a system preserves its H_∞ norm, i.e,
$\parallel \hat{\underline{G_d}}(z) \parallel_\infty = \parallel \hat{G_d}(z) \parallel_\infty$.

Throughout this chapter, we will assume the Lifting order to be the constant r defined in (7.4), and we will use the operator $\mathbf{L}$ to refer to $\mathbf{L_r}$. Finally, we present two important system relations that hold for sampled-data systems such as the one in Figure 7.1 using the Lifting operator (for proof refer to [15]):

$$S_f\, H \equiv \mathbf{L}^{-1}\, Q \tag{7.8}$$

where the operator Q is the static linear matrix $\begin{bmatrix} I_m & I_m & \ldots & I_m \end{bmatrix}^T_{1\times r}$.
And,

$$S\, P\, H_f \equiv R\, \mathbf{L}\, S_f\, P\, H_f \tag{7.9}$$

where the operator R is the static linear matrix $\begin{bmatrix} I_p & 0_p & \ldots & 0_p \end{bmatrix}_{1\times r}$.

7.2.2 Application to the SDO design problem

As mentioned in the beginning of section 7.2, the multirate system SPH_f (which maps the fast rate input $u_f(k)$ into the slow rate output $y_s(k)$ as in (7.10)) is needed to solve the SDO problem.

$$y_s(k) = SPH_f\, u_f(k) \tag{7.10}$$

To find a model for that system, it is first easy to see (by using the Lifting notation in (7.8)) that $u_f(k)$ is related to $u_s(k)$ by the equation:

$$\underline{u_f}(k) = Q\, u_s(k) \tag{7.11}$$

In order to reflect the response of the fast rate states $x_f(k)$, it is also important to remark that the model of P in (7.1) can also be represented as:

$$P = M_1 P' + M_2 \tag{7.12}$$

where $P' = \left[\begin{array}{c|c} A & B \\ \hline I_n & 0_{nm} \end{array}\right]$, $M_1 = \left[\begin{array}{c|c} 0_n & 0_n \\ \hline 0_{pn} & C \end{array}\right]$ and $M_2 = \left[\begin{array}{c|c} 0_n & 0_{nm} \\ \hline 0_{pn} & D \end{array}\right]$ (all the partitioned

matrices here represent *continuous-time* state space representations). Therefore, using the

Lifting properties introduced in section 7.2.1, along with equations (7.11) and (7.12), the

multirate system SPH_f can be represented by the following state space representation (see

Appendix A.5 for more details about the derivation of this model):

$$\xi(k+1) = A_f^r \, \xi(k) + \begin{bmatrix} A_f^{r-1}B_f & A_f^{r-2}B_f & \ldots & B_f \end{bmatrix} \underline{u_f}(k)$$

$$\underline{x_f}(k) = \underbrace{\begin{bmatrix} I_n \\ A_f \\ \vdots \\ A_f^{r-1} \end{bmatrix}}_{\bar{C}} \xi(k) + \underbrace{\begin{bmatrix} 0_{nm} & 0_{nm} & \ldots & 0_{nm} \\ B_f & 0_{nm} & \ldots & 0_{nm} \\ \vdots & \vdots & \vdots & \vdots \\ A_f^{r-2}B_f & A_f^{r-3}B_f & \ldots & 0_{nm} \end{bmatrix}}_{\bar{D}} \underline{u_f}(k) \qquad (7.13)$$

$$y_s(k) = \begin{bmatrix} C & 0_{pn} & \ldots & 0_{pn} \end{bmatrix} \underline{x_f}(k) + \begin{bmatrix} D & 0_{pm} & \ldots & 0_{pm} \end{bmatrix} \underline{u_f}(k)$$

The following theorem presents an observer for this model and provides conditions for

its convergence. The observer presented in this theorem is obtained by applying a classical

Luenberger observer structure to the state space model in (7.13).

Theorem 7.1 *The system described by the following equations:*

$$\hat{\xi}(k+1) = A_f^r \, \hat{\xi}(k) + \begin{bmatrix} A_f^{r-1}B_f & A_f^{r-2}B_f & \ldots & B_f \end{bmatrix} \underline{u_f}(k) + L_\ell \left(y_s(k) - \hat{y}_s(k)\right)$$

$$\underline{\hat{x}_f}(k) = \bar{C} \, \hat{\xi}(k) + \bar{D} \, \underline{u_f}(k) \qquad (7.14)$$

$$\hat{y}_s(k) = \begin{bmatrix} C & 0_{pn} & \ldots & 0_{pn} \end{bmatrix} \underline{\hat{x}_f}(k) + \begin{bmatrix} D & 0_{pm} & \ldots & 0_{pm} \end{bmatrix} \underline{u_f}(k)$$

is a sampled-data observer (SDO) for the system in Figure 7.1 if and only if the observer

gain L_ℓ is chosen such that $\left(A_f^r - L_\ell \bar{C}\right)$ is Hurwitz.

Proof: By defining the error variables as $e_x = \underline{x_f}(k) - \underline{\hat{x}_f}(k)$ and $e_\xi = \xi(k) - \hat{\xi}(k)$, we have:

$$e_x(k) = \bar{C} \, e_\xi(k)$$

But using (7.13) and (7.14) we have:

$$
\begin{aligned}
e_\xi(k+1) &= \xi(k+1) - \hat{\xi}(k+1) \\
&= A_f^r\, \xi(k) - \left(A_f^r\, \hat{\xi}(k) + L_\ell\, (y_s(k) - \hat{y}_s(k)) \right) \\
&= A_f^r\, e_\xi(k) - L_\ell \left(\begin{bmatrix} C & 0_{pn} & \ldots & 0_{pn} \end{bmatrix} e_x(k) \right) \\
&= A_f^r\, e_\xi(k) - L_\ell \begin{bmatrix} C & 0_{pn} & \ldots & 0_{pn} \end{bmatrix} \bar{C}\, e_\xi(k) \\
&= \left(A_f^r - L_\ell C \right) e_\xi(k)
\end{aligned}
$$

Therefore, $\left(A_f^r - L_\ell C \right)$ Hurwitz is a necessary and sufficient condition for the error $e_\xi(k)$ (and hence for the error $e_x(k)$) to converge to zero. It follows that (7.14) is an SDO for the system in Figure 7.1 with $\underline{\hat{x}}_f(k)$ as a fast rate state estimation. $\qquad\square$

Remarks:

1) A necessary and sufficient condition for arbitrary pole placement of the SDO introduced in theorem 7.1 is the observability of the pair $\left(A_f^r, C \right)$. It is important to note that this is not guaranteed by the "non-pathological" assumption for h_f in section 7.1.1.

2) The observer has a time delay of h_s (see [97] for more details about the lag problem associated with Lifting). This is clear by noting that $\underline{\hat{x}}_f(0)$ (the first group of state estimations in the first inter-sampling period) is based on the initial guess for $\hat{\xi}(0)$. The correction term $(y_s(k) - \hat{y}_s(k))$ has effect on $\underline{\hat{x}}_f(k)$ only starting from $k = 1$.

3) The observer developed in this section through the Lifting technique is equivalent to two *Luenberger* observers performing in parallel as follows: the first one is Ψ_s given in (7.5) which is a slow rate closed loop observer having $L_s \equiv L_\ell$ (of the Lifting observer), and the other is Ψ_f (also given in (7.5) but with $L_f = 0_{np}$) as an open loop observer which updates its initial conditions every "r" steps with the new state of Ψ_s.

7.3 H_∞ SDO Design

To avoid some of the drawbacks associated with the Lifting technique (and discussed at the end of section 7.2.2), a direct use of the available fast rate model in (7.3) to design a SDO is necessary. However, as we mentioned before, any Luenberger observer for this model (such as the observer Ψ_f in (7.5)) is not a feasible solution due to the unavailable fast rate output

information $y_f(k)$. Moreover, if $y_f(k)$ is replaced by $\tilde{y}_f(k)$:

$$\tilde{y}_f(k) = y_f(k) + d(k) \tag{7.15}$$

(which is an arbitrary approximation to $y_f(k)$ with an error vector $d(k)$), then the observer Ψ_f has an estimation error $e = x_f - \hat{x}_f$ with dynamics given from:

$$e(k+1) = (A_f - L_f C)\ e(k) - L_f\ d(k) \tag{7.16}$$

which is affected by $d(k)$ causing divergence of the observer. In this section, we solve the SDO design problem by using a dynamic observer structure (instead of the Luenberger structure in (7.5)). We apply the extra degrees of freedom to minimize the effect of $d(k)$ on the estimation error, offering a robust alternative to the trivial design obtained by Lifting. We show that the proposed design overcomes some of the drawbacks associated with the Lifting technique. Moreover, we show that the problem is equivalent to an H_∞ optimal control problem which satisfies the standard regularity assumptions in the H_∞ optimization theory, making the proposed design solvable using commercially available software, similar to the Lipschitz observer design problems introduced in Chapters 3, 4 and 5.

Towards that goal, the proposed dynamical observer for the fast rate model (7.3) is:

$$\hat{x}_f(k+1) = A_f\ \hat{x}_f(k) + B_f\ u_f(k) + \eta(k) \tag{7.17}$$

$$\hat{y}_f(k) = C\ \hat{x}_f(k) + D\ u_f(k) \tag{7.18}$$

where $\eta(k)$ is obtained by applying a dynamical compensator on the output estimation error. In other words $\eta(k)$ is given from

$$z(k+1) = A_L\ z(k) + B_L\ (\tilde{y}_f(k) - \hat{y}_f(k)); \qquad A_L \in \mathbb{R}^{q \times q}, B_L \in \mathbb{R}^{q \times p} \tag{7.19}$$

$$\eta(k) = C_L\ z(k) + D_L\ (\tilde{y}_f(k) - \hat{y}_f(k)); \qquad C_L \in \mathbb{R}^{n \times q}, D_L \in \mathbb{R}^{n \times p} \tag{7.20}$$

where $\tilde{y}_f(k)$ is an approximation to $y_f(k)$ with an error vector $d(k)$ as given in (7.15). We will also write

$$K = \left[\begin{array}{c|c} A_L & B_L \\ \hline C_L & D_L \end{array} \right] \tag{7.21}$$

to represent the "q^{th} order" compensator in (7.19)-(7.20). It is straightforward to see that the observer error dynamics in (7.16) is now given by

$$e(k+1) = A_f\ e(k) - \eta(k) \tag{7.22}$$

$$\eta(k) = K\ (Ce(k) + d(k)) \tag{7.23}$$

which can also be represented by the standard setup in Figure 7.2 having the variables in (7.24):

$$\omega = d(k)$$
$$\nu = \eta(k) \qquad (7.24)$$
$$\zeta = e(k) = x_f(k) - \hat{x}_f(k)$$
$$\varphi = Ce(k) + d(k)$$
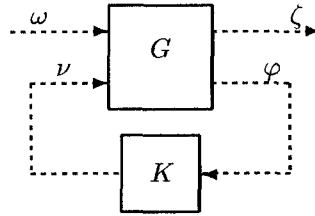
Figure 7.2: Standard Setup: the Discrete-time Case.

and the controller K in (7.21), and with the plant G as the standard state space representation in:

$$G \stackrel{\Delta}{=} \left[\begin{array}{c|cc} A & B_1 & B_2 \\ \hline C_1 & D_{11} & D_{12} \\ C_2 & D_{21} & D_{22} \end{array} \right] = \left[\begin{array}{c|cc} A_f & 0_{np} & -I_n \\ \hline I_n & 0_{np} & 0_n \\ C & I_p & 0_{pn} \end{array} \right] \qquad (7.25)$$

Therefore, the SDO design problem reduces to the *input/output* stability problem of the setup in Figure 7.2 which has as input the approximation error $d(k)$ and as output the observer estimation error $e(k)$. With an arbitrary choice for $\tilde{y}_f(k)$ in (7.15), one can ensure that $d(k)$ is a bounded signal and the problem in Figure 7.2 can then be solved as an $\mathcal{L}_1$ optimization problem. However, we here focus on the use of H_∞ optimization to solve this problem, assuming $d(k)$ to be of finite energy (i.e, $d(k) \in \ell_2$) or to have a certain frequency pattern reducing the problem to a weighted H_∞ optimal control problem. Unfortunately, the SDO design problem cannot be carried out directly using the standard H_∞ solution since the standard form in (7.25) does not satisfy all of the regularity assumptions in the H_∞ framework, summarized in section 7.3.1 (Notice that $D_{12}^T D_{12}$ is singular). In the following we show that this irregular H_∞ problem is equivalent to a modified H_∞ problem satisfying

all the regularity assumptions. Based on this result, we present a design procedure that can be used to compute the dynamic gain K for the SDO in (7.17)-(7.21).

7.3.1 Problem Regularization and H_∞ Design Procedure

By adding a "weighted" disturbance term $\epsilon\ \phi(k)$ in the state equation of the fast rate model (7.3), and extending the external output ζ to include the "weighted" vector $\beta\eta(k)$ (where $\beta > 0$), it can be seen that the observer error dynamics can still be represented by the setup in Figure 7.2 with the variables in (7.24), except for replacing ω by $\bar{\omega}$ defined as:

$$\bar{\omega} \stackrel{\Delta}{=} \begin{bmatrix} \phi(k) & d(k) \end{bmatrix}^T \tag{7.26}$$

and replacing ζ by $\bar{\zeta}$ defined as:

$$\bar{\zeta} = \begin{bmatrix} e(k) & \beta\eta(k) \end{bmatrix}^T \tag{7.27}$$

and redefining the plant G as:

$$G \stackrel{\Delta}{=} \left[\begin{array}{c|cc} A & B_1 & B_2 \\ \hline C_1 & D_{11} & D_{12} \\ C_2 & D_{21} & D_{22} \end{array} \right] = \left[\begin{array}{c|c|c} A_f & \begin{bmatrix} \epsilon I_n & 0_{np} \end{bmatrix} & -I_n \\ \hline \begin{bmatrix} I_n \\ 0_n \end{bmatrix} & \begin{bmatrix} 0_n & 0_{np} \\ 0_n & 0_{np} \end{bmatrix} & \begin{bmatrix} 0_n \\ \beta I_n \end{bmatrix} \\ \hline C & \begin{bmatrix} 0_{pn} & I_p \end{bmatrix} & 0_{pn} \end{array} \right] \tag{7.28}$$

which satisfies all of the regularity assumptions of the discrete H_∞ problem summarized below [15]:

1. (A,B_2) stabilizable: satisfied for any matrix A.

   (C_2,A) detectable: satisfied iff $(A_f,\ C)$ is detectable.

2. $D_{21}D_{21}^T = I_p$, which is nonsingular.

   $D_{12}^T D_{12} = \beta^2 I_n$, which is nonsingular.

3. $\text{rank} \begin{bmatrix} A - \lambda I & B_2 \\ C_1 & D_{12} \end{bmatrix} = 2n = \text{full column rank } \forall\lambda.$

   $\text{rank} \begin{bmatrix} A - \lambda I & B_1 \\ C_2 & D_{21} \end{bmatrix} = n + p = \text{full row rank } \forall\lambda.$

4. $D_{22} = 0.$

Therefore, all the regularity assumptions are satisfied iff the pair (A_f, C) is detectable which is implied by the "non pathological" assumption on h_f in section 7.1.1 (that guarantees (A_f, C) to be observable).

Similar to the Lipschitz case, a certain equivalence relationships among the setups T_1 and T_2 can be demonstrated (T_1 being the setup in Figure 7.2 associated with (7.25), while T_2 is the one associated with (7.28)):

Lemma 7.1 *Consider a stabilizing controller K for the setups T_1 and T_2, then $\| \hat{T}_1(z) \|_\infty < \gamma$ if and only if $\exists\ \epsilon > 0,\ \beta > 0$ such that $\| \hat{T}_3(z) \|_\infty < \gamma$.*

Proof: Similar to the proof of Lemmas 3.1 and 3.2 in Chapter 3, hence omitted.   □

We are now ready to present our main result in the form of a theorem showing that the observer gain K needed to minimize the energy (ℓ_2 norm) of the estimation error for the SDO in (7.17)-(7.21) must solve a regular H_∞ optimal control problem. To this end, we define the regular discrete H_∞ problem "Problem 1" as follows:

<u>Problem 1</u>: *Given $\epsilon > 0$ and $\beta > 0$, find S, the set of admissible controllers K satisfying $\| \hat{T}_{\zeta\omega}(z) \|_\infty < \gamma$ for the setup in Figure 7.2 with G having the state space representation in (7.28).*

The main result is summarized in the following theorem:

Theorem 7.2 *Consider the SDO design problem in Figure 7.1 with the plant P in (7.1) and the fast rate model in (7.3). Then the following two statements are equivalent:*

(i) The observer (7.17)-(7.21) with the dynamic gain K has a minimum estimation error energy.

(ii) $\exists\ \epsilon^* > 0,\ \beta^* > 0$ s.t $K \in S^*$ (the set of controllers solving "Problem 1" defined above with the minimum possible γ).

Proof: Since the observer's error dynamics is represented by T_1 (the setup in Figure 7.2 associated with (7.25)), then the estimation error's energy satisfies:

$$\|e\|_{\ell_2} \le \|\hat{T}_1(z)\|_\infty \|d\|_{\ell_2}$$

Then, $\|e\|_{\ell_2}$ is minimized, for a certain disturbance signal $d(k)$, if and only if the controller K minimizes $\|\hat{T}_1(z)\|_\infty$. The equivalence of the two statements then follows as a direct result of Lemma 7.1.   □

The following iterative "binary search" procedure is then proposed to evaluate the observer gain K that minimizes the estimation error's energy of the SDO observer in (7.17)-(7.21):

Design procedure:

Step 1 Set γ_{low} to an arbitrary small positive value and γ_{high} to an arbitrary large positive value.

Step 2 Set $\epsilon > 0$ and $\beta > 0$ and set $\gamma \leftarrow \frac{\gamma_{low} + \gamma_{high}}{2}$.

Step 3 Test solvability of Problem 1 (the regular H_∞ problem defined earlier). If test fails then go to Step 5 ; otherwise solve the problem (using available software packages), select any $K \in S$ as a candidate observer gain and set $\gamma_{high} \leftarrow \gamma$.

Step 4 If $|\gamma_{high} - \gamma_{low}| <$ a threshold value then *stop the algorithm*, otherwise go back to Step 2.

Step 5 Set $\epsilon \leftarrow \frac{\epsilon}{2}$ and $\beta \leftarrow \frac{\beta}{2}$. If ϵ or $\beta <$ a threshold value then $\gamma_{low} \leftarrow \gamma$ and go to Step 4, otherwise go to Step 3.

Remarks

- The H_∞ design procedure is guaranteed to converge if the pair (A_f, C) is detectable [15]. This detectability condition is guaranteed by the "non-pathological assumption" on h_f (unlike the observability condition of the Lifting technique as seen at the end of section 7.2.2).

- The H_∞ SDO does not introduce a time delay in the state estimation. This is another advantage of the H_∞ approach over the Lifting technique in section 7.2 (see the remarks at the end of section 7.2.2 for more details).

- The assumption of finite energy is easily satisfied in step tracking applications if $\tilde{y}_f(k)$ is selected as $\tilde{y}_f(k) = y_s(r \ (k \ mod \ r))$ (i.e, approximating the fast rate output as a constant signal between samples). In that case the approximation error term $d(k)$ in (7.15) is guaranteed to be a finite energy signal, i.e $d(k) \in \ell_2$.

7.4   Simulation Results

In this section we consider an illustrative example using the rotary inverted pendulum (ROT-PEN) introduced in Chapter 6. The linearized model about the pendant configuration, i.e the equilibrium point ($\theta_1 =$ constant, $\theta_2 = 180$ degrees *and* $u = 0$) gives the following 4th

order SISO-LTI model (state vector x and units for this model are same as in Chapter 6):

$$\dot{x} = \begin{bmatrix} 0 & 0 & 1 & 0 \\ 0 & 0 & 0 & 1 \\ 0 & -25.14 & -17.22 & -0.2210 \\ 0 & -68.13 & -16.57 & -0.599 \end{bmatrix} x + \begin{bmatrix} 0 \\ 0 \\ 26.3370 \\ 25.3596 \end{bmatrix} u \qquad (7.29)$$

$$y = \begin{bmatrix} 1 & 0 & 0 & 0 \end{bmatrix} x \qquad (7.30)$$

This model is open-loop unstable with the open-loop poles as $\{0, \ -13.3131, -0.9942 \pm 6.8510i\}$. In our simulation, we first stabilize the system, furthermore the closed-loop poles and the feedforward gain are chosen to make the output track a step input of magnitude of 10 degrees. This is for the purpose of validating the convergence of the proposed observer schemes and demonstrating the results in a controlled manner. But it is true that the observers can work for unstable systems. The simulation time is taken as 50 seconds.

The observer design in case of H_∞ was done with the help of the Matlab command *hinfsyn* and using the *Bilinear* transformation approach [15] to get a discrete H_∞ controller. In case of lifting, the command *place* was used to place the *discrete* poles of the observer (7.14) at $\{0.0183, \ 0.0025, -0.0563 \pm 0.1231i\}$.

The value of h_f is fixed to 0.1 and h_s is changed to take the values $\{0.2, 0.5, 0.8, \text{and } 1\}$. This represents a study for different values of r in equation (7.4). The approximated output $\tilde{y}_f(k)$ is chosen as the held output between samples (i.e, $\tilde{y}_f(k) = y_s(r \ (k \ mod \ r))$) as shown in figure 7.3 for the case $h_s = 1$. The approximation error $d(k)$ in (7.15) in this case is shown in Figure 7.4. It can be seen that the disturbance term $d(k)$ in Figure 7.4 is a decaying signal having a finite ℓ_2 norm (note that all ℓ_2 norms are computed for the interval $t = [0, \ 50 \ sec]$).

Case study 1: In this case, the simulation is conducted to study the difference between the Lifting technique introduced in section 7.2 and the H_∞ technique of section 7.3. The observer initial conditions (for both techniques) are taken as $\begin{bmatrix} 0.2 & 0 & 0 & 0 \end{bmatrix}^T$. Figure 7.5 shows the output estimation error for the two cases when $h_s = 1$. Table 7.1 shows the trend of state estimation error's ℓ_2 norm with the change of h_s. With the increase of r (the ratio between h_s and h_f), the number of inputs and outputs for the system defined by equation (7.13) increases making the implementation of the lifting technique more complex. It is also important to note that for very large values of h_s, the system in (7.13) could become unobservable making the use of the lifting technique impossible (as is the case for values of $h_s \gg 1$). Two factors are important in the choice of r: the computer speed to implement the observer in Figure 7.1;
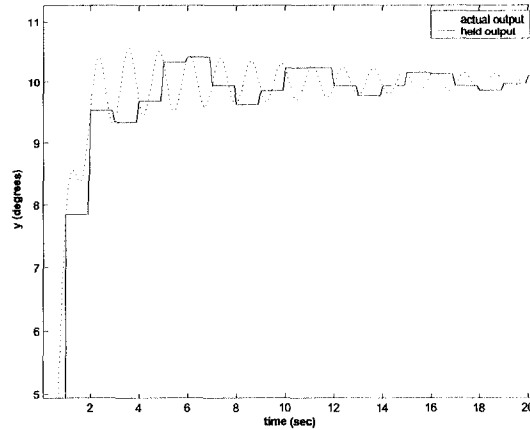
Figure 7.3: The Actual Output and the Approximated Output at $h_s = 1$ sec.
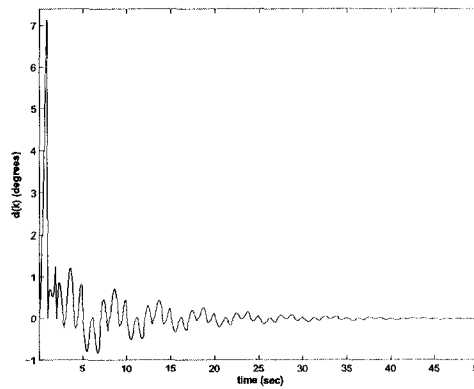
Figure 7.4: The Disturbance Term $d(k)$ at $h_s = 1$ sec.

and the required bound on the disturbance term since the norm of the vector $d(k)$ in (7.15) increases with the increase of r.

Case study 2: In this case, the simulation shows the application of the Lifting and H_∞ sampled-data observers in the fast rate fault detection problem. In this experiment, h_s is assumed to be 1 second, and a sensor fault is assumed to start after 20 seconds in the form of a small bias of magnitude 1.75 degrees. The residual signal $s(k)$ is taken as the summation of the output estimation error ($r(k)$) over a time window, and a simple decision scheme at step k is assumed as follows:

$$s(k) = \sum_{i=k-4}^{k} |r(k)| > \text{threshold} \Rightarrow \text{fault is detetected} \tag{7.31}$$

Applying both techniques (with the threshold in (7.31) as 2.0), the fault in H_∞ is detected at
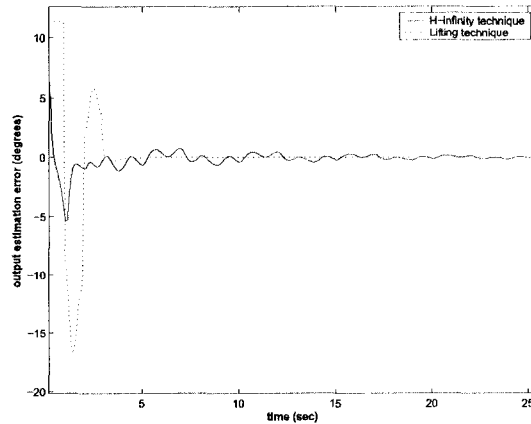
Figure 7.5: Output Estimation Error for Lifting and H_∞ at $h_s = 1$ sec.

Table 7.1: Case study 1 - effect of change of h_s on $\| e \|_{\ell_2}$

Value of h_s (in sec.)	0.2	0.5	0.8	1
H_∞ technique	16.0328	16.9887	18.3506	19.5616
Lifting technique	22.9438	36.9739	46.2796	57.2925

time = 20.1 seconds, while in Lifting it is detected at time = 22 seconds. The residual signals for both techniques are shown in Figure 7.6. This case study demonstrates that the proposed H_∞ observer scheme can provide updated residual signal in fast rate without introducing much time delay. This is important in the fault detection applications. However, in this example, no disturbance is added. In the case of unknown disturbance, more treatment needs to be taken to eliminate or attenuate the effects of disturbance which is a robust fault detection problem. The proposed H_∞ observer can find potential applications in this context.
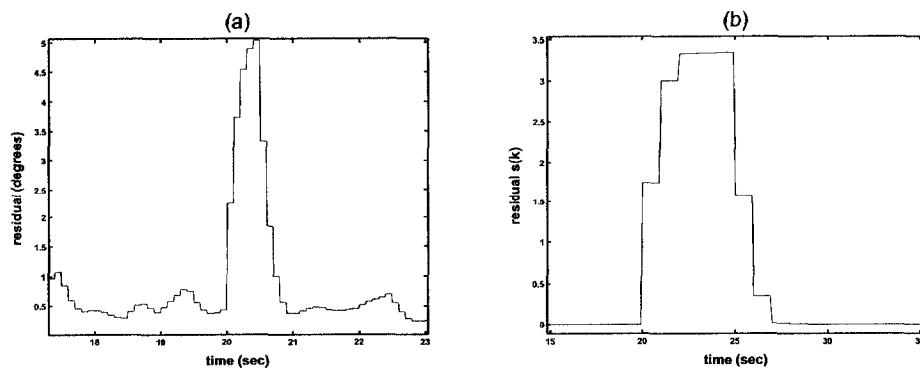
Figure 7.6: (a) Residual Signal for H_∞ Technique, (b) Residual Signal for Lifting.

7.5 Conclusion

In this chapter, we considered the problem of sampled-data state reconstruction in linear time invariant systems. An observer structure that can generate intersample state estimation is introduced and the problem is shown to be equivalent to a well defined H_∞ optimal control problem. A design algorithm to solve the H_∞ optimization problem is presented and can be carried out using commercially available software, such as MATLAB. The proposed H_∞ design has some important advantages over the classical lifting technique. This has been demonstrated through simulation experiments conducted on the rotary inverted pendulum. The solution of this problem in the Lipschitz case is suggested as future work.

Chapter 8

Conclusion and Future Work

This thesis undertook the observer-based approach for the solution of the fault diagnosis problem in a class of nonlinear control systems, known as Lipschitz systems. The observer-based approach adopted in this thesis falls in the category of analytical redundancy techniques where the powerful techniques of mathematical modelling, state estimation and system identification are used for Fault Detection and Isolation (FDI). The major advantages of analytical redundancy over hardware redundancy is that the former is cost-effective and can be implemented in software on the same process control computer.

8.1   Summary of Contributions

The main results of this thesis are as follows:

- The Lipschitz observer design approach in [91, 94] provided a good starting point for this research, but could not be applied directly to the FDI problem because of their restrictive observer structure and also because of their idealized natures that did not take into account uncertain model parameters and disturbances. A dynamic observer structure was proposed to solve the Lipschitz observer design problem. The main contributions of this structure were twofold: (i) The observer stability condition that ensures asymptotic convergence of the state estimates is satisfied by a family of observers, adding extra degrees of freedom to the observer and laying the ground to the addition of the FDI objective in the design problem, (ii) The observer design can be carried out using a systematic design procedure which is less restrictive than the existing design approaches and that can be solved using commercially available software.

- A sensor FDI formulation was introduced and applied to both the LTI and Lipschitz cases. The additional observer dynamics showed to be effective in adding the identification objective to the problem (in addition to the detection and isolation objectives). It was proven that the classical observer structure could not solve the problem in this case. An analytical solution was presented for the LTI case, while for the Lipschitz case the problem was shown to be equivalent to a standard convex optimization problem (solvable using LMIs). In these formulations, different frequency patterns for the sensor faults were considered, and systematic design procedures were presented to solve the problem.

- The robust FDI problem was considered by studying the case of additive uncertainties (modeling uncertainties, disturbances, noise). The Unknown Input Observer (UIO) technique, used to deal with additive uncertainties in the LTI case, was generalized to Lipschitz systems. The new observer was applied to the robust sensor FDI problem. The problem was modelled as a two-objective optimization problem (solvable using numerical techniques) where the first objective is to achieve observer stability, while the second one is total decoupling of the effect of uncertainties in the estimation error.

- The new Lipschitz observer and sensor FDI designs were applied in a practical example, namely the *Quanser* rotary inverted pendulum (ROTPEN) in the Control Systems Lab, Electrical and Computer Engineering department, University of Alberta. The ROTPEN model falls in the category of planar robot manipulators, and the experimental results illustrated the applicability of the proposed techniques in the robotics field. The experiments showed the following:

    i) How to model a robot manipulator as a standard Lipschitz system.

    ii) The importance of the dynamic Lipschitz observer in large operating regions where the linear observer normally fails.

    iii) The accurate velocity estimation obtained using the dynamic observer, alleviating the need to introduce velocity sensors in real-time.

    iv) How the static observer fails, unlike the dynamic observer, when applied to the ROTPEN due to the large Lipschitz constant that the system has.

    v) The efficiency of the dynamic observer in diagnosing and tolerating sensor faults of different frequencies (including an important bias introduced by the error in the initial conditions of the pendulum sensor).

- Other important contributions included the application of the dynamic observer structure in the sampled-data state reconstruction problem for the LTI case. Using the H_∞ framework, it was shown that the dynamic observer has some important advantages over the classical Lifting technique that has been used to study similar problems, including: shorter time delay and more relaxed observability conditions.

8.2 Future Work

The following are suggested areas that could be pursued in future research.

General Lipschitz fault diagnosis The question of solving the FDI problem in (5.35)-(5.36) remains an open research problem. Using the dynamical observer structure, the problem is equivalent to a three-objective optimization problem for which an analytical solution is hard to find. Finding approximate solutions to this problem is another area that is important to the improvement of Lipschitz FDI algorithms.

The Lipschitz dynamic sampled-data observer problem Extension of the SDO problem introduced in Chapter 7 to the Lipschitz case is an important proposition. More research needs to be done to integrate the sampled-data design with the overall dynamical observer structure. Such design may make the Lipschitz FDI strategies more reliable, especially in practical examples with large sampling times, where a continuous-time model is not a good approximation.

Experimental results for the robust Lipschitz FDI problem Applying the results in Chapter 5 to a real-time practical example could be pursued in future research. The ROTPEN model used in Chapter 6 is not affected by uncertainties in the state equations, and was therefore an infeasible example. A future research direction would be model any unknown centrifugal, coriolis, gravity or friction terms (in the dynamic equations of a robot manipulator) as modeling uncertainties of the form "$Ed(t)$" and show that one can always obtain a solution for the robust Lipschitz FDI problem in this case.

Application of the dynamic structure to bilinear systems For generalization to other nonlinear systems one can first try to extend this thesis results to the class of Bilinear systems, of the form (2.22)-(2.23). This class of systems has very important applications especially in chemical and nuclear engineering. The application of the dynamical

observer structure can add extra degrees of freedom to the observer design and the FDI

problems.

Bibliography

[1] C. Aboky, G. Sallet, J. C. Vivalda, "Observers for Lipschitz Non-linear Systems," *International Journal of Control*, Vol. 75, pp. 204-212, 2002.

[2] K. Adjallah, D. Maquin, J. Ragot, "Nonlinear Observer Based Fault Detection," *IEEE Transactions on Automatic Control*, pp. 1115-1120, 1994.

[3] K. J. Åström, "Intelligent Control," *Proceedings of the 1st European Control Conference, ECC*, Grenoble, France, pp. 2328-2339, 1991.

[4] C. Bakiotis, J. Raymond, A. Rault, "Parameter and Discriminat Analysis for Jet Engine Mechanical State Diagnosis," *Proceedings of the IEEE Conference on Decision and Control, CDC*, Fort Lauderale, USA, 1979.

[5] M. Basseville, "Detecting Changes in Signals and Systems - A Survey," *Automatica*, Vol. 24, No. 3, pp. 309-326, 1988.

[6] M. Basseville, I. V. Nikiforov, Detecting of Abrupt Changes: Theory and Applications, Information and System Science, Prentice Hall, New York, 1993.

[7] R. V. Beard, Failure Accommodation in Linear System through Self Reorganization, Ph.D thesis, Massachusetts Institute of Technology, Mass., USA, 1971.

[8] S. P. Bhattacharyya, "Observer Design for Linear Systems with Unknown Inputs," *IEEE Transactions on Automatic Control* , vol. 23, pp. 483-484, 1978.

[9] K. K. Busawon, M. Saif, "A State Observer for Nonlinear Systems," *IEEE Transactions on Automatic Control*, Vol. 44, No. 11, November 1999.

[10] F. Caccavale, L. Villani, Fault Diagnosis and Fault Tolerance for Mechatronic Systems: Recent Advances, Springer-Verlag Berlin, 2003.

[11] S. K. Chang, P. L. Hsu, K. L. Lin, "A Parametric Transfer-matrix Approach to Fault Identification Filter Design and Thershold Selection," *International Journal on Systems Science*, Vol. 26, No. 4, pp. 741-754, 1995.

[12] J. Chen, "Robust Residual Generation for Model-based Fault Diagnosis of Dynamic Systems", Ph.D thesis, Univ.of York, UK, 1995.

[13] J. Chen , R. J. Patton, Robust Model-based Fault Diagnosis for Dynamic Systems, Kluwer Academic Publishers, 1999.

[14] J. Chen, R. J. Patton, H. Zhang, "Design of Unknown Input Observers and Robust Fault Detection Filters," *International Journal of Control*, Vol. 63, No.1, pp. 85-105, 1996.

[15] T. Chen, B. A. Francis, Optimal Sampled-data Control Systems, Springer, London, 1995.

[16] E. Y. Chow, A. Willsky, "Issues in the Development of a General Algorithm for Reliable Failure Detection," *Proceedings of the 19th IEEE Conference on Decision and Control, CDC*, Albuquerque, NM, 1980.

[17] E. Y. Chow, A. Willsky, "Analytical Redundancy and the Design of Robust Failure Detection Systems," *IEEE Transactions on Automatic Control*, Vol. 29, No. 7, 1984.

[18] C. Ciccarella, M. Dalla Mora, A. Germani, "A Luenberger-like Observer for Nonlinear Systems," *International Journal of Control*, Vol. 57, pp. 537-556, 1993.

[19] R. N. Clark, D. C. Fosth, V. M. Walton, "Detecting Instrumental Malfunctions in Control Systems," *IEEE Trans. Aero. and Electron. Sys.*, Vol. 11, pp. 465-473, 1975.

[20] R. Da, "Failure Detection of Dynamical Systems with the State χ^2 Test," *Journal of Guidance, Control and Dynamics*, Vol. 17, No. 2, pp. 271-277, 1994.

[21] M. Darouach, M. Zasadzinski, S. J. Xu, "Full-order Observers for Linear Systems with Unknown Inputs," *IEEE Transactions on Automatic Control* , vol. 39, No.3, pp. 606-609, 1994.

[22] M. A. Demetriou, "Robust Adaptive Techniques for Sensor Fault Detection and Diagnosis," *Proceedings of the IEEE Conference on Decision and Control*, December 1998.

[23] F. Deza, D. Bossanne, E. Busvelle, J. P. Gauthier, D. Rakotopara, "Exponential Observer for Nonlinear Systems," *IEEE Transactions on Automatic Control*, Vol. 38, No. 3, pp. 482-484, 1993.

[24] X. Ding, P. M. Frank, "Frequency Domain Approach and Thershold Selector for Robust Model-based Fault Detection and Isolation," *Preprint of IFAC/IMACS Symposium: SAFEPROCESS 91*, Baden-Baden, pp. 307-312, 1991.

[25] X. Ding, P. M. Frank, "An Adaptive Observer-based Fault Detection Scheme for Nonlinear Dynamic Systems," *Proceedings of the 12th IFAC World Congress*, Sydney, Australia, pp. 307-310, 1993.

[26] X. Ding, L. Guo, "An Approach to Time Domain Optimization of Observer-based Fault Detection Systems," *International Journal of Control*, Vol. 69, No. 3, pp. 419-442, 1998.

[27] S. X. Ding, T. Jeinsch, P. M. Frank, E. L. Ding, "A Unified Approach to the Optimization of Fault Detection Systems," *International Journal of Adaptive Control and Signal Processing*, Vol. 14, pp. 725-745, 2000.

[28] J. Doyle, K. Glover, P. Khargonekar and B. Francis, "State Space Solutions to Standard H_2 and H_∞ Control Problems," *IEEE Transactions on Automatic Control*, Vol. 34, No. 8, pp. 831-847, August 1989.

[29] A. Edelmayer, J. Bokor, F. Szigeti, L. Keviczky, "Robust Detection Filter Design in the Presence of Time-varying System Perturbations", *Automatica*, vol. 33, No. 3, pp 471-475, 1997.

[30] F. W. Fairman, S. S. Mahil, L. Luk, "Disturbance Decoupled Observer Design via Singular Value Decomposition," *IEEE Transactions on Automatic Control* , vol. 29, No.1, pp. 84-86, 1984.

[31] P. M. Frank, "Fault Diagnosis in Dynamic Systems using Analytical and Knowledge-based Redundancy - A Survey and Some New Results," *Automatica*, Vol. 26, No. 3, pp. 459-474, 1990.

[32] P. M. Frank, "Enhancement of Robustness in Observer-based Fault Detection," *International Journal of Control*, Vol. 59, No. 4, pp. 955-981, 1994.

[33] P. M. Frank, "Analytical and Qualitative Model-based Fault Diagnosis - A Survey and Some New Results," *European Journal of Control*, Vol. 2, pp. 6-28, 1996.

[34] P. M. Frank, X. Ding, "Frequency Domain Approach to Optimally Robust Residual Generation and Evaluation for Model-based Fault Diagnosis," *Automatica*, Vol. 30, pp. 789-804, 1994.

[35] P. M. Frank, X. Ding, "Survey of Robust Residual Generation and Evaluation Methods in Observer-based Fault Detection Systems," *Journal of Process Control*, Vol. 7, No. 6, pp. 403-424, 1997.

[36] P. M. Frank, S. X. Ding, T. Marcu, "Model-based Fault Diagnosis in Technical Processes," *Transactions of the Institute of Measurement and Control*, Vol. 22, No. 1, pp. 57-101, 2000.

[37] P. M. Frank, B. Köppen-Seliger, "Fuzzy Logic and Neural Network Applications to Fault Diagnosis," *International Journal of Approximate Reasoning*, Vol. 16, No. 1, pp. 67-88, 1997.

[38] P. M. Frank, R. Seliger, "Fault Detection and Isolation in Automatic Processes," *Control and Dynamic Systems*, Vol. 49, Academic Press, pp. 241-287, 1991.

[39] P. M. Frank, J. Wünnenberg, "Robust Fault Diagnosis using Unknown Input Schemes", *System Fault Diagnosis in Dinamical Systems: Theory and Application*, R.J. Patton, P. M. Frank and R. N. Clark (eds), pp. 47-98, Prentice Hall, 1989.

[40] P. Gahinet, P. Apkarian, "A Linear Matrix Inequality Approach to H_∞ Control," *International Journal of Robust and Nonlinear Control*, Vol. 4, pp. 421-448, 1994.

[41] E. Garcia, P. M. Frank, "Deterministic Nonlinear Observer Based Approaches to Fault Diagnosis: A Survey," *Control Engineering Practice*, Vol. 5, No. 5, pp. 663-670, 1997.

[42] V. Garg, J. K. Hedrick, "Fault Detection Filters for a Class of Nonlinear Systems," *Proceedings of the American Control Conference, ACC*, Seattle, Washington, pp. 1647-1651, June 1996.

[43] J. P. Gauthier, H. Hammouri, S. Othman, "A Simple Observer for Nonlinear Systems Applications to Bioreactors," *IEEE Transactions on Automatic Control*, Vol. 37, No. 6, June 1992.

[44] J. Gertler, "Survey of Model-based Failure Detection and Isolation in Complex Plants," *IEEE Control Systems Magazine*, Vol. 8, No. 6, pp. 3-11, 1988.

[45] J. Gertler, "Analytical Redundancy Methods in Failure Detection and Isolation," *Control Theory and Advanced Technology*, Vol. 9, No. 1, pp. 259-285, 1993.

[46] J. Gertler, "Modelling Errors as Unknown Inputs", *Preprints of IFAC symposium on fault detection, supervision and safety for technical processes: SAFEPROCESS'94*, Espoo, Finland, pp 266-271 (Vol. 1), 1994.

[47] J. Gertler, M. K. Kunwer, "Optimal Residual Decoupling for Robust Fault Diagnosis", *International Journal of Control*, vol. 61, No. 2, pp 395-421, 1995.

[48] J. Gertler, Q. Luo, "Robust Isolable Models for Failure Diagnosis," *AIChE J.*, Vol. 35, No. 11, pp. 1856-1868, 1989.

[49] J. Gertler, D. Singer, "A New Structural Framework for Parity Equation-based Failure Detection and Isolation," *Automatica*, Vol. 26, No. 2, pp. 381-388, 1990.

[50] A. Glumineau, V. Lopez, "Transformation to State Affine System and Observer Design," *In collections*, H. Nijmeijer, T. I. Fossen, New Directions in Nonlinear Observer Design, Springer-Verlag, London, 1999.

[51] Y. Guan, M. Saif, "A Novel Approach to the Design of Unknown Input Observers," *IEEE Transactions on Automatic Control* , vol. 36, No.5, pp. 632-635, 1991.

[52] H. Hammouri, M. Kinnaert, E. H. El-Yaagoubi, "Residual Generator Synthesis for Bilinear Systems up to Output Injection," *Proceedings of the 33th Conference on Decsions and Control, CDC*, Florida, USA, pp. 1548-1553, 1994.

[53] H. Hammouri, M. Kinnaert, E. H. El-Yaagoubi, "Fault Detection and Isolation for State Affine Systems," *European Journal of Control*, Vol. 4, pp. 2-16, 1998.

[54] H. Hammouri, M. Kinnaert, E. H. El-Yaagoubi, "Observer-based Approach to Fault Detection and Isolation for Nonlinear Systems," *IEEE Transactions on Automatic Control*, Vol. 44, No. 10, October 1999.

[55] D. Hengy, P. M. Frank, "Component Failure Detection via Nonlinear State Observers," *Proceedings of IFAC Workshop on Fault Detection and Safety in Chemical Plants*, Kyoto, Japan, pp. 153-157, 1986.

[56] D. J. Hill and P. J. Moylan, "Stability Results for Nonlinear Feedback Systems," *Automatica*, Vol. 13, pp. 377-382, 1977.

[57] D. M. Himmelblau, R. W. Barker, W. Suewatanakul, "Fault Classification with the aid of Artificial Neural Networks," *Preprint of IFAC/IMACS Symposium: SAFEPROCESS 91*, Baden-Baden, pp. 369-373, 1991.

[58] T. Höfling, R. Isermann, "Fault Detection based on Adaptive Parity Equations and Single Parameter Tracking," *Control Engineering Practice*, Vol. 4, No. 10, pp. 1361-1369, 1996.

[59] M. Hou, K. Busawon, M. Saif, "Observer Design based on Triangular Form Generated by Injective Map," *IEEE Transactions on Automatic Control*, Vol. 45, No. 7, July 2000.

[60] M. Hou, P. C. Müller, "Design of Observers for Linear Systems with Unknown Inputs," *IEEE Transactions on Automatic Control*, vol. 37, No.6, pp. 871-875, 1992.

[61] M. Hou, P. C. Müller, "Disturbance Decoupled Observer Design: A Unified Viewpoint," *IEEE Transactions on Automatic Control*, vol. 39, No.6, pp. 1338-1341, 1994.

[62] M. Hou, A. C. Pugh, "Observing State in Bilinear Systems: a UIO Approach", *Proceedings of the IFAC Symposium on Fault Detection, Supervision and Safety for Technical Processes: SAFEPROCESS'97*, Pergamon, Univ. of Hull, UK, pp. 783-788, 1998.

[63] L. R. Hunt, M. S. Verma, "Observers for Nonlinear Systems in Steady State," *IEEE Transactions on Automatic Control*, Vol. 39, No. 10, October 1994.

[64] R. Isermann, "Fault Diagnosis of Machines via Parameter Estimation and Knowledge Processing - Tutorial Paper," *Automatica*, Vol. 29, No. 4, pp. 815-835, 1993.

[65] T. Iwasaki, R. E. Skelton, "All Controllers for the General H_∞ Control Problem: LMI Existence Conditions and State Space Formulas," *Automatica*, Vol. 30, No. 8, pp. 1307-1317, 1994.

[66] N. H. Jo, J. H. Seo, "A State Observer for Nonlinear Systems and its Application to Ball and Beam System," *IEEE Transactions on Automatic Control*, Vol. 45, No. 5, May 2000.

[67] N. H. Jo, J. H. Seo," Input Output Linearization Approach to State Observer Design for Nonlinear System," *IEEE Transactions on Automatic Control*, Vol. 45, No. 12, December 2000.

[68] P. Kabore, H. Wang, "Design of Fault Diagnosis Filters and Fault-tolerant Control for a Class of Nonlinear Systems," *IEEE Transactions on Automatic Control*, Vol. 46, No. 11, November 2001.

[69] N. Kbayashi, R. Nakamizo, "An Observer Design for Linear Systems with Unknown Inputs," *International Journal of Control* , vol. 35, pp. 605-619, 1982.

[70] P. Kudva, N. Viswanadham, A. Ramakrishna, "Observers for Linear System with Unknown Inputs," *IEEE Transactions on Automatic Control* , vol. 25, No.2, pp. 113-115, 1980.

[71] J. H. Lee, M. Morari, "Robust Measurement Selection", *Automatica*, Vol. 27, pp. 519-527, 1991.

[72] A. Lynch, Control Sytems II (Lab manual), University of Alberta, 2004.

[73] A. Lynch, S. Bortoff, "Nonlinear Observers with Approximately Linear Error Dynamics: the Multivariable Case," *IEEE Transactions on Automatic Control*, Vol. 46, No. 7, pp. 927-932, 2001.

[74] R. Marino, P. Tomei, Nonlinear Control Design - Geometric, Adaptive and Robust, Prentice Hall Europe, 1995.

[75] H. J. Marquez, Nonlinear Control Systems: Analysis and Design, Wiley, NY, 2003.

[76] H. J. Marquez, "A Frequency Domain Approach to State Estimation," *Journal of the Franklin Inst.*, Vol. 340, pp. 147-157, 2003.

[77] H. J. Marquez, M. Riaz, "Robust State Observer Design with Application to an Industrial Boiler System," *Control Engineering Practice*, Vol. 13, No. 6, pp. 713-728, 2005.

[78] R. K. Mehra, J. Peschon, "An Innovations Approach to Fault Detection and Diagnosis in Dynamic Systems," *Automatica*, Vol. 7, pp. 637-640, 1971.

[79] D. G. Meyer, "A parameterization of Stabilizing Controllers for Multirate Sampled-data Systems," *IEEE Transanctions on Automatic Control*, AC-35, pp. 233-236, 1990.

[80] D. G. Meyer, "Cost Translation and a Lifting Approach to the Multirate LQG Problem," *IEEE Transanctions on Automatic Control*, AC-37, pp. 1411-1415, 1992.

[81] L. A. Mironovski, "Functional Diagnosis of Linear Dynamic Systems," *Automn Remote Control*, Vol. 40, pp. 1198-1205, 1979.

[82] M. R. Napolitano, V. Casdorph, C. Neppach, S. Naylor, M. Innocenti, G. Silvestri, "Online Learning Neural Architectures and Cross-Correlation Analysis for Actuator Failure Detection and Identification," *International Journal of Control*, Vol. 63, No. 3, pp. 433-455, 1996.

[83] H. Nijmeijer, T. I. Fossen, New Directions in Nonlinear Observer Design, Springer-Verlag, London, 1999.

[84] R. Nikoukhah, "A New Methodology for Observer Design and Implementation," *IEEE Transactions on Automatic Control*, Vol. 43, No. 2, February 1998.

[85] R. J. Patton, "Robust Fault Detection using Eigenstructure Assignment," *Proceedings of the 12th IMACS World Congress on Scientific Computation*, Paris, pp. 431-434, 1988.

[86] R. J. Patton, J. Chen, "Robust Fault Detection using Eigenstructure Assignment: A Tutorial Consideration and Some New Results," *Proceedings of the 30th IEEE Conference on Decision and Control, CDC*, Brighton, UK, pp. 2242-2247, 1991.

[87] R. J. Patton, J. Chen, "Optimal Selection of Unkown Input Distribution Matrix in the Design of Robust Observers for Fault Diagnosis", *Automatica*, vol. 29, No. 4, pp 837-841, 1991.

[88] R. J. Patton, J. Chen, "Observer-based Fault Detection and Isolation: Robustness and Applications," *Control Engineering Practice*, Vol. 5, No. 5, pp. 671-682, 1997.

[89] R. J. Patton, J. Chen, H. Zhang, "Modelling Methods for Improving Robustness in Fault Diagnosis of Jet Engine System," *Prceedings of the 31st IEEE conference on decision and control*, Tucson, Arizona, pp. 2330-2335, 1992.

[90] R. J. Patton, S. W. Willcox, S. J. Winter, "A Parameter Insensitive Technique for Aircraft Sensor Fault Analysis," *J. of Guidance, Control and Dynamics*, Vol. 10, No. 3, pp. 359-367, 1986.

[91] S. Raghavan, Observers and Compensators for Nonlinear Systems with Application to Flexible Joint Robots, Ph.D dissertation, University of California at Berkely, 1992.

[92] S. Raghavan, J. K. Hedrick, "Observer Design for a Class of Nonlinear Systems," *International Journal of Control*, Vol. 59, No. 2, pp. 515-528, 1994.

[93] R. Rajamani, "Observers for Lipschitz Nonlinear Systems," *IEEE Transactions on Automatic Control*, Vol. 43, No. 3, pp. 397-401, March 1998.

[94] R. Rajamani, Observers for Nonlinear Systems with Application to Active Automotive Suspensions, Ph.D dissertation, University of California at Berkely, 1993.

[95] R. Rajamani, Y. M. Cho, "Existence and Design of Observers for Nonlinear Systems: Relation to Distance of Unobservability," *International Journal of Control*, Vol. 69, pp. 717-731, 1998.

[96] K. Reif, F. Sonnemann, R. Unbehauen, "Nonlinear State Observation using H_∞-filtering Riccati Design," *IEEE Transactions on Automatic Control*, Vol. 44, No. 1, pp. 203-208, January 1999.

[97] J. A. Rossiter, T. Chen, S. L. Shah, "A Comparison of Lifting and Inferential Control for Multi-rate Systems," *Proceedings of the American Control Conference*, Denver, Colorado, June 4-6, 2003.

[98] L. Sciavicco, B. Sicliano, Modeling and Control of Robot Manipulators, McGraw Hill, 1989.

[99] C. Scherer , "H_∞ Optimization without Assumptions on Finite or Infinite Zeros," *Int. J. Contr. and Optim.*, Vol. 30, No. 1, pp. 143-166, 1992.

[100] G. Schreier, J. Ragot, R. J. Patton, P. M. Frank, "Observer Design for a Class of Nonlinear Systems," *IFAC Fault detection, supervision and safety for technical processes*, Kingston Upon Hull, UK, 1997.

[101] R. Seliger, P. M. Frank, "Fault Diagnosis by Disturbance Decoupled Nonlinear Observers," *Proceedings of the 30th Conference on Decision and Control, CDC*, Brighton, England, pp. 2248-2255, December 1991.

[102] R. Seliger, P. M. Frank, "Robust Residual Evaluation by Thersohld Selction and a Performance Index for Nonlinear Observer-based Fault Diagnosis", *Proceedings of the International conference on fault diagnosis: TOOLDIAG'93*, Toulouse, pp 496-504, 1993.

[103] T. Sorsa, H. N. Koivo, "Application of Artificial Neural Networks in Process Fault Diagnosis," *Automatica*, Vol. 29, No. 4, pp. 843-849, 1993.

[104] R. F. Stengel, "Toward Intelligent Flight Control," *IEEE Transactions on Systems, Man and Cybernetics*, Vol. 11, No. 4, pp. 14-23, 1991.

[105] A. Stoorvogel, "The H_∞ Control Problem with Zeros on the Boundary of the Stability Domain," *International Journal of Control*, Vol. 63, pp. 1029-1053, 1996.

[106] F. E. Thau, "Observing the State of Non-linear Dynamic Systems," *International Journal of Control*, Vol. 17, No. 3, pp. 471-479, 1973.

[107] A. J. Van Der Schaft, "On Nonlinear Observers," *IEEE Transactions on Automatic Control*, Vol. 30, No. 12, December 1985.

[108] D. Van Schrick, "A Comparison of IFD Schemes: a Decision Aid for Designers," *Proceedings of the 3rd IEEE Conference on Control and Applications*, Glascow, Scotland, pp. 889-894, 1994.

[109] A. Vemuri, "Sensor Bias Fault Diagnosis in a Class of Nonlinear Systems," *IEEE Transactions on Automatic Control*, Vol. 46, No. 6, June 2001.

[110] S. H. Wang, E. J. Davison, P. Dorato, "Observing the States of Systems with Unmeasurable Disturbances," *IEEE Transactions on Automatic Control*, vol. 20, pp. 716-717, 1975.

[111] H. Wang, Z. J. Huang, S. Daley, "On the Use of Adaptive Updating Rules for Actuator and Sensor Fault Diagnosis," *Automatica*, Vol. 33, No. 2, pp. 217-225, 1997.

[112] H. Wang, W. Lin, "Applying Observer Based FDI Techniques to Detect Faults in Dynamic and Bounded Stochastic Distributions," *International Journal of Control*, Vol. 73, No. 15, pp. 1424-1436, 2000.

[113] K. Watanabe, D. M. Himmelblau, "Instrument Fault Detection in Systems with Uncertainty", *Int. J. Sys. Sci*, Vol 13, pp. 137-158, 1982.

[114] K. Watanabe, I. Matsuura, M. Abe, M. Kubota, D. M. Himmelblau, "Incipient Fault Diagnosis of Chemical Processes via Artificial Neural Networks," *AIChE J.*, Vol. 35, No. 11, pp. 1803-1812, 1989.

[115] R. Weber, C. Brosilow, "The Use of Secondary Measurements to Improve Control," *AIChE J.*, Vol. 18, pp. 614-623, 1972.

[116] A. S. Willsky, "A Survey of Design Methods for Failure Detection in Dynamic Systems," *Automatica*, Vol. 12, pp. 601-611, 1976.

[117] J. Wünnenberg, Observer-based Fault Detection in Dynamic Systems, Ph.D thesis, University of Duisburg, Germany, 1990.

[118] J. Wünnenberg, P. M. Frank, "Sensor Fault Using Detection via Robust Observer", *System Fault Diagnosis, Reliability& Related Knowledge-Based Approaches*, S.G. Tzafestas, M. G. Singh and G. Schmidt (eds), Reidel Press, Dordrecht, pp. 147-160, 1987.

[119] X. Xia, M. Zeitz, "On Nonlinear Continuous Observers," *International Journal of control*, Vol. 66, No. 6, pp. 943-954, 1997.

[120] D. Yu, D. N. Shields, "A Bilinear Fault Detection Observer," *Automatica*, Vol. 32, No. 11, pp. 1597-1602, 1996.

[121] S. H. Zak, "On the Stabilization and Observation of Nonlinear/Uncertain Dynamic Systems," *IEEE Transactions on Automatic Control*, Vol. 35, No. 5, pp. 604-607, May 1990.

[122] K. Zhou, J. C. Doyle, Essentials of Robust Control, Prentice-Hall, NY, 1998.

[123] F. Zhu, Z. Han, "A Note on Observers for Lipschitz Nonlinear Systems," *IEEE Transactions on Automatic Control*, Vol. 47, No. 10, pp. 1751-1754, October 2002.

[124] A. Zolghadri, "An Algorithm for Real-time Failure-detection in Kalman Filters," *IEEE Transactions on Automatic Control*, Vol. 41, No. 10, pp. 1537-1539, 1996.

Appendix A

Proofs

The purpose of this appendix is to provide a proof of several lemmas and theorems encountered throughout the book. For easy of reference we re-state the lemmas and theorems before each proof.

A.1 Proof of Lemmas 3.1 and 3.2

Lemma 3.1:

Consider a stabilizing controller K for the setups T_1 and T_2, then $\| \hat{T}_1(s) \|_\infty < \gamma$ if and only if $\exists \, \epsilon > 0$ such that $\| \hat{T}_2(s) \|_\infty < \gamma$.

Lemma 3.2:

Given $\epsilon > 0$ and a stabilizing controller K for the setups T_2 and T_3, then $\| \hat{T}_2(s) \|_\infty < \gamma$ if and only if $\exists \, \beta > 0$ such that $\| \hat{T}_3(s) \|_\infty < \gamma$.

Proof:

Using the definitions of T_1, T_2 and T_3, along with the definition of ζ, τ, $\bar{\zeta}$ and $\bar{\tau}$, the transfer matrix $\hat{T}_1(s)$ is given from (3.22), while $\hat{T}_2(s)$ and $\hat{T}_3(s)$ are given from:

$$\hat{T}_2(s) = \left[\begin{array}{cc|cc} A - D_L C & -C_L & I_n & -\epsilon D_L \\ B_L C & A_L & 0_{kn} & \epsilon B_L \\ \hline I_n & 0_{nk} & 0_n & 0_{np} \end{array} \right], \hat{T}_3(s) = \left[\begin{array}{cc|cc} A - D_L C & -C_L & I_n & -\epsilon D_L \\ B_L C & A_L & 0_{kn} & \epsilon B_L \\ \hline I_n & 0_{nk} & 0_n & 0_{np} \\ \beta D_L C & \beta C_L & 0_n & \epsilon \beta D_L \end{array} \right]$$

$$(A.1)$$

128

We will define $\bar{A}$ as the common state matrix $\begin{bmatrix} A - D_L C & -C_L \\ B_L C & A_L \end{bmatrix}$, and we will hence re-

fer to the state transition matrix of $\hat{T}_1(s)$, $\hat{T}_2(s)$ and $\hat{T}_3(s)$ as: $\hat{H}(s) \overset{\Delta}{=} \left(sI_{n+k} - \bar{A} \right)^{-1} = \begin{bmatrix} \hat{H}_{11}(s) & \hat{H}_{12}(s) \\ \hat{H}_{21}(s) & \hat{H}_{22}(s) \end{bmatrix}$.

From (3.22), (A.1), and from the definition of $\hat{H}(s)$, we have:

$$\hat{T}_1(s) = \hat{H}_{11}(s), \quad \hat{T}_2(s) = \begin{bmatrix} \hat{H}_{11}(s) & -\epsilon\hat{H}_{11}(s)D_L + \epsilon\hat{H}_{12}(s)B_L \end{bmatrix}, \quad \text{(A.2)}$$

$$\hat{T}_3(s) = \begin{bmatrix} \hat{H}_{11}(s) & -\epsilon\hat{H}_{11}(s)D_L + \epsilon\hat{H}_{12}(s)B_L \\ \beta\hat{N}_1(s) & \beta\hat{N}_2(s) \end{bmatrix}$$

$$\hat{N}_1(s) = D_L C\hat{H}_{11}(s) + C_L\hat{H}_{21}(s), \quad \hat{N}_2(s) = \epsilon\left(-\hat{N}_1(s)D_L + D_L C\hat{H}_{12}(s)B_L + C_L\hat{H}_{22}(s)B_L + D_L \right).$$

Proof of Lemma 3.1 (Sufficiency) For the "two input/one output" standard setup T_2, let $\exists \epsilon > 0$ and a stabilizing controller K s.t $\parallel \hat{T}_2(s) \parallel_\infty < \gamma$. But from (A.2) we have $\parallel \hat{T}_2(s) \parallel_\infty = \max\left(\parallel \hat{H}_{11}(s) \parallel_\infty, \parallel -\epsilon\hat{H}_{11}(s)D_L + \epsilon\hat{H}_{12}(s)B_L \parallel_\infty \right)$. Hence, $\parallel \hat{T}_1(s) \parallel_\infty < \gamma$.

(Necessity) Let $\exists$ a controller K such that $\parallel \hat{T}_1(s) \parallel_\infty < \gamma$. It follows that $\parallel \hat{H}_{11}(s) \parallel_\infty = \sigma < \gamma$.

$\therefore \parallel \hat{T}_2(s) \parallel_\infty = \max\left(\sigma, \epsilon \parallel -\hat{H}_{11}(s)D_L + \hat{H}_{12}(s)B_L \parallel_\infty \right)$.

But since K is a stabilizing controller, then $\parallel -\hat{H}_{11}(s)D_L + \hat{H}_{12}(s)B_L \parallel_\infty = \rho$ (where ρ is a finite number). Hence, $0 < \epsilon < \frac{\gamma}{\rho} \Rightarrow \parallel \hat{T}_2(s) \parallel_\infty < \gamma$.

Proof of Lemma 3.2 (Sufficiency) For the "two input/two output" setup T_3, let $\exists \epsilon > 0$, $\beta > 0$ and a controller K s.t $\parallel \hat{T}_3(s) \parallel_\infty < \gamma$. But $\parallel \hat{T}_3(s) \parallel_\infty = \max\left(\parallel \hat{H}_{11}(s) \parallel_\infty, \parallel -\epsilon\hat{H}_{11}(s)D_L + \epsilon\hat{H}_{12}(s)B_L \parallel_\infty, \parallel \beta\hat{N}_1(s) \parallel_\infty, \parallel \beta\hat{N}_2(s) \parallel_\infty \right)$.

Therefore, $\parallel \hat{T}_2(s) \parallel_\infty = \max\left(\parallel \hat{H}_{11}(s) \parallel_\infty, \parallel -\epsilon\hat{H}_{11}(s)D_L + \epsilon\hat{H}_{12}(s)B_L \parallel_\infty \right) < \gamma$.

(Necessity) Let $\exists \epsilon > 0$, K s.t $\parallel \hat{T}_2(s) \parallel_\infty = \sigma < \gamma$.

$\therefore \max\left(\parallel \hat{H}_{11}(s) \parallel_\infty, \epsilon \parallel \hat{H}_{11}(s)D_L - \hat{H}_{12}(s)B_L \parallel_\infty \right) = \sigma$.

$\therefore \parallel \hat{T}_3(s) \parallel_\infty = \max\left(\parallel \beta\hat{N}_1(s) \parallel_\infty, \parallel \beta\hat{N}_2(s) \parallel_\infty, \sigma \right)$.

But since K is a stabilizing controller, then $\parallel \hat{N}_1(s) \parallel_\infty = \rho_1$ and $\parallel \hat{N}_2(s) \parallel_\infty = \rho_2$ (where ρ_1 and ρ_2 are finite numbers). Hence, $0 < \beta < \frac{\gamma}{\max(\rho_1, \rho_2)} \Rightarrow \parallel \hat{T}_3(s) \parallel_\infty < \gamma$.

$\square$

A.2 Computation of the Transfer Matrix $\hat{Q}(s)$

Based on the results in theorem 4.3, it can be proven that, for $\hat{T}_{ef_s}(s)$ in (4.18), $\exists$ a transfer matrix $\hat{Q}(s) \in RH_\infty$ that satisfies $\hat{T}_{ef_s}(j\omega_o) = 0$

Proof: If $j\omega_o$ is not an eigenvalue of A, then (from theorem 4.3) the matrices $\hat{T}_2(j\omega_o)$ and $\hat{T}_3(j\omega_o)$ are invertible, and the matrix equation $\hat{T}_{ef_s}(j\omega_o) = 0$ can be solved for $\hat{Q}(j\omega_o)$ as follows:

$$\hat{Q}(j\omega_o) = -\hat{T}_2^{-1}(j\omega_o)\,\hat{T}_1(j\omega_o)\,\hat{T}_3^{-1}(j\omega_o) = \hat{Q}_{re} + j\hat{Q}_{im}$$

where $\hat{Q}_{re}$ and $\hat{Q}_{im}$ are $n \times p$ matrices that represent the real and imaginary parts respectively.

Let $\hat{Q}(s) = \left[\begin{array}{c|c} A_q & B_q \\ \hline C_q & D_q \end{array} \right]$; where $A_q \in \mathbb{R}^{\ell \times \ell}$, $B_q \in \mathbb{R}^{\ell \times p}$, $C_q \in \mathbb{R}^{n \times \ell}$ and $D_q \in \mathbb{R}^{n \times p}$ and where ℓ is the order of $\hat{Q}(s)$. Then the problem of computing $\hat{Q}(s) \in RH_\infty$ reduces to solving:

$$C_q\,(j\omega_o I_\ell - A_q)^{-1}\,B_q + D_q = \hat{Q}_{re} + j\hat{Q}_{im} \tag{A.3}$$

for a stable A_q with a suitable order ℓ, and for B_q, C_q and D_q. By choosing $\ell = n$, $C_q = I_n$ and $A_q = -I_\ell$, the problem in (A.3) reduces to:

$$\frac{1}{1+\omega_o^2}\,B_q^{(ij)} + D_q^{(ij)} = \hat{Q}_{re}^{(ij)};\quad i = 1,\cdots,n;\ j = 1,\cdots,p \tag{A.4}$$

$$\frac{-\omega_o}{1+\omega_o^2}\,B_q^{(ij)} = \hat{Q}_{im}^{(ij)};\quad i = 1,\cdots,n;\ j = 1,\cdots,p \tag{A.5}$$

where $B_q^{(ij)}$ and $D_q^{(ij)}$ are the elements in row i and column j of the $n \times p$ matrices B_q and D_q respectively. Equations (A.4) and (A.5) can be solved simultaneously for all the elements of B_q and D_q. This completes the solution for $\hat{Q}(s) \in RH_\infty$.

$\square$

A.3 Proof of Lemma 5.1

The error dynamics of (5.3)-(5.9) as an observer for (5.1)-(5.2) (with $f_s = 0$) is locally asymptotically stable and decoupled from the disturbance term $d(t)$ if conditions (5.10)-(5.16) are satisfied:

Proof: Using (5.3)-(5.9) as an observer for the system (5.1)-(5.2) (with $f_s = 0$) and defining the error $e_z = Tx - z$ and the state $\xi = \xi_2 - \xi_1$ we have (with the help of (5.10)-(5.12)):

$$\dot{e}_z = T(Ax + \Gamma(u,t) + Ed) - w_1 - w_2 - T\Gamma(u,t) + T(\Phi(x,u,t) - \Phi(\hat{x},u,t))$$

$$= TAx - (C_F\xi_1 + D_Fz) - (C_L\xi_2 + D_Ly) + T(\Phi(x,u,t) - \Phi(\hat{x},u,t))$$

$$= -C_F\xi_1 - C_L\xi_2 - [D_F(Tx - e_z) - TAx + D_LCx] + T(\Phi(x,u,t) - \Phi(\hat{x},u,t))$$

$$= C_F\xi + D_Fe_z - (D_FT - TA + D_LC)\,x + T(\Phi(x,u,t) - \Phi(\hat{x},u,t))$$

But from (5.11)-(5.13) and (5.16): $TA - D_F T = D_L C$.

$\therefore \dot{e}_z = C_F \xi + D_F e_z$.

For the state $\xi = \xi_2 - \xi_1$, we have:

$$\dot{\xi} = A_L \xi_2 + B_L y - A_F \xi_1 - B_F z$$

$$= A_L \xi_2 + B_L C x - A_F \xi_1 - B_F (Tx - e_z)$$

$$= A_F \xi + B_F e_z - (B_F T - B_L C)x$$

But from (5.11), (5.12), (5.14) and (5.15): $B_F T = B_L C$.

$\therefore \dot{\xi} = A_F \xi + B_F e_z$.

Therefore, the observer error is equivalent to

$$\dot{\xi} = A_F \xi + B_F e_z$$

$$\dot{e}_z = C_F \xi + D_F e_z + T \tilde{\phi}$$

And since $\begin{bmatrix} A_F & B_F \\ C_F & D_F \end{bmatrix}$ is stable from (5.12) and $\tilde{\phi}$ is bounded from the Lipschitz condition, then the error dynamics is locally asymptotically stable according to the "perturbation analysis theorem" (Theorem 4.6.1 in [75]) and decoupled from $d(t)$ and the proof is completed by noting that $e = x - \hat{x} = x - (z + Hy) = (I - HC)x - z = e_z$. $\qquad\qquad \square$

A.4 Derivation of the Robust Error Dynamics Model

In this section, we develop the error dynamics model (5.28)-(5.29). Similar to Appendix A.3, by assuming $e_z = Tx - z$ and the state $\xi = \xi_2 - \xi_1$ we have:

$$\dot{\xi} = A_L \xi_2 + B_L y - A_F \xi_1 - B_F z$$

$$= A_L \xi_2 + B_L (Cx + f_s) - A_F \xi_1 - B_F (Tx - e_z)$$

$$= A_F \xi + B_F e_z - (B_F T - B_L C)x + B_L f_s$$

$$= A_F \xi + B_F e_z + B_L f_s$$

and

$$\dot{e}_z = T(Ax + \Gamma(u,t) + Ed) - w_1 - w_2 - T\Gamma(u,t) + T(\Phi(x,u,t) - \Phi(\hat{x},u,t))$$

$$= TAx - (C_F\xi_1 + D_Fz) - (C_L\xi_2 + D_Ly) + T(\Phi(x,u,t) - \Phi(\hat{x},u,t))$$

$$= -C_F\xi_1 - C_L\xi_2 - [D_F(Tx - e_z) - TAx + D_LCx + D_Lf_s] + T(\Phi(x,u,t) - \Phi(\hat{x},u,t))$$

$$= C_F\xi + D_Fe_z - (D_FT - TA + D_LC)x + T(\Phi(x,u,t) - \Phi(\hat{x},u,t)) - D_Lf_s$$

$$= C_F\xi + D_Fe_z + T(\Phi(x,u,t) - \Phi(\hat{x},u,t)) - D_Lf_s$$

Defining $e = x - \hat{x}$, we have $e_z = Tx - (\hat{x} - Hy) = e + Hf_s$, and hence we get:

$$\dot{e} = C_F\xi + D_F(e + Hf_s) + T(\Phi(x,u,t) - \Phi(\hat{x},u,t)) - D_Lf_s - H\dot{f}_s$$

$$= C_F\xi + D_Fe + (D_FH - D_L)f_s + T(\Phi(x,u,t) - \Phi(\hat{x},u,t)) - H\dot{f}_s$$

$$= C_F\xi + D_Fe - D_{L1}f_s + T(\Phi(x,u,t) - \Phi(\hat{x},u,t)) - H\dot{f}_s$$

$\square$

A.5 Derivation of the Multirate Model

In this section, we develop the model in (7.13). The expression for $y_s(k)$ in (7.10) can be further reduced as:

$$y_s(k) = SPH_f\mathbf{L}^{-1}\underline{u_f}(k)$$

$$= SM_1P'H_f\mathbf{L}^{-1}\underline{u_f}(k) + SM_2H_f\mathbf{L}^{-1}\underline{u_f}(k)$$

$$= (RLS_fM_1P'H_f)\mathbf{L}^{-1}\underline{u_f}(k) + (RLS_fM_2H_f)\mathbf{L}^{-1}\underline{u_f}(k); \quad \text{by using (7.9)}.$$

$$= RM_1LS_fP'H_f\mathbf{L}^{-1}\underline{u_f}(k) + RM_2LS_fH_f\mathbf{L}^{-1}\underline{u_f}(k);$$

(since M_1 and M_2 are static matrices.)

$$= RM_1LS_fP'H_f\mathbf{L}^{-1}\underline{u_f}(k) + RM_2\underline{u_f}(k); \quad \text{since } S_fH_f \equiv I \text{ (the identitiy operator)}.$$

$$= \begin{bmatrix} C & 0_{pn} & \dots & 0_{pn} \end{bmatrix}\mathbf{L}P_d'\mathbf{L}^{-1}\underline{u_f}(k) + \begin{bmatrix} D & 0_{pm} & \dots & 0_{pm} \end{bmatrix}\underline{u_f}(k);$$

(by using (7.9) and (7.12).)

where P_d' is the step invariant transformation of P' (i.e, $S_fP'H_f$) defined as $P_d' = \begin{bmatrix} A_f & B_f \\ \hline I_n & 0_{nm} \end{bmatrix}$

with $A_f = e^{h_fA}$, and $B_f = \int_0^{h_f} e^{\tau A}d\tau B$.

$$\therefore y_s(k) = \begin{bmatrix} C & 0_{pn} & \dots & 0_{pn} \end{bmatrix}\underline{P_d'}\underline{u_f}(k) + \begin{bmatrix} D & 0_{pm} & \dots & 0_{pm} \end{bmatrix}\underline{u_f}(k)$$

The state space model (7.13) is then obtained by using (7.7) to get a representation for $\underline{P_d'}$.

Appendix B

Simulation and Experimental Models

B.1 Model Matrices of the Tank System

$$A = \begin{bmatrix} -0.0084 & -0.0012 & 0.0155 & 0.0280 & 0.0017 \\ -0.0046 & -0.0352 & -0.0227 & 0.0150 & 0.0082 \\ -0.0825 & -0.0122 & -0.0773 & 0.0661 & 0.3209 \\ -0.2105 & 0.0336 & -0.0929 & -0.3418 & -0.1551 \\ 0.0388 & -0.0754 & -0.1532 & 0.0126 & -0.1602 \end{bmatrix}, \ B = \begin{bmatrix} 0.0028 & -0.0022 \\ -0.0016 & 0.0118 \\ -0.1157 & 0.2819 \\ -0.2818 & -0.1153 \\ 0.0552 & -0.2418 \end{bmatrix},$$

$$C = \begin{bmatrix} -6.7795 & -0.7974 & 0.0766 & 0.1585 & 0.0444 \\ -0.1862 & 19.2450 & -0.4087 & -0.0602 & -0.3102 \end{bmatrix}, \ D = \begin{bmatrix} 0 & 0.0090 \\ 0 & -0.0388 \end{bmatrix}.$$

B.2 The ROTPEN Model

The system parameters are: $l_1 = 0.215$ m, $l_2 = 0.335$ m, $m_2 = 0.1246$ Kg, $\beta = 0.135 Nm/s$, $\mu = 0.2065 Nm/V$, $b_2 = 0.0018 Kg/s$, $g = 9.81 m/s^2$, and $J_1 = 0.0064$ Kg.m^2. With the state defined as $x = [x_1 \ x_2 \ x_3 \ x_4]^T = [\theta_1(\text{rad}) \ \theta_2(\text{rad}) \ \dot{\theta}_1(\text{rad/s}) \ \dot{\theta}_2(\text{rad/s})]^T$, the state space model

133

has the form $\dot{x} = f(x) + g(x)u$ as follows (This model was derived in [72]):

$$\dot{x} = \begin{bmatrix} x_3 \\ x_4 \\ h_3(x) - \dfrac{m_2 l_2^2 \beta x_3}{3\Delta} \\ h_4(x) + \dfrac{m_2 l_1 l_2 \beta c_2}{2\Delta} \end{bmatrix} + \begin{bmatrix} 0 \\ 0 \\ \dfrac{\mu m_2 l_2^2}{3\Delta} \\ \dfrac{-\mu m_2 l_1 l_2 c_2}{2\Delta} \end{bmatrix} u$$

where $s_k = sin(x_k)$, $c_k = cos(x_k)$ are used to simplify notation, and where:

$$h_3(x) = \frac{m_2^2 l_2^2 \left(-\frac{1}{2} g l_1 s_2 c_2 - \frac{1}{4} l_1 l_2 x_3^2 s_2 c_2^2 + b_2 l_1 x_4 c_2/(m_2 l_2) + \frac{1}{3} l_1 l_2 x_4^2 s_2 - \frac{1}{3} l_2^2 x_3 x_4 s_2 c_2 \right)}{2\Delta}$$

$$h_4(x) = \frac{\frac{1}{2} m_2 g l_2 \left(m_2 l_1^2 + \frac{1}{4} m_2 l_2^2 s_2^2 + J_1 \right) s_2}{\Delta} - \frac{\left(m_2 l_1^2 + \frac{1}{4} m_2 l_2^2 s_2^2 + J_1 \right) b_2 x_4}{\Delta}$$
$$+ \frac{\frac{1}{4} m_2 l_2^2 [m_2 l_1^2 (x_3^2 - x_4^2) s_2 c_2 + \frac{1}{4} m_2 l_2^2 x_3^2 s_2^3 c_2 + J_1 x_3^2 s_2 c_2 + m_2 l_1 l_2 x_3 x_4 s_2 c_2^2]}{\Delta}$$

$$\Delta = m_2 l_2^2 \left(\frac{1}{3} m_2 l_1^2 + \frac{1}{12} m_2 l_2^2 s_2^2 + \frac{1}{3} J_1 - \frac{1}{4} m_2 l_1^2 c_2^2 \right).$$

B.3   Models and Parameters for Experiment A

Linear model parameters :

$$A = \begin{bmatrix} 0 & 0 & 1 & 0 \\ 0 & 0 & 0 & 1 \\ 0 & -25.14 & -17.22 & 0.2210 \\ 0 & 68.13 & 16.57 & -0.599 \end{bmatrix} ; \quad B = \begin{bmatrix} 0 \\ 0 \\ 26.3370 \\ -25.3596 \end{bmatrix}$$

Control parameters :

$$F = \begin{bmatrix} -2.5207 & -35.9896 & -2.4878 & -3.4189 \end{bmatrix} ; \quad p = -2.5207$$

Reduced-order model for observer design $(\bar{x} = [\theta_2\ \dot{\theta}_1\ \dot{\theta}_2]^T)$:

$$\dot{\bar{x}} = \begin{bmatrix} 0 & 0 & 1 \\ -25.14 & -17.22 & 0.2210 \\ 68.13 & 16.57 & -0.599 \end{bmatrix} \bar{x} + \begin{bmatrix} 0 \\ 26.3370 \\ -25.3596 \end{bmatrix} u$$
$$\bar{y} = \begin{bmatrix} 1 & 0 & 0 \end{bmatrix} \bar{x}$$

Luenberger observer :

$$L_1 = \begin{bmatrix} 92.2 & 95.7 & 1643.9 \end{bmatrix}^T .$$

Linear dynamic observer for sensor bias : (K_1)

$$
A_{L1} = \begin{bmatrix} 93 & 0 & 0 & 0 & 0 \\ 11850 & -150 & 0 & 0 & 0 \\ 20836 & 0 & -200 & 0 & 0 \\ 0 & 0 & 0 & -1 & 0 \\ 0 & 0 & 0 & 0 & -1 \end{bmatrix}, \ B_{L1} = \begin{bmatrix} -103 \\ -11850 \\ -20836 \\ 0 \\ 0 \end{bmatrix},
$$

$$
C_{L1} = \begin{bmatrix} -197 & 0 & 1 & 0 & 0 \\ -10280 & 133 & 0 & 0 & 0 \\ -22713 & 17 & 199 & 0 & 0 \end{bmatrix}, \ D_{L1} = \begin{bmatrix} 207 \\ 10255 \\ 22781 \end{bmatrix}.
$$

Linear dynamic observer for low frequencies : (K_2, obtained for $a = 0.1$, $b = 1$, $c = 0.001$, $\beta = 1$, $\gamma = 10$)

$$
A_{L2} = \begin{bmatrix} 10.6178 & 10.6118 & 0.0049 & -0.0349 \\ -34.9216 & -63.2524 & -2.9453 & -3.3428 \\ 34.1085 & 6.0292 & -17.5710 & -0.3241 \\ -240.9994 & -177.2030 & 16.0249 & -0.9341 \end{bmatrix}, \ B_{L2} = \begin{bmatrix} -47.5 \\ 155.9 \\ -152.6 \\ 1077.7 \end{bmatrix},
$$

$$
C_{L2} = \begin{bmatrix} 0.0126 & 6.3495 & 0.6567 & 0.9843 \\ 0.0013 & 0.6567 & 0.0803 & 0.1090 \\ 0.0020 & 0.9843 & 0.1090 & 0.1661 \end{bmatrix}, \ D_{L2} = \begin{bmatrix} 0 \\ 0 \\ 0 \end{bmatrix}.
$$

B.4   Models and Parameters for Experiment B

Luenberger observer with small gain :

$$
L_{3-small} = \begin{bmatrix} 5.9207 & -7.4414 & -13.0209 & -9.9019 \\ -1.5356 & 21.6603 & -7.2493 & 108.1343 \end{bmatrix}^T.
$$

High-gain Luenberger observer :

$$
L_{3-large} = 10^3 \begin{bmatrix} 0.0716 & 0.0070 & 0.1432 & -0.5022 \\ 0.0203 & 0.2206 & 1.4312 & 4.4841 \end{bmatrix}^T.
$$

Dynamic Lipschitz observer : $(K_3$, obtained for $\alpha = 44.45$, $\epsilon = \beta = 0.00048828)$

$$A_{L3} = 10^4 \begin{bmatrix} -0.3428 & 0 & 0 & 0 \\ 0 & -0.3428 & 0 & 0 \\ -6.2073 & 0 & -0.2048 & 0 \\ 0 & -6.2073 & 0 & -0.2048 \end{bmatrix}, \quad B_{L3} = 10^4 \begin{bmatrix} 0.138 & 0 \\ 0 & 0.138 \\ 6.2072 & 0 \\ 0 & 6.2072 \end{bmatrix},$$

$$C_{L3} = 10^3 \begin{bmatrix} 2.048 & 0 & 0.0005 & 0 \\ 0 & 2.048 & 0 & 0.0005 \\ 0.0005 & 0 & 2.0480 & \\ 0 & 0.0005 & 0 & 2.0485 \end{bmatrix}, \quad D_{L3} = \begin{bmatrix} 0 & 0 \\ 0 & 0 \\ 0 & 0 \\ 0 & 0 \end{bmatrix}.$$

Nonlinear "normal form" Controller :

By considering $y = x_2$, and using the nonlinear model of the ROTPEN in Appendix B.2, the following coordinate transformation:

$$\begin{bmatrix} \xi_1 \\ \xi_2 \\ \eta_1 \\ \eta_2 \end{bmatrix} = \begin{bmatrix} x_2 \\ x_4 \\ x_1 \\ x_3 \left(\frac{l_1}{2}c_2\right) + x_4 \frac{l_2}{3} \end{bmatrix}$$

is used to put the system in the so-called *normal* or *tracking form* [74], that is:

$$\begin{bmatrix} \dot{\xi}_1 \\ \dot{\xi}_2 \\ \dot{\eta}_1 \\ \dot{\eta}_2 \end{bmatrix} = \begin{bmatrix} \xi_2 \\ f_4(x) + g_4(x)u \\ x_3 \\ -\frac{l_1}{2}x_3 x_4 s_2 + \frac{l_1}{2}c_2 f_3(x) + \frac{l_2}{3}f_4(x) \end{bmatrix}$$

and using the control law:

$$u = \frac{1}{g_4(x)}\left[-9x_2 - 6x_4 - f_4(x)\right]$$

where $f_4(x)$ and $g_4(x)$ denote the 4th elements of $f(x)$ and $g(x)$ in Appendix B.2 respectively. The subsystem (ξ_1, ξ_2) is then stabilized. It is important to note that the the zero dynamics in this case, i.e the subsystem (η_1, η_2) is unstable, and therefore the motor angle is not guaranteed to converge to the reference input.

Static Lipschitz observer : (obtained for $\alpha = 1$, $\varepsilon = 0.5$)

$$L_5 = \begin{bmatrix} 1.7108 & -2.1247 & 1.9837 & -5.4019 \\ 0.4338 & -0.2089 & 1.1030 & -2.8972 \end{bmatrix}^T.$$

B.5 Models and Parameters for Experiment C

LQR control scheme with integrator :

$$u = -K_{\ell qr}\, x + \frac{K_i}{s}\left(\theta_1^{\text{``ref''}} - \theta_1^{\text{``measured''}}\right),$$

$$K_i = -2.6310,$$

$$K_{\ell qr} = \begin{bmatrix} -4.4721 & -63.9745 & -5.2972 & -9.2556 \end{bmatrix}.$$

obtained using the MATLAB command

$$[K_{\ell qr}] = LQR(A, B, Q, R),$$

$$Q = diag(300, 1000, 150, 50),$$

$$R = 15.$$

Lipschitz reduced-order model for observer design $(\bar{x} = [\theta_2\ \dot{\theta}_1\ \dot{\theta}_2]^T)$:

$$\dot{\bar{x}} = \begin{bmatrix} 0 & 0 & 1 \\ -25.14 & -17.22 & 0.2210 \\ 68.13 & 16.57 & -0.599 \end{bmatrix} \bar{x} + \begin{bmatrix} 0 \\ \phi_1(\bar{x}, u) \\ \phi_2(\bar{x}, u) \end{bmatrix}$$

$$\bar{y} = \begin{bmatrix} 1 & 0 & 0 \end{bmatrix} \bar{x}$$

Lipschitz dynamic observer for sensor bias : $(K_6,$ obtained for $\lambda = 10^{-12},\ \epsilon = 0.1)$

$$A_{L6} = \begin{bmatrix} -175.7353 & 3.8503 & 0.1710 & -30.6336 \\ 16.8182 & -171.9539 & 26.7652 & 32.1257 \\ 35.1361 & 16.5360 & -97.3465 & 114.1349 \\ -87.9041 & 25.7568 & 62.1442 & -87.8099 \end{bmatrix},\ B_{L6} = \begin{bmatrix} 5.0462 \\ -44.8932 \\ -75.4539 \\ 106.5497 \end{bmatrix},$$

$$C_{L6} = \begin{bmatrix} 167.6750 & -5.0531 & -8.5208 & 42.0138 \\ -7.1899 & 155.5373 & -42.6804 & -11.1441 \\ 5.3053 & -18.7128 & -120.8293 & 171.1055 \end{bmatrix},\ D_{L6} = \begin{bmatrix} 0 \\ 0 \\ 0 \end{bmatrix}.$$

Lipschitz dynamic observer for fault of 2 rad/sec : (K_7, obtained for $\lambda = 10^{-12}$, $\epsilon = 0.1$)

$$A_{L7} = \begin{bmatrix} -816.9997 & -12.5050 & -51.0842 & -64.0861 & 31.8003 \\ 23.8482 & -772.7024 & 149.1621 & 122.7602 & -75.3718 \\ -3.0714 & 139.9543 & -412.1421 & 361.2027 & -176.7926 \\ -193.3011 & 128.2831 & 346.2370 & -405.3024 & 201.2094 \\ 71.5547 & -47.7237 & -104.0209 & 129.8922 & -64.7247 \end{bmatrix} , \quad B_{L7} = \begin{bmatrix} 9.2096 \\ -73.6540 \\ -80.3861 \\ 177.6628 \\ -67.4227 \end{bmatrix} ,$$

$$C_{L7} = \begin{bmatrix} 809.4037 & 11.3091 & 28.1928 & 88.3295 & -43.7581 \\ -13.1309 & 758.2718 & -276.6110 & 4.7255 & 12.0717 \\ -15.9908 & -176.8554 & -509.7118 & 587.8999 & -294.7496 \end{bmatrix} , \quad D_{L7} = \begin{bmatrix} 0 \\ 0 \\ 0 \end{bmatrix} .$$

Lipschitz dynamic observer for low frequencies : (K_8, obtained for $\lambda = 10^{-12}$, $\epsilon = 0.1$)

$$A_{L8} = \begin{bmatrix} -217.7814 & 1.8898 & -4.8573 & -38.2385 \\ -1.5288 & -185.0261 & 38.1186 & 36.8585 \\ 108.5437 & 28.4810 & -87.0920 & 135.1710 \\ -618.9648 & 28.9348 & 82.1016 & -164.6086 \end{bmatrix} , \quad B_{L8} = \begin{bmatrix} -30.2950 \\ 26.3896 \\ 147.7784 \\ -637.5223 \end{bmatrix} ,$$

$$C_{L8} = \begin{bmatrix} -184.6168 & 3.4213 & 1.8716 & -51.2266 \\ 6.5728 & -171.5615 & 49.1851 & 16.3542 \\ -4.3022 & 15.0586 & 114.2413 & -224.5769 \end{bmatrix} , \quad D_{L8} = \begin{bmatrix} 0 \\ 0 \\ 0 \end{bmatrix} .$$